Robust Adaptive Control of Switched Systems

by

Khalid El Rifai

Submitted to the Department of Mechanical Engineering
in partial fulfillment of the requirements for the degree of

Doctoral of Philosophy in Mechanical Engineering

at the

MASSACHUSETTS INSTITUTE OF TECHNOLOGY

May 2007
[June 2007]

Author .....
Department of Mechanical Engineering
May 23, 2007

Certified by .....
Kamal Youcef-Toumi
Professor
Thesis Supervisor

Accepted by .....
Lallit Anand
Chairman, Department Committee on Graduate Students

Robust Adaptive Control of Switched Systems

by

Khalid El Rifai

Submitted to the Department of Mechanical Engineering
on May 23, 2007, in partial fulfillment of the
requirements for the degree of
Doctoral of Philosophy in Mechanical Engineering

Abstract

In this thesis, robust adaptive controllers are developed for classes of switched nonlinear systems. Switched systems are those governed by differential equations, which undergo vector field switching due to sudden changes in model characteristics. Such systems arise in many applications such as mechanical systems with contacts, electrical systems with switches, and thermal-fluidic systems with valves and phase changes. The presented controllers guarantee system stability, under typical adaptive control assumptions, for systems with piecewise differentiable bounded parameters and piecewise continuous disturbances without requiring a priori knowledge on such parameters or disturbances. The effect of plant variation and switching is reduced to piecewise continuous and impulsive inputs acting on a Bounded Input Bounded State (BIBS) stable closed loop system. This, in turn, provides a separation between the robust stability and robust performance control problems. The developed methodology provides clear guidelines for steady-sate and transient performance optimization and allows for parameter scheduling and multiple model controller adjustment techniques to be utilized with no stability concerns. The results are illustrated for various systems including contact-based robotic manipulation and Atomic Force Microscope (AFM) based nano-manipulation.

Thesis Supervisor: Kamal Youcef-Toumi
Title: Professor

Acknowledgments

I would like to start with my family espeically my parents who have been the driving force to any success I have had, I owe them everything. A special mention goes to my brother Osamah who has been an inspiration for me all through my academic career. I would also like to thank all my friends here in Boston and in Egypt for their support and encouragement.

I would like to thank my advisor Kamal for the great experience I had at MIT during both by S.M. and Ph.D.. Kamal has not only been an excellent advisor to work with but also a great person to deal with. His expertise and insight in the systems and control area have been a valuable asset to this thesis. His understanding, patience, and support have made this work a great personal experience.

I am very thankful to my committee members Jean-Jacques Slotine and Daniela De Farias for their valueable technical input as well as their cooepration and flexibility in dealing with committee meetings and defense scheduling despite being on sabbattical away from MIT during my last semester.

Finally, I would like to extend my thanks to all the great people I recievd my education from both at Purude and MIT. Your comments and advice are intangible references to this work.

Contents

List of Figures

Chapter 1

Introduction

In today's era of real-time intelligent control systems, the characteristics of which are autonomy, versatility, and complexity, hybrid, i.e., continuous and discrete, dynamics plays a major role. Systems with hybrid dynamics are those characterized by continuous evolution of a process variables, governed by differential equations or difference equations, along with discrete transitions. The analysis and control of systems characterized by hybrid, i.e., continuous and discrete, dynamics has been attracting many research efforts in recent years. This is motivated by the need to achieve reliably, repeatable, and safe control schemes to handel complex systems with switching dynamics of large, rapid, and sudden changes in model characteristics due to either natural physical changes or controlled decision making based changes. Such systems arise in many application such as mechatronics and robotics, biological and chemical processes, power and communication networks. The ability to design controls for switched and hybrid systems with a priori stability and performance guarantees would not only extend the range of capabilities of control engineering practice to new horizons but also allow for operating existing systems at unprecedented levels of autonomy, versatility, and performance.

1.1 Motivation

This thesis seeks the development of control schemes for reliable and repeatable control of hybrid switched systems. A hybrid switched system is a system that switches between

different vector fields in a differential equation (or a difference equation) each active during a period of time. This recently introduced definition is motivated by the need for control schemes that can handel systems with time varying switching dynamics of large, rapid, and sudden changes in model characteristics due to either natural (physical) changes or controlled (decision making based) changes. These issues arise in systems with discrete changes in energy exchange elements due to intermittent interaction with other systems or with an environment. This is common in electrical circuits with switches such as power converters as well as robotic and mechatronic systems with contact and impact effects. Fluidic systems with valves and phase changes also display switching dynamics. Switched systems also arise when the governing dynamics of a system depends on certain discrete events, which is common in multi-stage chemical process, gene regulatory networks, power and communication networks.

Hybrid switched systems also arise due to modeling reasons. This is the case when modeling multi-time scale dynamics or complex dynamics for which only simple models valid under certain conditions are known, which can be integrated and switched between based on the corresponding validity conditions. Switched systems also arise in modeling for the purpose of control of rapidly varying systems. This includes the notion of gain scheduling, where a complex plant is represented by a family of plants each active during a period of time and control is scheduled according to the current representative plant. This approach is widely used in many industries such as aerospace, automotive, and process control industries, yet remains used in an ad-hoc time consuming manner with very little guarantees or guidelines.

1.2 Problem Formulation

A hybrid switched system is a system that switches between different vector fields in a differential equation (or a difference equation) each active during a period of time. In this thesis, we consider feedback control of continuous-time hybrid switched time varying

systems. These systems are given by:

$$\begin{aligned} \dot{x}(t) &= f_i(x(t), t, u, d),\ t_{i-1} \leq t < t_i \\ y &= h_i(x, t),\ t_{i-1} \leq t < t_i \\ i(t)^+ &= g(i(t), x, t) \end{aligned} \tag{1.1}$$

Where x is the continuous state, d is the disturbances, u is the control input and y is the measured output. Furthermore, $i(t) \in \{1, 2, 3 \dots\}$ is a piecewise constant signal with i denoting the i^{th} switched subsystem active during a period of time $t_i - t_{i-1}$, where t_i is the i^{th} switching time. The signal $i(t)$, usually referred to as the switching function, is the discrete state of this hybrid system. The discrete state is updated by the discrete dynamics $i(t)^+$ governed by $g(i(t), x, t)$, which is driven by the continuous state cx as an input. This means switching may be triggered by a time event or a state event, e.g. x reaching certain threshold values, or even memory, i.e, past values for $i(t)$. This type of system is a continuous-time switched system, whereas discrete-time switched systems are similarly defined by replacing differential equations with difference equations. In this thesis, we will focus on continuous-time switched systems, which will be referred to as switched systems.

An important assumption is that only a finite number of distinct switches can occur within a finite period of time, i.e., the set of switches is countable, with a nonzero period of time $t_i - t_{i-1} > 0\ \forall\, i$ between each consecutive pair of switches and thus infinitely fast switching, the Zeno phenomena [74], is excluded. This is a reasonable assumption since this is how most physical systems behave and we will choose not to introduce any controller switching with infinitely fast switching since it's a typically undesirable behavior. Also note that with this definition and assumption, the effect of switching based on state on the continuous dynamics is similar to time dependent switching since the switching depends on state only implicitly. In fact, we can always find a time-based switching sequence producing equivalent behavior to a state-based switching since we assume an infinitely countable set of switches with nonzero time between each consecutive pair of switches.

There are two main challenges with control of switched systems. First, stability and response of switched systems even when each subsystem is stable and known are difficult

to predict/guarantee. The robustness of stability and performance of switched systems with respect to uncertainties is another challenging problem, which not only includes the existing fundamental limitations in controlling uncertain systems but also introduces challenges associated with different mode-dependent levels/types of uncertainties. Therefore, there is a need for constructive implementable control schemes that can handel systems with switching dynamics of of large, rapid, and sudden changes in model characteristics. The raised issues can then be cast into the following problem. Need to develop a control scheme that guarantees :

1-Stability.

2-Steady state and dynamic performance.

for **uncertain time varying switched** systems subject to:

(i) Large and rapidly varying parametric uncertainty.

(ii) Disturbances and unstructured uncertainties.

(iii) Switching dynamics including parametric, structural, and external effects.

Next, we discuss the status of the state of the art with respect to addressing the aforementioned issues and solving the stated problem.

1.3 Literature Survey

This section reviews the key achievements and limitations of existing literature of relevance. Despite numerous efforts on analysis of hybrid and switched dynamical systems as well as switched control of non-switched systems, there isn't a single constructive synthesis method or technique available for control of a nontrivial class of switched systems with a priori stability and performance guarantees. Two main categories are considered, which are analysis and control of switched systems and the control of uncertain systems.

In terms of stability and response of switched systems, several conservative sufficient conditions have been obtained in recent years, see survey papers [36, 8]. In this context, sufficient conditions for stability such as common Lyapunov functions and average dwell time [36] are the most commonly studied results. One class of results requires that all subsystems share a *common Lyapunov function*, then stability is guaranteed for any switch-

ing speed/order, which for linear-time-invariant (LTI) systems requires system matrices to commute or be symmetric. This is a very restrictive requirement. A corresponding control design requires switching controller gains such that all subsystems are made stable and such that a common Lyapunov function condition is satisfied. In order to verify that such a condition is met, the system is partitioned into known subsystems and a set of linear matrix inequalities (LMI) of the number of subsystems is solved. A feasible solution to such LMI's is usually difficult to obtain and the problem is considered computationally intractable. The other class of results requires that all subsystems are stable (or with some brief known instabilities) and switching is slow enough on the average, *average dwell time condition* [36]. The corresponding controller design requires gains to be adjusted to guarantee the stability of each frozen configuration and knowledge of worst case decay rates among subsystems and condition numbers of Lyapunov matrices in order to compute the maximum admissible switching speed. If plant switching exceeds this switching speed then stability can no longer be guaranteed.

It should be noted that work done on another class of systems referred to linear-parameter varying (LPV) systems, which originate from gain scheduling has recently arrived at analogous conditions for stability of such systems, see for instance [70]. Most of the aforementioned results assume that the system is known exactly and unforced. Analogous analysis results have been extended for systems with disturbances [79] and with some uncertainties [81]. A recent survey [84] summarizes different theorems and conditions for existence of stabilizing controllers and controllability of switched linear systems.

In summary, the available results for control of switched systems have all utilized recently developed sufficient conditions for stability of switched system to state some conditions and properties, which if satisfied by a control system, then stability and response of the switched system can be guaranteed. However, none of these results provide any technique or method that can be constructively used to control a switched system with guarantees on the system's stability and response independent of the success of heuristics or feasibility of complex computational methods.

The other problem of interest is that of dealing with uncertainty. More recently, switching control has been introduced to deal with uncertain time-invariant plants. This line

of work is known as multiple model adaptive or supervisory control where a plant is assumed to belong to a set of known plants from available data and candidate controllers are switched between based on estimation to control the plant. The supervisory control work of [1, 86] and related references therein, uses LTI controllers and estimation-based switching between controllers is made in order to implement the best possible controller. As noted by the authors the problem of freezing an unstable plant/controller configuration is a concern to safety. Furthermore, the stability of the overall system, a switched system, even when each frozen configuration is stable, needs to be verified via complex and not always verifiable conditions. In this approach stability is either based on the common Lyapunov function condition [86] or the average dwell time condition [1] discussed earlier. In fact, the safe multiple model control work developed in [1] to address this issue requires that any change in controller is "small enough" in an identification based sense so that it does not result in a frozen unstable closed loop and that the initial controller chosen is a stabilizing controller. Whereas methods based on a conventional adaptive control architecture have better stability potential for controller switching via re-initializing the adaptation by switching between fixed estimates or resetting the adaptive estimate during transients. However, as suggested by the authors [49, 29, 52], these efforts are solely for improving transients, which is possible only if such fixed estimates are good. Furthermore, the robustness with respect to disturbances and parameter variations was not considered in these efforts. All of these efforts were for a an LTI plant yet a few of the multiple model control schemes considered infrequent jumps and slowly varying parameters of a linear system [86]. Similar ideas were introduced for classes of nonlinear systems, see for instance [31, 75].

Adaptive control [68, 69, 27] is another popular approach to deal with system uncertainty. The problem with conventional adaptive controllers is that the transient performance is not characterized and stability with respect to bounded parameter variations or disturbances is not guaranteed. Robust adaptive controllers, [27], developed to address the presence of disturbances and non-parametric uncertainties, are typically based on projection, switching-sigma or deadzone adaptation laws that require a priori known bounds on parameters, and in some cases disturbances as well, in order ensure state boundedness. Extensions to some classes of time varying systems have been developed in [42, 17, 43, 44, 83]. How-

ever, the results are restricted to smoothly varying parameters with known bounds and typically require additional restrictive conditions such as slowly varying unknown parameters [83] or constant and known input vector parameters [43], in order ensure state boundedness. In this case, such a conclusion is of very little practical importance if the error can not be reduced to an acceptable level by increasing the adaptation or feedback gains or using a better nominal estimate of the plant parameters. Furthermore, performance with respect to rejection of disturbances as well as the transient response remain primarily unknown.

Another type of robust adaptive controllers known as leakage or fixed-sigma modification has been less popular than projection and switching-sigma modifications due to its inability to achieve zero steady-state tracking when parameters are constant and disturbances vanish. However, this is irrelevant for time-varying switched systems of interest to this thesis. Again existing results with this technique concluded boundedness of the closed loop states in the presence of disturbances and exponential stability of the system if persistently excited [27], which is a condition that is usually not satisfied in practice and is sometimes very difficult to check [27, 30]. However, the robust adaptive controller presented in this thesis, which is a generalization of the leakage adaptive controller, is shown to achieve internal exponential and BIBS stability, for the class of systems under consideration, without the need for a persistence of excitation condition as required in [27]. This provides strong stability and performance robustness for time varying switched systems, which yields a new approach to the control of such systems.

1.4 Thesis Scope and Contribution

In this thesis we consider feedback control of continuous-time hybrid switched time varying systems. First, we view a switched system as one parameterized by a time varying vector of parameters, $a(t)$, which is piecewise differentiable and described by the following state equations:

$$
\begin{aligned}
\dot{x} &= f(x, a, u, d) \\
y &= h(x, a) \\
a(t) &= a_i(t),\ t_{i-1} \leq t < t_i,\ i = 1, 2, \ldots \\
i(t)^+ &= g(i(t), x, t)
\end{aligned} \tag{1.2}
$$

Where the last two equations are not needed and are only repeated for the purpose of comparison with (1.1). Therefore, we embed the switching behavior in the piecewise changes in $a(t)$, which again may be triggered by state or time driven events. It is assumed that $a_i(t) \in C^1$, i.e., at least one time continuously differentiable. This means $a(t)$ is piecewise differentiable, i.e., with a well defined bounded derivative everywhere except at points t_i where $\dot{a}$ consists of dirac-delta functions. Also the points of discontinuity of a, which are distinct and form an infinitely countable set, are separated by a nonzero time $t_i - t_{i-1} > 0$ $\forall\, i$, i.e., there is no infinitely fast switching and the dynamics is well defined. Note that by allowing piecewise changes in parameter vector a the parametrization allows structural changes in the system if the parameter vector is overparametrized such that all possible structural terms are included. Then some parameters may switch to or from the value of zero as structural changes take place in the system.

The parametrization of system dynamics in terms of a parameter vector a allows for using adaptive control, where an additional controller state $\hat{a}$ is introduced to adapt for uncertainty and variation in parameter a. The approach used here is based on using an adaptive control architecture, which is modified through the adaptation law, and possibly the control law, to enforce different system properties. These properties are key to enabling the control of switched systems with a priori known guarantees on the system's stability and response independent of the success of heuristics or feasibility of complex computational methods. The idea is driven from the fact that adaptive systems allow arbitrary uncertainty in constant parameters as long as they belong to an admissible set, specified by adaptive stabilizability assumptions. Therefore, if we allow plant parameters to vary as bounded functions within this admissible set, we are left with dealing with the effect of

these variations on stability and performance of the closed loop system, which is addressed by the modified adaptation law used here.

The major contributions of this thesis are:

1. Development of a control scheme that:
    - Guarantees stability for large classes of uncertain time varying switched systems including nonlinear, multi-input-multi-output (MIMO), and output feedback systems.
    - Provides clear guidelines for steady-state and transient performance optimization.
    - Allows for stable gain scheduling and data-based control design.
2. Development of maximum likelihood and Bayesian learning based algorithms for adjusting controller parameters in the presence of data models.
3. Verification of control system performance and characteristics via case studies including contact-based robotic manipulation and Atomic Force Microscope based nano-manipulation.

This thesis develops a generalization of leakage, also known as fixed-sigma, adaptive controllers [27] and shows, for the classes of problems of interest, that the closed loop system is exponentially stable and BIBS stable without the need for persistence of excitation as typically required in [27]. This analysis yielded a control scheme which guarantees stability in the presence of piecewise differentiable bounded parameters, under otherwise typical adaptive control assumptions, without any a priori knowledge of such parameters or restriction on their finite rate of variation. This is the case as the problem reduces to a BIBS stable closed loop driven by parameter variations and uncertainty as well as disturbances as inputs. This approach has yielded explicit dynamic bounds on the size of tracking error and its dependence on these inputs (disturbances, parametric uncertainty and variation) as well as chosen control gains and parameters. As a result, this provides a separation between the robust stability and robust performance control problems. This in turn provides a constructive design method to control a large class of switched systems with clear guidelines for

steady-state and transient performance optimization, which has been lacking in the control literature.

The developed control scheme allows for stable gain scheduling and data-based control design by adjusting a chosen parameter vector estimate in the adaptation law referred to as a^*. This is the case since the difference between the actual plant parameter vector a and the chosen parameter vector a^* acts as an input to the closed loop system. Therefore, a choice of a^* which makes $a^* - a$ smaller improves tracking error and can be varied in an arbitrarily bounded manner since it's only an input to a BIBS stable closed loop system. Gain scheduling, maximum likelihood, and Bayesian learning based algorithms have been developed for adjusting the control when data models are available.

The developed methodology has been used to construct detailed control procedures for several classes of systems. The control system's performance and characteristics have been verified via case studies including contact-based robotic manipulation and Atomic Force Microscope (AFM) based nano-manipulation. The focus of these simulations has been on demonstrating that the developed controllers not only successfully handel switched systems but also clearly follow the predictions and design guidelines provided by the developed theory. The latter is paramount to a practically useful control design methodology.

1.5 Thesis Organization

The reminder of thesis is organized as follows. Chapter 2 provides an introduction to switched systems including detailed application examples from different fields. Chapter 3 presents the basic theory and methodology for adaptive control of switched systems. Whereas, Chapters 4 and 5 provide control design details following the developed methodology of Chapter 3 for systems in companion form and parametric-strict forms, respectively. This includes case study applications to contact-based robotic manipulation in Chapter 4 and Atomic Force Microscope (AFM) based nano-manipulation in chapter 5. In Chapter 6, the control methodology is extended to allow for switching and parameter varying control techniques to be utilized in the presence of more data about the system. Conclusions and Recommendations are given in Chapter 7. The appendix includes proofs

of the main theorems and necessary mathematical notations.

Chapter 2

Introduction to Switched Systems

2.1 Introduction

The following chapter introduces switched systems with emphasis on practical examples where such systems arise. An introduction to switched systems and their mathematical representation is presented. This is followed by detailed examples and models from electrical, mechanical, fluidic, and other domains.

2.2 Switched Systems

A hybrid switched system is a system that switches between different vector fields in a differential equation (or a difference equation) each active during a period of time. This recently introduced definition is motivated by the need for control schemes that can handel systems with time varying switching dynamics of large, rapid, and sudden changes in model characteristics due to either natural (physical) changes or controlled (decision making based) changes. These issues arise in systems with discrete changes in energy exchange elements due to intermittent interaction with other systems or with an environment. This is common in electrical circuits with switches such as power converters as well as robotic and mechatronic systems with contact and impact effects. This includes contact in manipulation from macro- to nano- scales, and numerous contact-based micro- devices used as relays. Fluidic systems with valves and phase changes also display switching dynamics.

Discrete changes in energy exchange elements can also occur in an internal manner for nano-scale dynamics where quantum effects yield discrete changes in energy states and energy exchange elements.

Switched systems also arise when the governing dynamics of a system depends on certain discrete events, which is common in multi-stage chemical process, gene regulatory networks, power and communication networks. The introduction of catalysts, agents, or controlled changes in the environment gives rise to new chemical reactions in a process, when certain critical conditions are satisfied. This yields discrete changes in the dynamics governing the concentrations of targeted chemicals in this process, which are the state variables of this dynamical system. Gene regulatory networks, as well as many other physiological regulatory systems, behave as "switches" in the sense that multiple reaction pathways, and thus dynamics, are taken depending on availability of stimuli and concentrations of proteins, RNA, or other molecules reaching certain threshold values. The principles of operation of many power and communication networks rely on activation/connection of different links and components in the network either in some scheduled manner or in a reactive manner when certain logic based conditions are met. This is done to adjust the network's usage of resources while minimizing congestions and delays along with changes in sources and sizes of demands. This yields discrete changes in the active architecture of the networks and the data/power flow dynamics.

A hybrid switched system is a system that switches between different vector fields in a differential equation (or a difference equation) each active during a period of time. In this thesis, we consider feedback control of continuous-time switched time varying systems described by:

$$\begin{aligned} \dot{x}(t) &= f_i(x,t,u,d),\ t_{i-1} \leq t < t_i \\ y(t) &= h_i(x,t),\ t_{i-1} \leq t < t_i \\ i(t)^+ &= g(i(t),x,t) \end{aligned} \tag{2.1}$$

where x is the continuous state, d is the disturbances, u is the control input, and y is the measured output. Furthermore, $i(t) \in \{1,2,3\dots\}$ is a piecewise constant signal with i

denoting the i^{th} switched subsystem active during a time interval $[t_{i-1}, t_i)$, where t_i is the i^{th} switching time. The signal $i(t)$, usually referred to as the switching function, is the discrete state of this hybrid system. The discrete state is governed by the discrete dynamics of $g(i(t), x, t)$, which is driven by the continuous state x as an input. This means switching may be triggered by a time event or a state event, e.g. x reaching certain threshold values, or even memory, i.e, past values of $i(t)$.

In this thesis, we view a switching system as one parameterized by a time varying vector of parameters, which is piecewise differentiable, see Equation (2.2). This is a reasonable representation since it captures many physical systems that undergo switching dynamics, thus we will focus on such systems described by:

$$\begin{aligned} \dot{x} &= f(x, a, u, d) \\ y &= h(x, a) \\ a(t) &= a_i(t),\ t_{i-1} \leq t < t_i,\ i = 1, 2, \ldots \\ i(t)^+ &= g(i(t), x, t) \end{aligned} \tag{2.2}$$

Therefore, we embed the switching behavior in the piecewise changes in $a(t)$, which again may be triggered by state or time events. Where $a_i(t) \in C^1$, i.e., at least one time continuously differentiable. This means $a(t)$ is piecewise continuous, with a well defined bounded derivative everywhere except at points t_i where $\dot{a} = da/dt$ consists of dirac-delta functions. Also the points of discontinuity of a, which are distinct and form an infinitely countable set, are separated by a nonzero dwell time, i.e., there are no Zeno phenomena [37, 74]. This is a reasonable assumption since this is how most physical systems behave. Note that by allowing piecewise changes in a the parametrization allows structural changes in the system if we overparametrize such that all possible structural terms are included. Then some parameters may switch to or from the value of zero as structural changes take place in the system.

2.3 Examples of Switched Systems

In this section different examples of switched systems arising in engineering and non-engineering problems are discussed. These examples are categorized based on their main physical domain.

2.3.1 Electrical Systems

Electrical systems are one of the most common type of systems where switching dynamics are observed. Any circuit containing a switch such as a diode or thyristor is regarded as a switched systems, see [3] for analysis and classification of different type of switches. Switching circuits have been arising in many applications for a long time but usually have very specific switching behavior such as periodic switching between two modes. This has yielded specialized analysis and control results based on averaging and periodic-specific techniques well before formal switched system theory has emerged. Nevertheless, more formal and general switched system results are expected to enable higher performance and more diverse capabilities for switching circuits.

Converter	Topology	A_1	A_2	B_1	B_2	$C_1 = C_2$
Buck	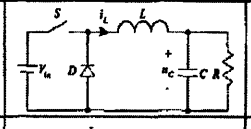	$\begin{bmatrix} 0 & -\frac{1}{L} \\ \frac{1}{C} & -\frac{1}{RC} \end{bmatrix}$	$\begin{bmatrix} 0 & -\frac{1}{L} \\ \frac{1}{C} & -\frac{1}{RC} \end{bmatrix}$	$\begin{bmatrix} \frac{1}{L} \\ 0 \end{bmatrix}$	$\begin{bmatrix} 0 \\ 0 \end{bmatrix}$	$[0 \ 1]$
Boost	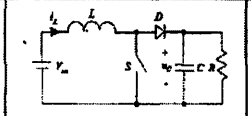	$\begin{bmatrix} 0 & 0 \\ 0 & -\frac{1}{RC} \end{bmatrix}$	$\begin{bmatrix} 0 & -\frac{1}{L} \\ \frac{1}{C} & -\frac{1}{RC} \end{bmatrix}$	$\begin{bmatrix} \frac{1}{L} \\ 0 \end{bmatrix}$	$\begin{bmatrix} \frac{1}{L} \\ 0 \end{bmatrix}$	$[0 \ 1]$
Buck/boost	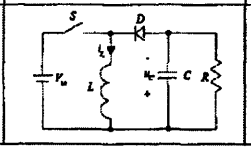	$\begin{bmatrix} 0 & 0 \\ 0 & -\frac{1}{RC} \end{bmatrix}$	$\begin{bmatrix} 0 & -\frac{1}{L} \\ \frac{1}{C} & -\frac{1}{RC} \end{bmatrix}$	$\begin{bmatrix} \frac{1}{L} \\ 0 \end{bmatrix}$	$\begin{bmatrix} 0 \\ 0 \end{bmatrix}$	$[0 \ 1]$

Table 2.1: DC-DC Power Converters [25].

Power and communication systems include many switching circuits such as routers,

converters, rectifiers. A famous example of switching circuits is a DC-DC power converter, which falls under the broad class of switching power supplies. Table 2.1 shows a schematic of Buck, Boost, and Buck-Boost converter circuits. These systems can be modeled as two-mode linear switching systems according to:

$$\dot{x} = \begin{cases} A_1 x + B_1 u & \text{ON} \\ A_2 x + B_2 u & \text{OFF} \end{cases}$$

$$y = \begin{cases} C_1 x & \text{ON} \\ C_2 x & \text{OFF} \end{cases}$$

Where the state is given by $x = [i_L, u_c]^T$ and the input voltage is $u = V_{in}$, and the output is voltage $y = u_c$. The system matrices A_i, B_i and C_i are given in Table 2.1 for the different power converters. Note that since the same output is measured in all cases $C_1 = C_2$ for all three types of converters. Whereas, the Buck converter displays switching in the input matrix B_i and the Boost converter undergoes switching in system matrix A_i with both types of switching observed for the Buck/Boost converter. Clearly, switching is represented by piecewise changes in parameters of system matrices.

2.3.2 Mechanical Systems

Mechanical systems with contact display switching dynamics analogous to electrical systems with switches. This takes place in many common systems. One such system is manual transmissions in an automobile, where clutch engagement gives rise to switching dynamics. In particular, Figure 2-1 shows a diagram of different elements in a manual transmission and focuses further on the engaged and slipping modes of clutch dynamics, which cause switching in the overall system dynamics. A clutch is a system consisting of two parallel rotating disks being moved closer or further from each other. Below is the equations governing the clutch dynamics [46]. In the slipping phase, the clutch dynamics consists of two

disks governed by the dynamics:

$$\begin{aligned} J_1\dot{\omega}_1 &= \tau_1 - \tau_s \\ J_2\dot{\omega}_2 &= \tau_s - \tau_2 \end{aligned}$$

where ω_1, ω_2 are the angular velocities of the clutch disks, J_1, J_2 are their polar inertias, τ_1, τ_2 are torques acting on these disks due to coupling with engine and gearbox, respectively. The friction torque τ_s consists of Coulomb and static friction torques during clutch slipping. The same equations apply to the engaged state but with the condition that $\omega_1 = \omega_2$ adding the two disks' dynamic equations, the dynamics of the engaged mode may be reduced to:

$$\begin{aligned} (J_1 + J_2)\,\dot{\omega}_1 &= \tau_1 - \tau_2 \\ \omega_2 &= \omega_1 \end{aligned}$$

Therefore, in the engaged clutch mode, the system is a first order system with effective inertia $J_1 + J_2$, whereas the slipping clutch mode yields 2^{nd} order dynamics with two inertias J_1, J_2 and friction and other torques acting on these inertias.

The overall dynamics may be compactly described by the Equations [46]:

$$\begin{aligned} J_1\dot{\omega}_1 &= \tau_1 - \mu_{1,2} \\ J_2\dot{\omega}_2 &= \mu_{1,2} - \tau_2 \\ \mu_{1,2} &= \begin{cases} k_{1,2}sign(\omega_1 - \omega_2) & \text{if } \omega_1 - \omega_2 \neq 0 \\ \lambda_{1,2} & \text{if } |\lambda_{1,2}| \leq K_{1,2} \text{ and } \omega_1 - \omega_2 = 0 \\ K_{1,2}sign(\lambda_{1,2}) & \text{if } |\lambda_{1,2}| > K_{1,2} \text{ and } \omega_1 - \omega_2 = 0 \end{cases} \\ \lambda_{1,2} &= \frac{J_1\tau_2 + J_2\tau_1}{J_1 + J_2} \end{aligned}$$

where the switching is embedded in the overall friction torque $\mu_{1,2}$ consisting of Coulomb friction $k_{1,2}sign(\omega_1 - \omega_2)$ when the relative velocity between the disks is nonzero and static friction otherwise. Coulomb friction works to reduce the relative velocity between

the disks whereas static friction works to maintain the disks' contact. The expression for the static friction torque needed for the clutch to be engaged $\lambda_{1,2}$ is computed by enforcing that $\dot{\omega}_1 = \dot{\omega}_2$ and solving for this torque. Therefore, $\mu_{1,2} = \lambda_{1,2}$ during the engaged phase. However, this must be smaller than the maximum static friction amplitude $K_{1,2}$, hence slipping still occurs when $|\lambda_{1,2}| > K_{1,2}$ although $\omega_1 - \omega_2 = 0$. As discussed in Section 2.1, switching can be represented by changes in parameters, such as $a_1(t) = K_1 2sign(\lambda_{1,2}))$ being a parameter that switches between values $a_1 = K_{12}$ and $a_1 = -K_{12}$ or from either one of theses values to the value $a_1 = 0$ when static friction is not active and $\omega_1 - \omega_2 \neq 0$.

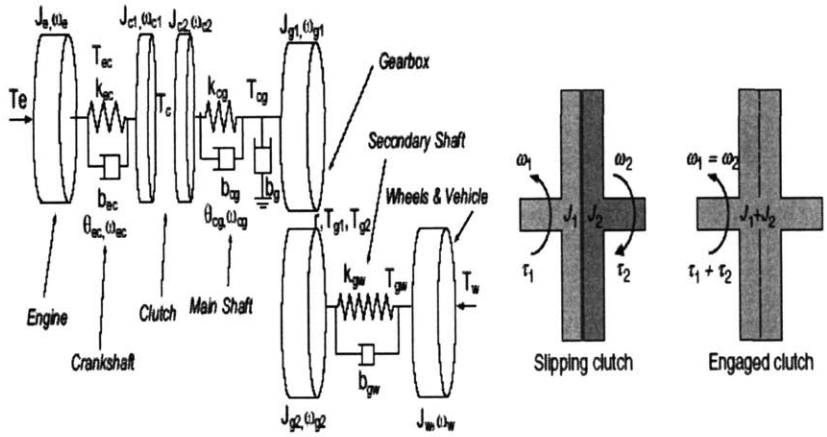

Figure 2-1: Clutch Engagement in Manual transmission Systems [41, 46].

This clutch switching behavior is coupled with the rest of the transmission system, yielding a complex switched system. This problem has received considerable interest recently due to the increasing popularity of automanual transmissions. These systems differ from standard automatic transmissions in the sense that they have the same architecture as a manual transmission given in Figure 2-1 but with the clutch engagement being feedback controlled by an actuator rather than the human depressing the clutch. One of the main issue with these systems is the tarde-off between smoothness and speed of shifting, which is due to the switching nature of the dynamics. A fast and sudden change in system dynamics while maintaining smooth behavior with very little transients is an understandably

challenging task from a control system dynamics point of view. Leading car manufacturers such as Ferrari and BMW are continuously developing these control systems with the fastest shifting times of 200 milliseconds during 2004 are now replaced with a 100 millisecond figure. Nevertheless, smoothness while maintaining such high speeds is still lacking either on upshifts or downshifts. The switching dynamics of clutch engagement are also seen in clutch-type car differentials and other clutch based machines and systems.

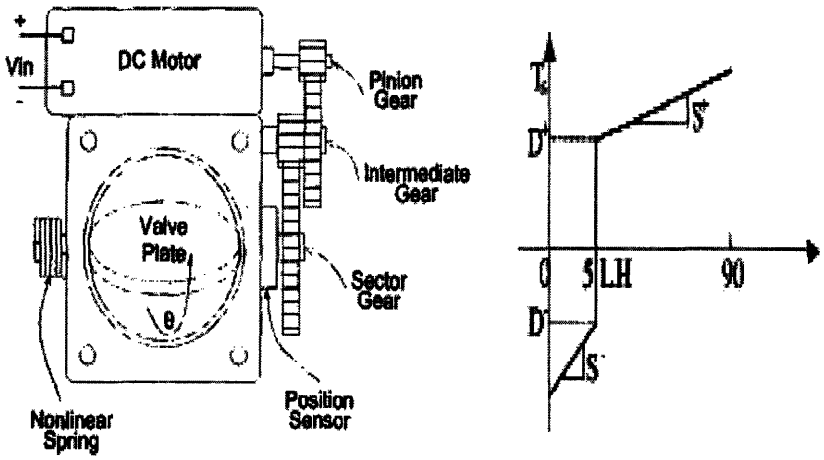

Figure 2-2: Electronic Throttle Body [51, 60].

Another example of contact based switching is seen in electronic throttle body systems, which are commercially know as drive by wire systems. The main switching characteristic in this system is the asymmetrical piecewise spring, see Figure 2-2 from [51]. This is a dual return spring mechanism with stops in order to yield a nonzero equilibrium position for the throttle referred to as the limp-home position, at about $3 - 15°$, so that when power fails the driver can limp home to the nearest service station or parking lot. Furthermore, asymmetry in spring rate is introduced by the two return springs such that contact with stops enforces the higher rate spring for angles below the limp home position and the low rate spring otherwise. This is introduced to yield less sensitive throttle body motion at idle and low loads for improved drivability while allowing for more responsive motion and less power consumption when more throttle travel is needed. The downside of this is that the

torque jump due to this switching stiffness is significant, [60] at about 40% of the nominal motor torque with uncertainty in limp-home position of about 10°, which can deteriorate the control performance. Note that the contact based return spring involves contact with a second plate for angles beyond the limp-home position, which suggests a jump in total inertia J as well, yet the added inertia due to the second plate is insignificant compared to that of the rotor's inertia [53]. The throttle body may be described by the following equations [51]:

$$\begin{aligned}
\dot{\theta} &= k_g\omega \\
\dot{\omega} &= \frac{1}{J}(-B\omega - T_f(\omega) - T_s(\theta) + T_L + k_t z) \\
\dot{z} &= \frac{1}{L}(-Rz - k_v\omega + u) \\
y &= \theta
\end{aligned}$$

where k_g, is an effective gear ratio, J and B are effective inertia and damping of rotor, valve plate, and gearing, T_f is friction torque and T_s is the piecewise linear dual spring torque, see Figure 2-2, k_t is the motor constant, R is motor resistance, and k_v is emf constant, z is the motor current, u is the motor input voltage, and T_L is load torque, which is primarily due to aerodynamic forces from air flow past throttle body. The controlled output is the throttle position θ, which is measured via a potentiometer. The system is basically a DC motor with gearing combined with a piecewise linear return spring as well as friction and aerodynamic torques. The switching spring torque T_s of Figure 2-2 may be represented by:

$$T_s = \begin{cases} S^-(\theta - \theta_o) - D^- & \text{if } \theta \leq \theta_o \\ S^+(\theta - \theta_o) + D^+ & \text{if } \theta > \theta_o \end{cases}$$

where $S^- > S^+$ are the two spring rates acting for angles below and beyond the limp home position θ_o, and D^+, D^- are torque offsets.

Another application where switching dynamics arises due to piecewise spring forces is seen in engine fuel injectors such as the piezo injector in Figure 2-3. In order to avoid fuel leakage for the closed valve under all operating conditions, an idle lift is introduced as a safety margin for small deflections. Opening the valve, one can divide the procedure into three principal phases [58]: 1) Deflection of the piezo actuator within the idle lift, 2) Impact of the piezo actuator bolt on the servo valve and deflection until the servo valve opens, 3) Opening the servo valve. Piecewise changes in effective spring rates are observed between these modes. The injector will operate at a high switching speed, 0.1 millisecond per stroke, between the open and closed states of the injector, meaning switching dynamics is an intrinsic part of the system's operation rather than an initial transient. Other common application where mechanical contact yields switching dynamics are in contact based robotic manipulation including macro-, micro-, and nano- scale manipulation. Detailed examples along with control design will be presented in upcoming chapters.

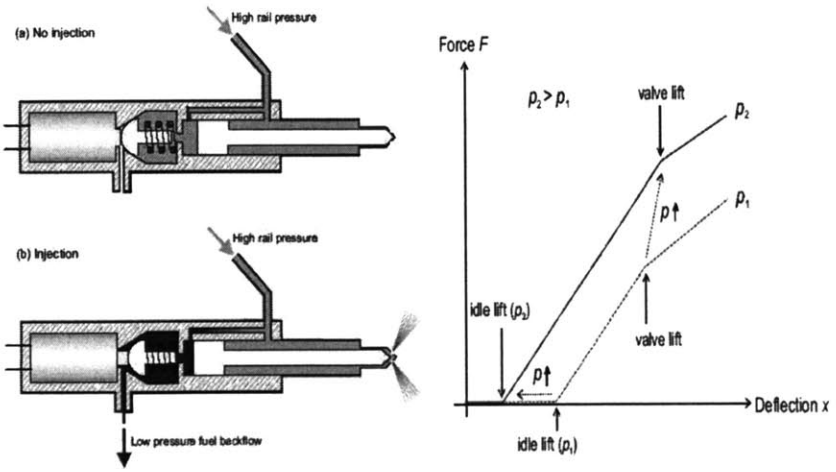

Figure 2-3: Engine Piezo Injector [58].

2.3.3 Fluidic Systems

Fluidic systems are another class of systems where switching dynamics arises due to discrete changes in energy exchange elements. Switching fluidic systems are commonly ob-

served in systems with valves. Figure 2-4 shows a hydraulic piston actuator, which is a popular actuator due to its strength and durability. These types of actuators utilize servo-valves, which introduce switching in the pressure dynamics in these actuators. The dynamics of this system can be described by [50]:

$$
\begin{aligned}
\dot{x}_{sv} &= -\frac{1}{\tau_{sv}} x_{sv} + \frac{K_{sv}}{\tau_{sv}} V_{sv} \\
\dot{P}_L &= \frac{4\beta}{2V_h + A_2 L}\left[K x_{sv}\left(S(x_v)\sqrt{\frac{P_S - P_L}{2}} + S(-x_v)\sqrt{\frac{P_S + P_L}{2}}\right)\right] \\
&\quad -\frac{4\beta}{2V_h + A_2 L}\left[\left(\frac{A_1 + A_2}{2}\right)\dot{x}_p\right] \\
\ddot{x}_p &= \frac{1}{M}\left[\left(\frac{A_1 - A_2}{2}\right)(P_s + P_L) + F_{pf}\right] \\
S(x_v) &= \begin{cases} 1 & \text{if } x_{sv} \geq 0 \\ 0 & \text{if } x_{sv} < 0 \end{cases} \\
y &= x_p
\end{aligned}
$$

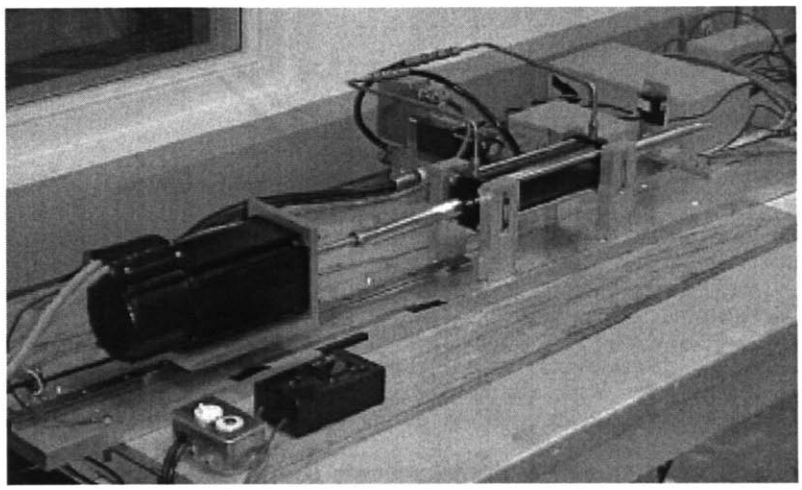

Figure 2-4: Hydraulic Piston Actuator [50].

Where x_{sv} is the spool valve position, V_{sv} is the control voltage, K_{sv} is the servo-valve position gain and τ_{sv} is the time constant of the valve. Whereas, P_L and P_S are the load

and supply pressures, respectively. Parameters K the servo-valve flow gain, A_1 and A_2 are piston inlet and outlet areas, L is the actuator stroke length, V_h is the hose volume between the servo valve and the actuator, and β is the effective bulk modulus of the oil. Finally, x_p is the piston position, which is the controlled output, M is the total mass, and F_{pf} is the friction forces acting on the piston, see [50] and references therein for details. The switching function S, which is controlled by the spool valve position, introduces switching in the system dynamics between two modes. In particular, the position of the servo-valve spool controls the flow rate in and out of the actuator, which introduces switching in the load pressure dynamics.

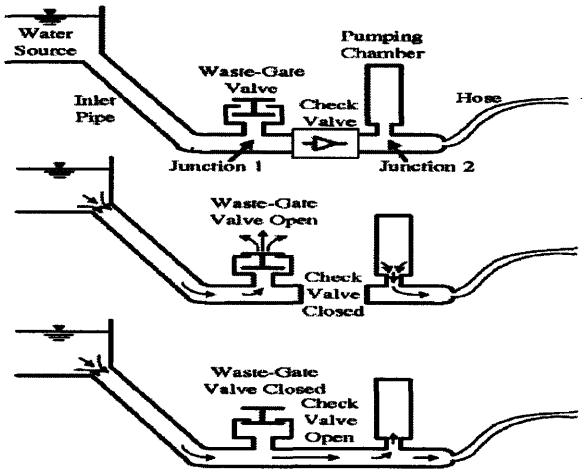

Figure 2-5: Hydraulic-Ram Pump [34].

Many other hydraulic systems with valves undergo switching dynamics. Figure 2-5 shows a hydraulic-ram pump, which also undergoes switching in its dynamics due two valves yielding three possible dynamic modes of operation, see [34] for details.

Another phenomena in fluidic systems where switching dynamics arises is in the presence of phase changes. Heat exchangers are a common example where phases transitions repeatedly occur causing switching in the system dynamics with changes in its order. In particular, when a refrigerant's phase disappears, the states associated with it become redundant and the order of the system is reduced. Figure 2-6 shows the phase transitions

in a heat exchanger, where three possible dynamics are observed due to vapor, liquid, or two-phase modes, see [6] for details.

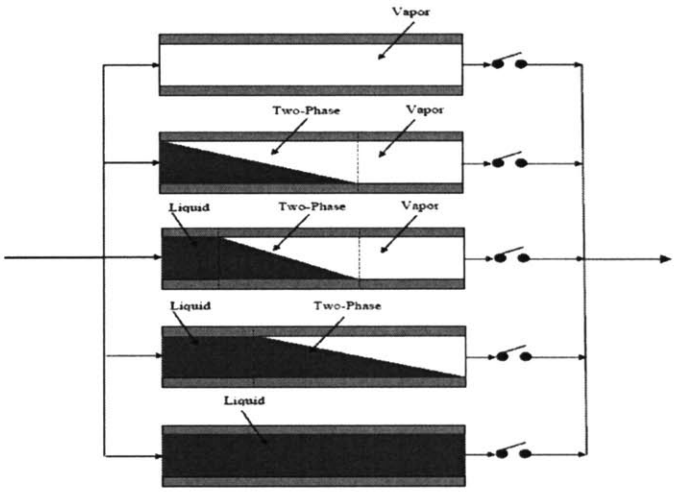

Figure 2-6: Phase Transitions in Heat Exchanger [6].

2.3.4 Other Systems

The last three sections discussed electrical, mechanical, and fluidic switched systems. In this section, a few extra examples from other domains are discussed.

Switched systems are commonly found in chemical process control systems. These systems are thermal-fluidic systems but with concentrations of chemicals being key state variables of interest. Figure 2-7 is a continuously stirred tank with switching between two available inlet streams. An irreversible, first-order exothermic reaction takes place. The operation schedule requires switching between two available inlet streams consisting of pure specie A at flow rates F_{A1}, F_{A2}, concentrations C_{A1}, C_{A2} and temperatures T_{A1}, T_{A2} respectively. The dynamics of the system is modeled by:

$$\begin{aligned} \dot{C}_A &= \frac{F_i}{V}(C_{Ai} - C_A) - k_0 e^{-E/RT_R} C_A \\ \dot{T}_R &= \frac{F_i}{V}(T_{Ai} - T_R) - \frac{\Delta H}{\rho c_p} k_0 e^{-E/RT_R} C_A + \frac{Q}{\rho c_p} \end{aligned}$$

Where i denotes the i^{th} inlet stream for $i = 1, 2$, C_A denotes the concentration of the species, T_R denotes the temperature of the reactor, Q is the heat removed from the reactor, V is the volume of the reactor, k_0, E, ΔH are the pre-exponential constant, the activation energy, and the enthalpy of the reaction. Whereas, c_p and ρ are the heat capacity and density of the fluid in the reactor. The control objective is to stabilize the reactor at the desired operating setpoint using the rate of heat input q and change in inlet concentration i.

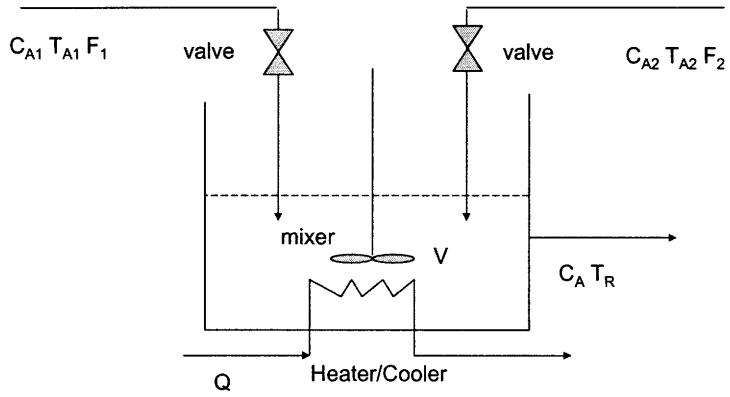

Figure 2-7: A Continuously Stirred Tank Chemical Process [45].

Switching dynamics is also found in biological systems. Gene regulatory systems are an example of a biological system, which can be modeled as a switched system, among other methods to capture their switch-like behavior [9]. Gene expressions are represented by the existence or absence of certain proteins. Protein production is switched ON or OFF depending on the the presence of other genes in sufficient concentrations. A simple switching linear model of these systems is given by [9]:

$$\begin{aligned} \dot{x}_i &= g_i(x) - \gamma_i x_i \\ g_i(x) &= \sum_{l \in L} \kappa_{il} b_{il}(x) \end{aligned}$$

Where x_i is the cellular concentration of the product of gene i and $\gamma_i > 0$ is the degradation rate of x_i. The function $g_i(x) \geq 0$ where $\kappa_{il} > 0$ is a rate parameter, b_{il} is a switching function defined in terms of sums and multiplications of step functions, and L is a set of indices. Figure 2-8 shows an example of a three genes network. This system can be modeled by the following switched system [9]:

$$\begin{aligned} \dot{x}_1 &= \kappa_1 s(x_2, \theta_{21}) - \gamma_1 x_1 \\ \dot{x}_2 &= \kappa_2 (1 - s(x_1, \theta_{11}) s(x_3, \theta_{3,1})) - \gamma_2 x_2 \\ \dot{x}_3 &= \kappa_3 (1 - s(x_1, \theta_{12})) + \kappa_4 (1 - s(x_3, \theta_{3,2})) - \gamma_3 x_3 \\ s(x_j, \theta_j) &= \begin{cases} 1 & \text{if } x_j \geq \theta_j \\ 0 & \text{if } x_j < \theta_j \end{cases} \end{aligned}$$

The system follows the general form with $g_1(x_2) = \kappa_1 s(x_2, \theta_{21})$, meaning that protein 1 is synthesized at a rate κ_1, if the concentration of protein 2 is above the threshold concentration θ_{21} where $s(x_j, \theta_j)$ is a unit step function with switching threshold θ_j. Combined dependencies are shown for gene 2, which is expressed at a rate k_2, if the concentration of either of proteins 1 and 3 remains below its respective threshold by using $g_2(x_1, x_3) = \kappa_2 (1 - s(x_1, \theta_{11}) s(x_3, \theta_{3,1}))$, see [9] for more details.

Other examples of switching dynamics are seen in non-physical phenomena such as planning, management, and production problems. A switching production system is discussed in [59]. When the stock level of a product is positive, some of the perishable produced parts are being stored and will deteriorate with time at a given rate. When the stock level is negative it leads to backorders, which means that orders for production of parts are coming in and there are no stocked parts to immediately meet the demand. This can be

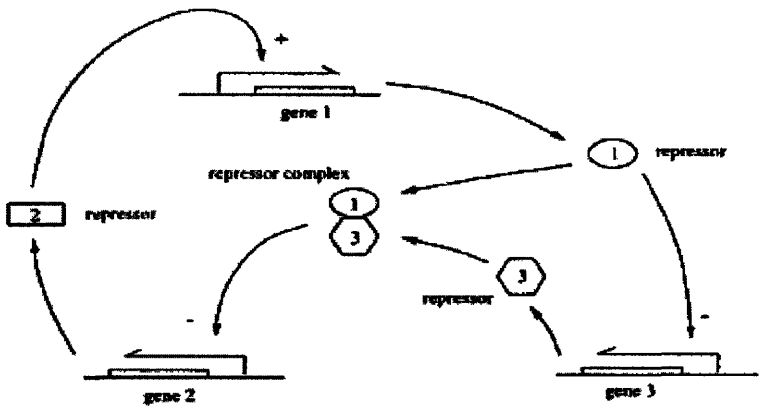

Figure 2-8: Example regulatory network of three genes [9].

represented by the following simple model:

$$\dot{x} = \begin{cases} -\rho x + u - d & \text{if } x > 0 \\ u - d & \text{if } x \leq 0 \end{cases}$$

Where $x(t), u(t)$, and $d(t)$ are stock level, the production rate and the demand rate at time t, respectively. The model represents the fact that, when the stock is non-empty $x > 0$, the stocked parts may deteriorate with time, which is assumed to be at a linear rate factor ρ. Whereas, when the product is on backorder, its evolution only depends on production rate and given demand. The goal of this system is to design a controller u that adjusts the production rate despite the difference in system dynamics near the zero stock level point. Models containing additional constraints such as capacity limitations as well as higher order systems including multiple dependent products may be developed, see [59] and reference therein.

2.4 Summary

This chapter formally introduced switched systems and their representation by parameterized systems with piecewise parameters. Examples from electrical, mechanical, fluidic, chemical, biological, and other areas demonstrate the importance of switched systems as well as their challenging dynamics and control.

Chapter 3

A Robust Adaptive Controller for Switched Systems

3.1 Introduction

The following chapter presents a methodology for robust adaptive control design for a class of switched nonlinear systems. Under typical adaptive control assumptions, the control scheme guarantees system stability for bounded disturbances and parameters without requiring a priori knowledge on such parameters. The problem reduces to an analysis of an exponentially stable system driven by piecewise continuous and impulsive inputs due to plant parameter switching and variation. This system is a modification of the closed loop error dynamics in standard adaptive control systems, through a generalized leakage-type adaptation law.

3.2 Methodology

3.2.1 Parameterized Switched Systems

A hybrid switched system is a system that switches between different vector fields in a differential equation (or a difference equation) each active during a period of time. In this thesis, we consider feedback control of continuous-time switched time varying systems

described by:

$$\begin{aligned} \dot{x}(t) &= f_i(x,t,u,d),\ t_{i-1} \le t < t_i \\ y(t) &= h_i(x,t),\ t_{i-1} \le t < t_i \\ i(t)^+ &= g(i(t),x,t) \end{aligned} \tag{3.1}$$

where x is the continuous state, d is the disturbances, u is the control input, and y is the measured output. Furthermore, $i(t) \in \{1,2,3\dots\}$ is a piecewise constant signal with i denoting the i^{th} switched subsystem active during a time interval $[t_{i-1}, t_i)$, where t_i is the i^{th} switching time. The signal $i(t)$, usually referred to as the switching function, is the discrete state of this hybrid system. The discrete state is updated by the discrete dynamics $i(t)^+$ governed by $g(i(t),x,t)$, which is driven by the continuous state x as an input. This means switching may be triggered by a time event or a state event, e.g. x reaching certain threshold values, or even memory, i.e, past values of $i(t)$.

In this thesis, we view a switching system as one parameterized by a time varying vector of parameters, which is piecewise differentiable, see Equation (3.2). This is a reasonable representation since it captures many physical systems that undergo switching dynamics, thus we will focus on such systems described by:

$$\begin{aligned} \dot{x} &= f(x,a,u,d) \\ y &= h(x,a) \\ a(t) &= a_i(t),\ t_{i-1} \le t < t_i,\ i = 1,2,\dots \\ i(t)^+ &= g(i(t),x,t) \end{aligned} \tag{3.2}$$

Therefore, we embed the switching behavior in the piecewise changes in $a(t)$, which again may be triggered by state or time driven events. $a_i(t) \in C^1$, i.e., at least one time continuously differentiable. This means $a(t)$ is piecewise continuous, with a well defined bounded derivative everywhere except at points t_i where $\dot{a} = d\,a/dt$ consists of dirac-delta functions. Also the points of discontinuity of a, which are distinct and form an infinitely countable set, are separated by a nonzero dwell time, i.e., there are no Zeno phenomena [37, 74].

This is a reasonable assumption since this is how most physical systems behave. The main assumptions on the class of systems under consideration are formally stated below:

Assumption 3.2.1.
For a switched system given by Equation (3.1) or Equation (3.2) the set of switches associated with a switching sequence $\{(t_i, f_i)\}$ *or* $\{(t_i, a_i)\}$ *is infinitely countable and* $\exists$ *a scalar* $\mu > 0$ *such that* $t_i - t_{i-1} \geq \mu \ \forall i$.

Assumption 3.2.2. $d \in \mathbb{R}^k$ *is uniformly bounded and piecewise continuous.*

Assumption 3.2.3. $a \in \mathcal{S}_a$ *is uniformly bounded and piecewise differentiable, where the set* $\mathcal{S}_a$ *is an admissible, but not necessarily known, set of parameters.*

Note that by allowing piecewise changes in a the parametrization allows structural changes in the system if we overparametrize such that all possible structural terms are included. Then some parameters may switch to or from the value of zero as structural changes take place in the system.

3.2.2 Robust Adaptive Control

In this section, we discuss the basic methodology based on the general structure of the adaptive control problem. In standard adaptive control for linearly-parameterized systems we usually have control and adaptation laws of the form [**?**, 27]:

$$\begin{aligned} u &= g(x_m, \hat{a}, \dot{\hat{a}}, y_r, t) \\ \dot{\hat{a}} &= f_a(x_m, \hat{a}, y_r, t) \end{aligned} \tag{3.3}$$

Where u is the control signal, $\hat{a}$ is an estimate of plant parameter vector $a \in S_a$, where S_a is an admissible set of parameters, x_m is measured state variables, and y_r is a desired reference trajectory to be followed. The adaptation law f_a in Equation (3.3) though not specified is usually a gradient-like adaptation law.

This yields the following closed loop error dynamics :

$$\begin{aligned} \dot{e}_c &= f_e(e_c, \tilde{a}, t) + d(t) \\ \dot{\tilde{a}} &= f_a(e_c, \hat{a}, t) - \dot{a} \end{aligned} \tag{3.4}$$

where e_c represents a generalized tracking error, includes state estimation error in general output feedback problems, $\tilde{a} = \hat{a} - a$ is parameter estimation error, and d is the disturbance.

In standard adaptive control we typically design the control and adaptation laws, Equation (3.3), such that $\forall\, a \in S_a$ we have:

$$e_c^T P f_e + \tilde{a}^T \Gamma^{-1} f_a \;\leq\; -e_c^T C e_c \tag{3.5}$$

where matrices $P > 0$ and $C > 0$ are chosen depending on the particular algorithm, e.g. choice of reference model and the diagonal matrix $\Gamma > 0$ is the adaptation gain matrix. This is sufficient to stabilize the system with constant parameters and no disturbances $d = \dot{a} = 0$. However, since the error dynamics is not BIBS stable, stability is no longer guaranteed in the presence of bounded inputs such as d and $\dot{a}$. In order to deal with time varying and switching dynamics, a modification to the adaptation law will be pursued.

Now consider the following modified adaptation law:

$$\dot{\hat{a}} = f_a(e_c, \hat{a}, t) - L(\hat{a} - a^*) \tag{3.6}$$

with the diagonal matrix $L > 0$ and $a^*(t)$ is an arbitrarily chosen piecewise continuous bounded vector, which is an additional estimate of the plant parameter vector. Then the same system in Equation (3.4) with the modified adaptation law becomes:

$$\begin{aligned} \dot{e}_c &= f_e(e_c, \tilde{a}, t) + d(t) \\ \dot{\tilde{a}} &= f_a(e_c, \hat{a}, t) - L\tilde{a} + L(a^* - a) - \dot{a} \end{aligned} \tag{3.7}$$

This system, as Theorem 1 below states, possesses strong robustness and stability properties with respect to time variation in parameter a. The modified adaptation law shown above

is a generalization of leakage adaptive laws [27], which have been used to improve robustness with respect to unstructured uncertainties. The leakage adaptation law, also known as fixed-sigma, uses $L = \sigma\,\Gamma$, where $\sigma > 0$ is a scalar and the vector $a^*(t)$ above is usually not included or is a constant. In fact, the key contribution from the generalization presented here is not in the significance of the algebraic difference relative to leakage adaptive laws [27] but rather in how the algorithm is utilized and proven to achieve new capabilities for control of rapidly varying and switching systems.

Theorem 1. *If there exits matrices $P, C > 0$ and diagonal matrix $\Gamma > 0$ such that (3.5) is satisfied for $\dot{a} = d = 0$ then the system given by Equation (3.7) with $d, \dot{a} \neq 0$ and diagonal $L > 0$ is:*
(i) Uniformly internally exponentially stable and BIBS stable.
(ii) If Assumptions (3.1.1-3.1.3) are satisfied and $a^*(t)$ is chosen as a piecewise continuous bounded vector then state $x_c = [e_c, \tilde{a}]^T$ is bounded with

$$\|e_c(t)\| \leq c_1\|x_c(t_o)\|e^{-\alpha(t-t_o)} + c_2\int_{t_o}^{t} e^{\alpha(\tau-t)}\|v(\tau)\|\,d\tau \tag{3.8}$$

where c_1, c_2 are constants, $\alpha = \underline{\lambda}(diag(P^{-1}C, L))$, and $v = [P^{1/2}d, \Gamma^{-1/2}(L(a^*-a)-\dot{a})]^T$.

The proof of this result is found in Appendix A.

3.2.3 Remarks

This section presents some remarks summarizing the implications of this result.

- The role of the extra term $-L(\hat{a} - a^*)$ in the adaptation law is to transform the Lyapunov stable homogenous adaptive control system into an exponentially and BIBS stable system, via the term $-L\tilde{a}$, driven by an input $L(a^* - a)$.

- BIBS stability of the closed loop system guarantees that the system is *robustly stable* with respect to any bounded magnitude parametric uncertainty and bounded disturbance *without requiring any a priori knowledge of such bounds* since they appear as

inputs to the closed loop system. This, in turn, provides a separation between the robust stability and robust performance control problems.

- Plant parameter switching no longer affects internal dynamics and stability but enters as a step change in input $L(a^* - a)$ and an impulse in input $\dot{a}$ at the switching instant.

- Controller switching of a^* does not affect internal dynamics but enters as a step change in input $L(a^* - a)$, which is a very powerful feature that can be used to utilize available information about the system. This gives rise to a robust control philosophy, using an adaptive control architecture, for time varying switching systems for which satisfactory control methods are lacking even when the plant is known exactly.

- Allowed arbitrary time variation and switching in the parameter vector a are for admissible plants with parameters within the admissible set of parameters S_a. As will be seen in subsequent chapters, this is defined by extensions of typical adaptive control assumptions. Such assumptions include linearly-parameterized dynamics of known structure, exponentially stable zero dynamics, known and constant relative degrees and signs of the control direction.

- The modified adaptation law is a slightly more general version of the leakage modification, also known as fixed-sigma, [27], where $L = \sigma\,\Gamma$, where $\sigma > 0$ is a scalar and the vector $a^*(t)$ above is usually not included or is a constant. This is a robust adaptive control method that has been less popular than projection and switching-sigma modifications due to its inability to achieve zero steady-state tracking when parameters are constant and disturbances vanish. However, as shown here the modified adaptive controller achieves internal exponential and BIBS stability, for the class of systems under consideration, without need for persistence of excitation as required in [27]. This yields stronger stability and performance robustness for time varying switching systems for which the constant parameter case is irrelevant.

- Note that the enforced choice of chosen gain matrices Γ and L being diagonal is not necessary but is made for simplicity and common usage. It is sufficient to chose them in any way such that $\Gamma^{-1}L > 0$ and symmetric.

3.3 Extensions

3.3.1 Adapting For Disturbances

An additional feature that will be augmented with the methodology described earlier is additional estimators to adapt for disturbances. Adapting for constant disturbances or for constant magnitudes of disturbances of known form is common in adaptive control. This is the case as they appear as constant parameters in the system. However, since the adaptation approach used in this chapter can be used for rapidly varying parameters, we can then use it for time varying disturbances with no restriction.

Then using the following modified control law with an additional update law for disturbance estimate $\hat{d}$:

$$\begin{aligned} u &= g(x_m, \hat{a}, \dot{\hat{a}}, y_r, w_d, t) \\ \dot{\hat{\theta}} &= f_\theta(x_m, \hat{a}, y_r, w_d, t) - L(\hat{\theta} - \theta^*) \\ \dot{\hat{d}} &= f_d(x_m, \hat{a}, y_r, w_d, t) - L_d\hat{d} \end{aligned}$$

where θ replaces a and the matrix $w_d(t) \in R^{l \times m}$ for $\hat{d} \in R^l$ and $u \in R^m$ is the assumed internal model of disturbance, e.g., a sinusoidal function, if available. This updated system still yields error dynamics of the form given by Equation (3.7) and satisfies Equation (3.5) upon redefining some variables. This means that if there is no assumed content for the disturbance, then w $\hat{d}$ is simply adapting for an arbitrary time varying disturbance. Whereas, including some terms in w_d such as squares or sine functions allows for an application of the internal model principle to improve the controller's response to such disturbances.

This updated system still yields error dynamics of the form given by Equation (3.7) and satisfies Equation (3.5) upon redefining some variables. In this regard, defining a new parameter $a = [\theta, 0]^T$ and parameter estimation error $\tilde{a} = [\tilde{\theta}, \hat{d}]^T$ yields results analogous to those of Theorem 1. The disturbance adaptation parameter $\hat{d}$ is augmented in $\hat{a}$ with an assumed nominal value of 0 in a and in $a^* = [\theta^*, 0]^T$. The condition given by Equation (3.5) is now satisfied with a redefined matrix $\Gamma^{-1} = diag(\Gamma_o^{-1}, \Gamma_d^{-1})$ where Γ_o is the original adaptation gain used for $\hat{\theta}$ and Γ_d is the adaptation gain used for updating $\hat{d}$ above.

Similarly, the overall filter gain is redefined as $L = diag(L_o, L_d)$ where L_o is the original filter gain used for $\hat{\theta}$. The proof for this extension is omitted and will be seen in design specific developments in subsequent chapters.

3.3.2 An Extended Form with Parameter Dependent Matrix Γ

An additional parameter, which is usually the high frequency gain or a control input parameter, appears in many algorithms as part of matrix Γ in Equation (3.5) causing a deviation from the forms presented earlier. In particular, we have:

$$\begin{aligned} u &= g(x_m, \hat{a}, \dot{\hat{a}}, y_r, w_d, t) \\ \dot{\hat{\theta}} &= f_\theta(x_m, \hat{a}, y_r, w_d, t) - L_o(\hat{\theta} - \theta^*) \\ \dot{\hat{\rho}} &= f_\rho(x_m, \hat{a}, y_r, w_d, t) - L_\rho(\hat{\rho} - \rho^*) \\ \dot{\hat{d}} &= f_d((x_m, \hat{a}, y_r, w_d, t) - L_d\hat{d} \end{aligned}$$

Again this updated system still yields error dynamics of the form given by Equation (3.7) and satisfies Equation (3.5) upon redefining some variables. In this regard, defining a new parameter $a = [\theta, \rho, 0]^T$ and parameter estimation error $\tilde{a} = [\tilde{\theta}, \tilde{\rho}, \hat{d}]^T$ yields results analogous to those of Theorem 1 with $a^* = [\theta^*, \rho^*, 0]^T$. The condition given by Equation (3.5) is now satisfied with a redefined matrix $\Gamma^{-1} = diag(\Gamma_o^{-1}, \gamma_\rho^{-1}|b(t)|, \Gamma_d^{-1})$ and $L = diag(L_o, L_\rho, L_d)$, where $b(t) = 1/\rho$ is a scalar plant parameter of known and constant sign.

The only real issue added here is the dependence of Γ on the time varying parameter $b(t)$, which is part of the overall parameter $a = [\theta, 1/b, 0]^T$ since $b(t) = 1/\rho$. The inclusion of the time varying scalar $b(t)$ should affect the stability of the system, however, it turns out that this only affects the scalars c_1, c_2 in Theorem 1 if the following additional assumption is satisfied:

Assumption 3.3.1. *$b(t)$ is an unknown scalar function such that $b(t) \neq 0\ \forall t$, and sign of $b(t)$ is known and constant.*

Theorem 2 states the extended result below:

Theorem 2. *If there exits matrices* $P, \Gamma_o, \Gamma_d, \gamma_\rho, C > 0$ *such that (3.5) is satisfied for* $\dot{a} = d = 0$ *with* $\Gamma^{-1} = diag(\Gamma_o^{-1}, \gamma_\rho^{-1}|b(t)|, \Gamma_d^{-1})$ *and Assumption 3.2.1 is satisfied then the system given by Equation (3.7) with* $d, \dot{a} \neq 0$ *and* $L > 0$ *and diagonal is :*
(i) Uniformly internally exponentially stable and BIBS stable.
(ii) If Assumptions (3.1.1-3.1.3) are satisfied and $a^*(t)$ *is chosen as a piecewise continuous bounded vector then state* $x_c = [e_c, \tilde{a}]^T$ *is bounded with*

$$\|e_c(t)\| \leq c_1 \|x_c(t_o)\| e^{-\alpha(t-t_o)} + c_2 \int_{t_o}^{t} e^{\alpha(\tau - t)} \|v(\tau)\| \, d\tau$$

where c_1, c_2 *are constants,* $\alpha = \bar{\lambda}(diag(P^{-1}C, L))$, *and* $v = [P^{1/2}d, \Gamma^{-1/2}(L(a^* - a) - \dot{a})]^T$.

The proof of this result is found in the Appendix. Note that the extended proof is only needed if $b(t)$ is time varying, whereas the proof of Theorem 1 is sufficient for this case if b is constant.

3.4 Performance of the Control System

In this section, the tracking performance of the obtained control system is discussed. A key feature in the obtained result is the separation between the robust stability and robust performance control problems. Therefore, this section focuses solely on the robust performance problem.

3.4.1 Dynamic Response

Note that the bound obtained in Theorem 1, Equation (3.8), can be represented by a familiar linear-like response. First denote the norm of the input v by the signal $v_n(t) = \|v(t)\|$ and the laplace transform of this signal by $V_n(s)$ with s being the laplace variable then we have:

$$\|e_c\| \leq c_1 \|x_c(t_o)\| e^{-\alpha(t-t_o)} + c_2 \mathcal{L}^{-1}(H(s)V_n(s))$$

where $\mathcal{L}^{-1}$ is the inverse laplace transform and $H(s) = 1/(s+\alpha)$ is a first order stable filter with filter frequency α. The result follows from the fact the integral in Equation (3.8) is just a convolution.

Therefore, after decay of the zero-input response, which depends on the full vector $x_c(t_o)$ and not only the tracking error, the system's response is upper bounded by the response of a pre-specified low pass filter to the input v_n. Thus the response to step and impulse inputs is as expected for such a linear filter. However, in this case such inputs will not arise from disturbances but also from parameters and their variation. In particular, switches in parameters $a(t)$ yields step changes in a and impulses in $\dot{a}(t)$. The response of the system follows the response of filter $H(s)$ to such inputs. Furthermore, the system display the frequency response characteristics of such a filter such as in-bandwidth disturbance attenuation and more importantly the attenuation of high frequency inputs due to roll-off. These two properties are the essence of low and high frequency disturbance attenuation commonly used in linear control. Such simple practical features are rarely found in nonlinear and adaptive control designs nevertheless for an uncertain rapidly varying and switching system. As will be seen in Section 3.4, simulations of the system's response will follow these predictions and trends exactly.

3.4.2 Tracking Error

Since stability and dynamic response of the system have been established independent of uncertainty, the remaining design task is the optimization the control parameters and gains a^*, L, Γ, P, and C for minimal tracking error. This is the case as the obtained result provides a separation between the robust stability and robust performance control problems. The obtained dynamic bound on the size of tracking error, Equation (3.8), and its dependence on disturbances, parametric uncertainty and variation as well as chosen control gains and parameters yields clear guidelines for performance optimization. Different methods for improving tracking error are described below with reference to Equation (3.8):

1. *Increasing the system input-output gain* $\alpha = \underline{\lambda}(diag(P^{-1}C, L))$, which as discussed earlier, acts on the overall input uncertainty v. This attenuation, however, increases

the system bandwidth. This can be achieved by increasing the filter gain L and $P^{-1}C$, which corresponds to feedback gains.

2. *Increasing adaptation gain* Γ, which has the effect of attenuating parametric uncertainty and variation independent of system bandwidth (Recall that α is independent of Γ from Theorem 1). This is the case since the size of the input v is reduced by reducing the component $\Gamma^{-1/2}(L(a^* - a) - \dot{a})$. Note that a very large Γ has the effect of amplifying measurement noise and introducing excessive oscillations in the control, which can be seen from the adaptation law.

3. *Using a small gain* $\Gamma^{-1/2}L$, which has the effect of attenuating parametric uncertainty. This can be achieved by either increasing the adaptation gain matrix Γ or by reducing the size of L. This is the case since this condition implies having *approximate integral action* in the adaptation law of Equation (3.7), i.e., approaching integral action in the standard adaptation law.

4. *Adjusting and updating parameter estimate* a^* , which can be any piecewise continuous bounded function. This allows for reducing the effect of parametric uncertainty through reducing size of input $a^* - a$ independent of system bandwidth and control gains. This will be discussed in more detail in Chapter 5.

3.4.3 Remarks

- Exponential stability allows for shaping the transient response, e.g. settling time, and frequency response of the system to low/high frequency dynamics and inputs by adjusting the decay rate α, see Theorem 1. This is to be done independent of the parametric uncertainty $a^* - a$, which is contrasted to LTI feedback where closed loop poles change with parametric uncertainty.

- The attenuation of uncertainty by high input-output system gain in this scheme differs from robust control by the fact that BIBS stability, the pre-requisite to such attenuation, is never lost due to large parametric uncertainty $a^* - a$. This is the case since

parametric uncertainty no longer enters as a function of the plant's state but rather as an input $L(a^* - a)$.

- In switching between different a^* values many of the useful and interesting ideas to monitor, select, and switch between different candidate controllers via multiple models such as those in [1, 49] can be used with a_i^* values playing the role of the i^{th} candidate controller. The difference is that this is to be done without frozen-time instability or switched system instability concerns (verifying dwell time or common Lyapunov function conditions) as a^* is just an input to the closed loop system. Similarly, gain scheduling and Linear Parameter Varying (LPV) control [40, 62, 70] can be applied with a^* playing the role of the scheduled parameter vector to be varied, again with no concerns with instability and transient behavior since $a^* - a$ enter as an input to the system, see Chapter 5 for details.

- For control switches of a^*, the actual control signal is smooth, which is attractive for practical implementation. This is the case since a^* only enters in the adaptation law with $\dot{\hat{a}}$ piecewise continuous and thus $\hat{a}$ is continuous and the control signal is given by $u(t) = W(t)\hat{a}$ or equivalent.

3.5 Example

Consider the following unstable 2^{nd} order plant of relative degree 1 with a 2-mode periodic switching:

$$\begin{aligned} \dot{x}_1 &= a_1 x_1^3 + x_2 + (1 + x_1^2) b_1 u + d \\ \dot{x}_2 &= a_2 x_1 + (1 + x_1^2) b_2 u \\ y &= x_1 + n \end{aligned}$$

Where u, d, and n are control signal, disturbance, and measurement noise, respectively. Whereas, the plant parameters are given by:

$$\begin{aligned} a_1 &= 3 + 30\, square(2\pi\omega t) \quad , a_2 = -2 - 20\, square(2\pi\omega t) \\ b_1 &= 5 + \ square(2\pi\omega t) \quad , b_2 = 20 + 10\, square(2\pi\omega t) \end{aligned} \tag{3.9}$$

Where $square$ denotes the square function and ω is the plant switching frequency in Hz.

3.5.1 Control System Evaluation

The control design is based on the backstepping design procedure [33], which is modified along the lines of the developed methodology, see Chapter 5 for detailed design procedures. Let us choose the nominal gains $C = 100$ (feedback gain), adaptation filter gain $L = I$, where I is the identity matrix, then we have from Theorem 1 that the decay rate $\alpha = 1$ rad/sec. This should yield a settling time of at most 4 seconds for the closed loop system. Also the nominal value of the adaptation gain $\Gamma = 100I$ will be used. Whereas, a^* is chosen to be a constant vector a_{ave} taking the average values of the parameters in Equation (3.9), i.e., when square functions are set to zero.

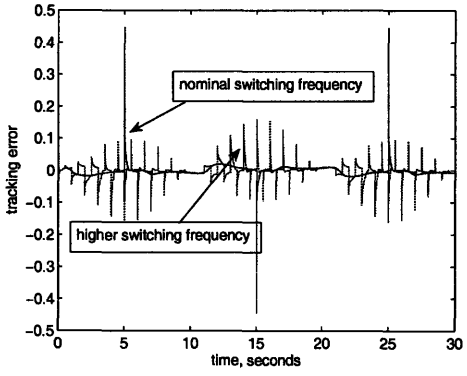

Figure 3-1: Tracking error for different plant switching frequencies for modified adaptive controller.

Figure 3-1 shows the response of the modified adaptive controller for the output of the plant tracking a sinusoidal reference of amplitude 2 and frequency 0.3 rad/sec; the

disturbance is set to zero for this case. The response follows the predicted theoretical behavior. The system responds to the corresponding impulse change in $\dot{a}$ and step change in a due to switching in plant parameter vector a with the error settling after exponentially decaying transient according to the system decay rate α. The figure displays exactly that at the plant switching times of 5, 15, an 25 seconds for the nominal switching frequency $\omega = 0.1\ Hz$, see Equation (3.9). The second case in the Figure 3-1 shows the effect of increasing plant switching frequency. The same trend follows with no concern of instability. In fact, as the developed theory suggests, plant parametric uncertainty and variation are inputs to the closed loop system. Therefore, increasing the frequency of this input, 6 rads/sec in this case, relative system bandwidth, 1 rads/sec, will lead to attenuation of this input due to system roll-off as in linear systems. This result is clearly displayed in the figure as the maximum tracking error is smaller for the faster switching case, without any other changes in plant or control parameter values.

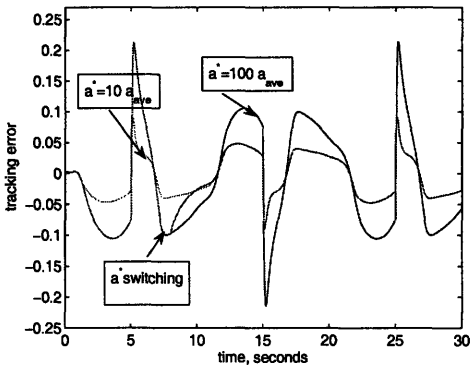

Figure 3-2: Effect of parameter estimate a^* on tracking error for modified adaptive controller.

Figure 3-2 shows the effect of different choices of the additional parameter estimate a^* for the nominal case of Figure 3-1. First, consider the case of a constant a^* where $a^* = 100\, a_{ave}$ and $a^* = 10\, a_{ave}$, where a_{ave} is the average parameter vector for parameters in Equation (3.9), i.e., when square functions are set to zero. The figure shows that the average tracking error is larger when $a^* = 100\, a_{ave}$, since it corresponds to a larger size of the input $a^* - a$, as predicted by Equation (3.8). Note that the average tracking error in

both cases is larger than that of the nominal case in Figure 3-1, which is due to the size of $a^* - a$. The third case in Figure 3-2 shows the effect of switching the choice of a^* starting from a $a^* = 100\, a_{ave}$ to $a^* = 10\, a_{ave}$ at $t = 8$ seconds. The response obviously matches that of the $a^* = 100\, a_{ave}$ case until controller switching of a^* takes place, which is followed by a quick transition to a response matching that of the $a^* = 10\, a_{ave}$ case. Note that the transition between these two response takes place within the estimated settling time of 4 seconds based on a designed for decay rate of $\alpha = 1$ rads/ sec. This case shows that upon switching to a better estimate of a the system will converge, within the estimated settling time, to an output corresponding to smaller tracking error. This is a key capability that can be utilized in practice to perform robust and stable gain scheduling and online controller adjustments, see Chapter 6 for details.

Figure 3-3 shows the tracking error for the nominal plant of Figure 3-1 when sinusoidal parameter variation is introduced. The plant parameters are given by:

$$\begin{aligned} a_1 &= 3 + 30\, square(2\pi\omega\, t) + 30\, sine(2\pi\, t) \\ a_2 &= -2 - 20\, square(2\pi\omega\, t) - 20\, sine(2\pi\, t) \\ b_1 &= 5 + \ square(2\pi\omega\, t) + 2\, sine(2\pi\, t) \\ b_2 &= 20 + 10\, square(2\pi\omega\, t) + 6\, sine(2\pi\, t) \end{aligned}$$

Where the nominal switching frequency of $\omega = 0.1$ Hz was used. The system displays the predicted response of the closed loop system responding to a sinusoidal input due to inputs $\dot{a}$ and $a^* - a$ with the tracking error remaining small.

Next, Figures 3-4-3-6 will include the addition of a sinusoidal disturbance $d = 50\sin(\pi\, t)$ to the nominal case discussed above for switching frequency $\omega = 0.1\ Hz$. Figure 3-4 displays the response of the nominal case of Figure 3-1 with the addition of a sinusoidal disturbance $d = 50\sin(\pi\, t)$, which introduces a clear sinusoidal content to the tracking error. Whereas, increasing feedback gain, which corresponds to the matrix C in Theorem 1, significantly reduces the tracking error due to both plant switching (jumps and other steady errors) and disturbances. This is consistent with the bound Equation (3.8) in that increasing system bandwidth α (via feedback gain) attenuates total input (disturbance an parametric

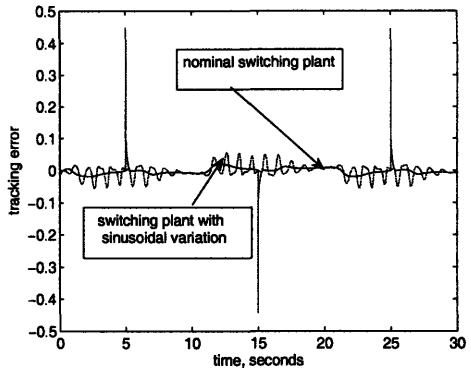

Figure 3-3: Effect of sinusoidal parameter variation on tracking error for modified adaptive controller.

uncertainties and variations) as well as increases the system bandwidth.

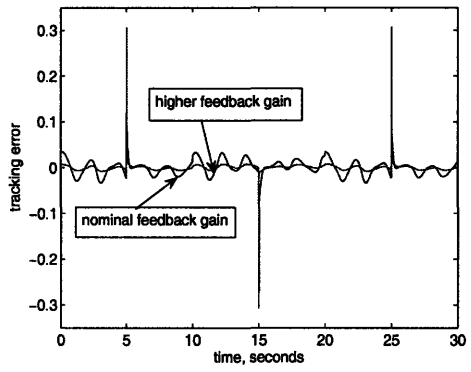

Figure 3-4: Effect of feedback gain on tracking error for modified adaptive controller.

Whereas, Figure 3-5 considers the same situation in Figure 3-4 but with increasing adaptation gain instead of feedback gain. Again similar performance improvements are achieved along the lines of Equation (3.8) yet without increasing system bandwidth. Finally Figure 3-6 shows the effect of introducing disturbance adaptation estimator $\hat{d}$, using the same gain magnitudes as for parameter estimators, $L_d = 1$ and $\Gamma_d = 100$. Although tracking error is reduced, The use of $\hat{d}$ reduces the disturbance effect on tracking error (the sinusoidal content in tracking error) yet is less effective than increasing feedback and adaptation gains in reducing the jump in tracking error due to plant switching. Similarly,

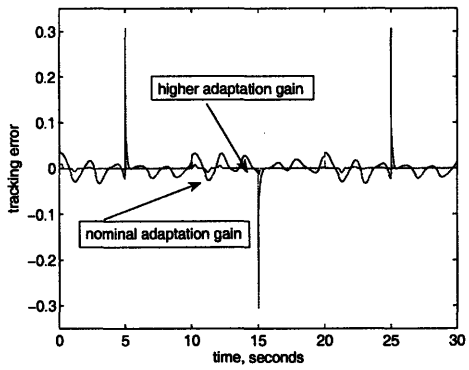

Figure 3-5: Effect of adaptation gain Γ on tracking error for modified adaptive controller.

increasing adaption gain Γ_d for the disturbance adaptation can improve tracking.

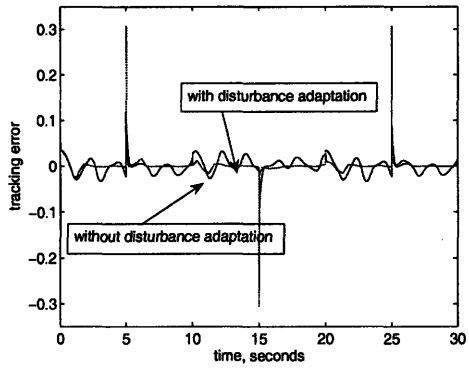

Figure 3-6: Effect of disturbance adaptation on tracking error for modified adaptive controller.

Figures 3-3-3-6 show that the tracking error can be reduced by adjusting a^*, increasing feedback and adaptation gains, as well as the use of an additional adaptation $\hat{d}$ with different levels of effectiveness relative to disturbances, parametric uncertainty, and variation. This allows adjustment and tuning of the respective control parameters to achieve desired performance given practical limitations such bandwidth, noise, and control effort. The important message from this case study is not only that the developed control methodology can successfully handel systems with large and rapid switching dynamics but also that this approach yields systematic and practical means to optimize performance, which follow the

developed theory.

3.5.2 Comparison with Other Techniques

Finally, let us compare the system's response with the developed adaptive controller to other control techniques. We consider the same system of Section 3.4 with switching frequency $\omega = 1$ Hz case. The system is required to follow a constant reference of amplitude 2. As mentioned earlier, the control design is based on the backstepping design procedure [33]. First consider a non-adaptive backstepping controller, where the parameter estimate $\hat{a}$, in the developed control scheme of Section 3.4.1 is replaced with a fixed value $\hat{a} = a_{ave}$, which is the same value chosen for the vector a^* in Section 3.4.1. Recall that a_{ave} uses the average values of the parameters in Equation (3.9), which is a reasonable choice for a nominal guess of the plant parameters. Figure 3-7 shows that the non-adaptive controller yields an unstable closed loop despite using the same assumed value of plant parameter vector, which has been used by the modified adaptive controller with $a^* = a_{ave}$. This is seen where the tracking is zero since $a = a_{ave}$ until switching starts due to the square function in Equation (3.9), where the tracking error grows unbounded.

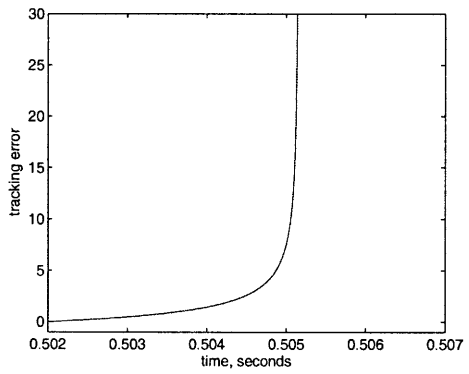

Figure 3-7: Tracking error for non-adaptive backstepping controller with $\hat{a} = a_{ave}$.

Next, Figure 3-8 shows the response of the parameter estimates $\hat{a}$, when the equivalent standard adaptive controller, Equation (3.3), is used. This corresponds to setting $L = 0$ in the modified adaptive controller of Equation (3.6). In this case, some of the parameter

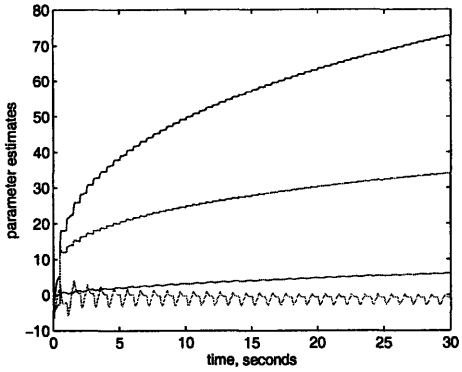

Figure 3-8: Parameter estimates $\hat{a}$ for standard adaptive controller.

estimates $\hat{a}$ grow unbounded, which could yield an unstable system in practical implementation. This is a known issue with standard adaptive control in the presence of parameter variations or even disturbances, which is usually referred to as parameter drift [69, 27]. In contrast, the modified adaptive controller for the same situation maintains bounded parameter estimates due to BIBS stability of the closed loop, see Figure 3-9.

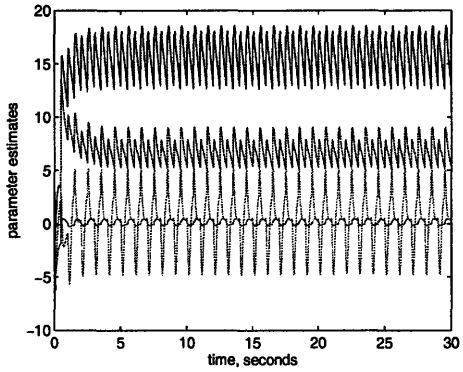

Figure 3-9: Parameter estimates $\hat{a}$ for modified adaptive controller.

The poor robustness of standard adaptive controllers with respect to time varying parameters and disturbances has lead to modifying the adaptation law by robust adaptation laws such as deadzone, projection, and leakage modifications [27]. Although there have not been any results reporting guaranteed stability and performance characteristics for rapidly varying switching systems using these techniques, we will compare the leakage-based mod-

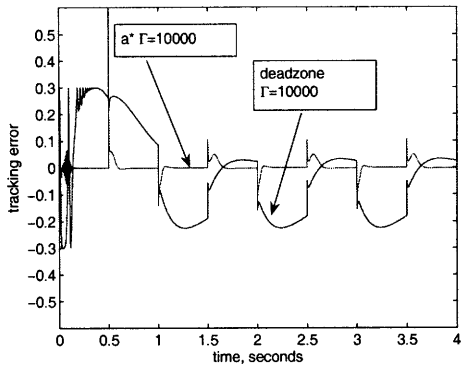

Figure 3-10: Tracking error comparison for modified adaptive controller and a deadzone adaptive controller.

ification developed in this thesis with deadzone and projection modifications.

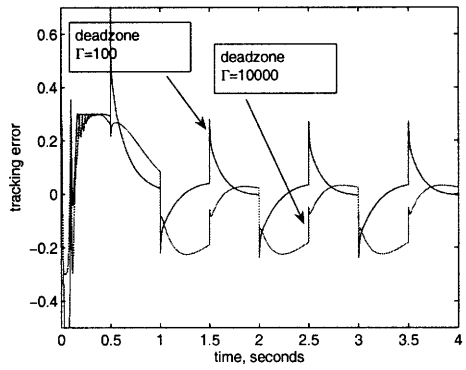

Figure 3-11: Effect of adaptation gain Γ on tracking error for deadzone adaptive controller.

A deadzone modification to the standard adaptation law of Equation (3.3) can be given by:

$$\dot{\hat{a}} = \begin{cases} f_a(x_m, \hat{a}, y_r, t) & \text{if } \|e\| > \epsilon \\ 0 & \text{otherwise} \end{cases}$$

This simply means to turn off the adaptation when the tracking error is less than some acceptable threshold ϵ. Figure 3-10 compares the modified adaptive controller with $a^* =$

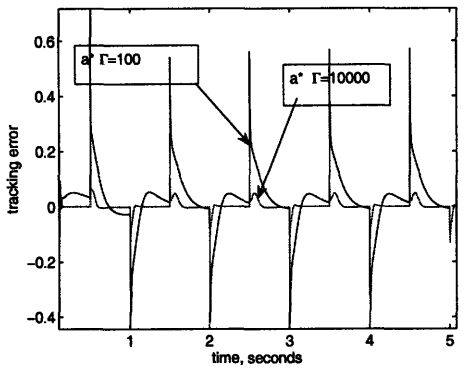

Figure 3-12: Effect of adaptation gain Γ on tracking error for modified adaptive controller.

a_{ave} to an equivalent deadzone adaptive controller with the same adaptation gain $\Gamma = 10000I$, where I is the identity matrix, and a deadzone threshold of $\epsilon = 0.3$. In this case, the modified adaptive controller outperforms the deadzone adaptive controller in the tracking error. Furthermore, when attempting to reduce the size of the tracking error threshold for the deadzone, ϵ, to allow for improvement in tracking error, the parameter estimates grew unboundedly as in the standard adaptive controller case of Figure 3-8. This is expected as the deadzone adaptive controller approaches that of a standard adaptive controller as $\epsilon \rightarrow 0$. Another limitation to the deadzone controller is the lack of systematic dependence on control parameters such as the adaptation gain Γ unlike the modified adaptive controller. Figure 3-11 shows how increasing the adaptation gain from $\Gamma = 100I$ to $\Gamma = 10000I$ does not necessarily improve tracking but rather yields reduction and increase in tracking at different times and of different signs. This is contrasted with the modified adaptive controller when tested under the same conditions, Figure 3-12, where a clear reduction in tracking error is observed with increasing Γ, in accordance with the scaling relationship in Equation (3.8).

Next, we consider a parameter projection modification to the standard adaptive controller of Equation (3.3). The projection modification [27] used here is given by:

$$\dot{\hat{a}} = \begin{cases} f_a & \text{if } \|\hat{a}\| \leq M \text{ or } \hat{a}^T f_a \leq 0 \\ f_a - \frac{\hat{a}\,\hat{a}^T}{\|\hat{a}\|^2}\left(\frac{\|\hat{a}\|^2 - M^2}{M^2}\right) f_a & \text{otherwise} \end{cases}$$

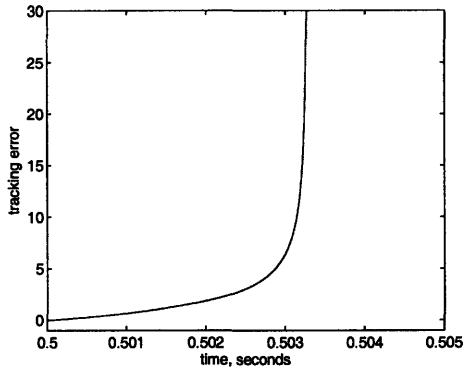

Figure 3-13: Tracking error for projection adaptive controller with small parameter bound $M = 1$.

Which uses an assumed bound on parameters $\|a\| \leq M$. This assumption is critical to projection algorithms. Figure 3-13 shows the tracking error growing unbounded when a projection algorithm was implemented with a tight bound $M = 1$. In this case, the assumed bound on parameters was too tight as soon as the system switched to a different mode leading to instability. This is in contrast to the developed adaptive controller, which does not require such information to guarantee stability. This is the case as the assumed parameter vector a^* only affects the size of tracking error for a given choice of control gains.

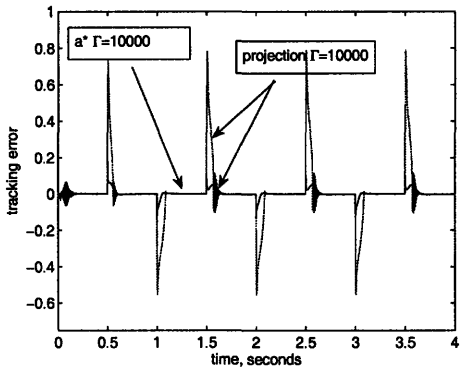

Figure 3-14: Tracking error comparison for modified adaptive controller and a projection adaptive controller.

Nevertheless, it was possible to obtain a choice for the projection bound, $M = 10$,

where the system remained stable. Figure 3-14 compares the tracking error for this projection adaptive controller and the developed adaptive controller with $a^* = a_{ave}$ for the same adaptation gain. Again, the developed adaptive controller achieved smaller tracking error. As was the case with deadzone controller, the projection controller does not display the systematic dependence on the adaptation gain Γ unlike the proposed adaptive controller, see Figure 3-15.

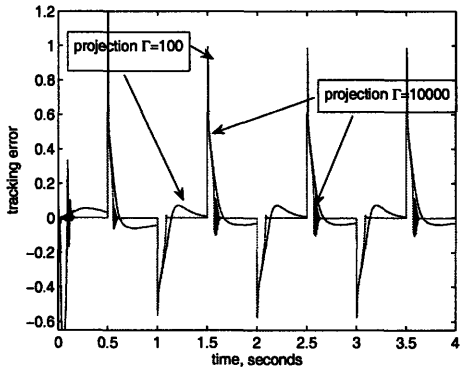

Figure 3-15: Effect of adaptation gain Γ on tracking error for projection adaptive controller.

This section demonstrates and highlights the advantages of using the developed technique over various other adaptive and non-adaptive techniques. In addition to the fact that the proven stability characteristics of Theorem 1 have yet to be proven for any other method, the developed controller demonstrated superior performance and practical usability relative to the tested methods based on the performed simulations. Instability of the system was observed with the other techniques for situations where the developed controller maintained system stability as proven without the need for a priori bounds on system parameters. Furthermore, when the other adaptive techniques were able to maintain system stability, the tracking error was smaller with the developed technique. This, however, does not suggest that the tracking error with these other techniques will always be larger since there is no proof of such a claim. More importantly, it was shown that the developed adaptive controller follows the provided design guidelines for optimizing performance according to Equation (3.8) and the corresponding discussion of Section 3.3.2. Whereas, projection and deadzone adaptive controllers did not display a clear performance

improvement with increasing adaptation gain Γ in the performed simulations. This is the case since both projection and deadzone modification do not achieve a clear bound due to BIBS stability as that in Equation (3.8). In fact, most results using such techniques to deal with disturbances or parameter variations only conclude boundedness. In this case, such a conclusion is of very little practical importance if the error can not be reduced to an acceptable level by increasing the adaptation gain or using a better nominal estimate of the plant parameters as with using a^* in the proposed adaptation law, see Figure 3-2. In fact, the use of a^* to utilize available information for performance optimization is not possible in other adaptive control techniques such as projection or deadzone controllers.

3.6 Summary

This chapter presents a control methodology for stable robust adaptive control of time-varying switched nonlinear systems. The control scheme guarantees system stability for systems with piecewise differentiable bounded parameters and piecewise continuous bounded disturbances without requiring a priori knowledge on such parameters or disturbances. A leakage-type adaptive control modification is shown to achieve internal exponential and BIBS stability without need for persistence of excitation. The effect of plant variation and switching is reduced to piecewise continuous and impulsive inputs acting on this BIBS stable closed loop system. The developed methodology provides clear guidelines for steady-sate and transient performance optimization. The results are demonstrated through example simulations, which follow the developed theory. In the simulations, the proposed controller demonstrated superior robustness of stability and performance as well as practical usability relative to non-adaptive and other adaptive methods such as projection and deadzone adaptive controllers.

Chapter 4

Design for Systems in Companion Form

4.1 Introduction

This chapter is concerned with control of systems in the MIMO companion form. The developed methodology of Chapter 3 is applied to these systems yielding a detailed design procedure. The results are illustrated through a case study for contact-based manipulation via a 2-link planar manipulator.

Consider m-input-m-output systems in the MIMO companion form given below:

$$y^{(r)} = f(x,t) + B(x,t)u + d \tag{4.1}$$

where the output $y = [y_1, \ldots, y_m]^T \in \mathbb{R}^m$, $y^{(r)} = [y_1^{(r_1)}, \ldots, y_m^{(r_m)}]^T \in \mathbb{R}^m$ is a vector consisting of the ri^{th} derivative of each output with $r = \sum_i^m r_i$ is the relative degree index for the vector relative degree $[r_1, \ldots, r_m]^T$ of the system. The vector $x = [y_1, \ldots, y^{(r_1-1)}, \ldots, y_m, \ldots, y_m^{(r_m-1)}]^T \in \mathbb{R}^r$. Whereas, $u \in \mathbb{R}^m$ is the control input and $d \in \mathbb{R}^m$ is the disturbances. The adaptive control literature contains various results on adaptive control of MIMO systems in companion form when parameters are constant, see [68, 69, 7, 82, 76] and references therein. Adaptive control of time varying robotic and mechanical systems in MIMO companion form has been developed in [73, 55, 72] based on the procedure in [69]. However, these results are all restricted to smoothly varying parameters and assume a priori known bounds on parameters, in addition to their varia-

tions in some cases, in order to perform projection or a time expansion-based estimation to guarantee bundedness of the system.

The basic assumptions for this class of systems are given below:

Assumption 4.1.1. *The vector relative degree* $[r_1, \ldots, r_m]^T$ *of the system given by Equation (4.1) is a well defined and known constant vector.*

Assumption 4.1.2. *The vector*
$x = [y_1, \ldots, y^{(r_1-1)}, \ldots, y_m, \ldots, y_m^{(r_m-1)}]^T \in \mathbb{R}^r$ *is measured.*

Assumption 4.1.3. *The zero dynamics associated with the system given by Equation (4.1) is uniformly exponentially stable.*

Assumption 4.1.4. *The reference trajectory* $y_d = [y_{d1}, \ldots, y_{dm}]^T$ *and its first* r *derivatives* $y_d^{(1)} = [y_{d1}^{(1)}, \ldots, y_{dm}^{(1)}]^T$, ..., $y_d^{(r)} = [y_{d1}^{(r_1)}, \ldots, y_{dm}^{(r_m)}]^T$ *are known, bounded and, piecewise continuous.*

Assumption 4.1.5. $d \in \mathbb{R}^n$ *is uniformly bounded and piecewise continuous.*

Two different design procedures are presented based on different assumptions on the input matrix $B(x,t)$, which are presented next. The procedure is based on creating a filtered version of the actual tracking error to create first order equivalent subsystems [68, 69, 82]. Let the tracking error variable $s_i = (d/dt + \lambda_i)^{r_i-1}\tilde{y}_i$ where scalars $\lambda_i > 0$, $s = [s_1, \ldots, s_m]^T$, $\tilde{y}_i = y_i - y_{di}$ is the unfiltered tracking error for a desired reference $y_{di}(t)$. We will also use the notation $\tilde{y} = [\tilde{y}_1, \ldots, \tilde{y}_m]^T$ and $y_d = [y_{d1}, \ldots, y_{dm}]^T$. Denote by $v_i = y_i^{(r_i)} - \dot{s}_i$ and $v = [v_1, \ldots, v_m]^T$. Note that $v = f(x, y_d, y_d^{(1)}, \ldots, y_d^{(r)})$ only, which are all available signals.

4.2 Design Method I

The first design procedure is presented in this section with the additional assumptions for the design are given by:

Assumption 4.2.1. *The input matrix is given by* $B(x,t) = b(t)M^{-1}(x,t)\,\beta(x)$, *where:*
- $M(x,t) \in \mathbb{R}^{m\times m}$ *is an unknown bounded symmetric positive definite matrix,* $M(x,t) > 0$

and $\|M(x,t\| \leq c$ *for some constant c.*

-$\beta(x) \in \mathbb{R}^{m \times m}$ *is a known nonsingular square matrix in* x*.*

- $b(t)$ *is an unknown scalar function such that* $b(t) \neq 0 \; \forall \, t$*, and sign of* $b(t)$ *is known and constant.*

Assumption 4.2.2. *The scalar parameter* $b(t) \neq 0 \; \forall \, t$ *is piecewise differentiable bounded with finite discontinuities in finite time.*

Assumption 4.2.3. $Mf(x,t) + Mv(t) + \frac{1}{2}\dot{M}s(t) = -W(x,t)\theta + Gs$ *where* θ *is piecewise differentiable bounded with finite discontinuities in finite time,* $W(x,t)$ *is a matrix of known functions, and* G *is skew-symmetric* $s^T G s = 0$*.*

Then based on the assumptions we have:

$$\begin{aligned} y^{(r)} &= f(x,t) + b(t)M^{-1}(x,t)\,\beta(x)u + d \\ My^{(r)} &= Mf(x,t) + b(t)\beta(x)u + Md \\ M\dot{s} &= Mv(t) + Mf(x,t) + b(t)\beta(x)u + Md \end{aligned}$$

Using a design procedure based on that in [69], the control and adaptation law are given by:

$$\begin{aligned} u &= \hat{\rho}\beta(x)^{-1}u_d \\ \dot{\hat{\theta}} &= -\Gamma_o W^T s - L_o(\hat{\theta} - \theta^*) \\ \dot{\hat{\rho}} &= -\gamma sign(b) s^T u_d - L_\rho(\hat{\rho} - \rho^*) \\ \dot{\hat{d}} &= -\Gamma_d W_d\, s - L_d \hat{d} \end{aligned} \tag{4.2}$$

where

$$\begin{aligned} u_d &= -Ks + W\hat{\theta} + W_d^T \hat{d} \\ W\theta &= -Mf - Mv - \frac{1}{2}\dot{M}s + Gs \end{aligned}$$

Where the diagonal matrixes $\Gamma_o, \Gamma_d > 0$ and scalar $\gamma_\rho > 0$ are adaptation gains and diagonal matrix $K > 0$ is the control gain matrix. Adaptation filter gains are the diagonal matrices $L_o, L_d > 0$ and scalar $L_\rho > 0$. The matrix $w_d \in R^{l \times m}$ for $\hat{d} \in R^l$ and $u \in R^m$

is assumed internal model of disturbance, e.g., a sinusoidal function. If no assumed disturbance content is available then W_d^T is just a truncated identity matrix such that $W_d^T \hat{d}$ is replace by $\hat{d}$. If no disturbance adaptation is used then $W_d = 0$ and the update law for $\hat{d}$ is removed.

Denote the vector $\hat{a} = [\hat{\theta}^T, \hat{\rho}, \hat{d}]$, which is an estimate of the total parameter vector $a = [\theta^T, \rho, 0]^T$, where $\rho = 1/b$ and the disturbance adaptation parameter $\hat{d}$ is augmented in $\hat{a}$ with an assumed nominal value of 0 with $a = [\theta^T, \rho, 0]^T$. Also denote by $e_c = s$ and $C = K$ for this design method. where $\Gamma^{-1} = diag(\Gamma_o^{-1}, \gamma_\rho^{-1}|b|, \Gamma_d^{-1})$ and $L = diag(L_o, L_\rho, L_d)$. Then the closed loop error dynamics is given by:

$$
\begin{aligned}
M\dot{e}_c &= -Ke_c + W\tilde{\theta} - \frac{1}{2}\dot{M}e_c + Ge_c + b\tilde{\rho}u_d + W_d^T\hat{d} + Md \\
\dot{\tilde{a}} &= \begin{bmatrix} -\Gamma_o W^T e_c - L_o(\hat{\theta} - \theta^*) - \dot{\theta} \\ -\gamma_\rho sign(b) e_c^T u_d - L_\rho(\hat{\rho} - \rho^*) - \dot{\rho} \\ -\Gamma_d W_d e_c - L_d\hat{d} \end{bmatrix}
\end{aligned}
$$

Where $\tilde{a} = [\tilde{\theta}, \tilde{\rho}, \hat{d}]$. Theorem 3 below establishes the properties of the controlled system, see Appendix for proof.

Theorem 3. *If the system given by Equation (4.1) satisfies the assumptions (4.0.1-4.0.5) and (4.1.1-4.1.3) then the adaptive feedback control given by Equation (4.2) yields:*
(i) Uniformly internally exponentially stable and BIBS stable system with state $x_c = [e_c, \tilde{a}]^T$.
(ii) state $x_c = [e_c, \tilde{a}]^T$ *is bounded with*
$\|y - y_r\| \leq \epsilon[c_1\|x_c(t_o)\|e^{-\alpha(t-t_o)} + c_2\int_{t_o}^{t} e^{\alpha(\tau-t)}\|v(\tau)\|\, d\tau]$. *where* c_1, c_2, ϵ *are constants,* $\alpha = \underline{\lambda}(diag(M^{-1}K, L))$, *and* $v = [M^{3/2}d, \Gamma^{-1/2}(L(a^* - a) - \dot{a})]^T$.

The assumptions on the input matrix $B(x,t)$ are used to yield a form directly generalizing the SISO companion form given below:

$$
y^{(r)} = -W(x)^T\theta + b\beta(x)u + d \tag{4.3}
$$

where $\beta(x)$ and $W(x) = [w_1(x), w_2(x), \ldots, w_m(x)]$ are known functions with $M(x,t) = 1$ in MIMO form. Therefore, the results presented earlier apply directly to systems in SISO

companion form above. The next section, presents another design based on a different set of assumptions on the input matrix $B(x,t)$.

4.3 Design Method II

This section presents an alternative design procedure with the additional assumptions for the design are given by:

Assumption 4.3.1. *The input matrix is given by* $B(x,t) = M(x,t)^{-1}T(x,t)$, *where*
-$M(x,t) \in \mathbb{R}^{m\times m}$ *is an unknown bounded symmetric positive definite matrix ,* $M(x,t) >$ *and* $\|M(x,t\| \leq c$ *for some unknown constant c.*
-$T(x,t) \in \mathbb{R}^{m\times m}$ *is an unknown unity upper triangular matrix.*

Assumption 4.3.2. $Mf(x,t) + Mv(t) + \frac{1}{2}\dot{M}s + (T(x,t) - I)u = -W(x,t)\theta + Gs$ *where* θ *is piecewise differentiable bounded with finite discontinuities in finite time,* $W(x,t)$ *is a matrix of known functions, and G is skew-symmetric* $s^T Gs = 0$.

Then based on the assumptions we have:

$$\begin{aligned} y^{(r)} &= f(x,t) + b(t)M(x,t)^{-1}T(x,t)u + d \\ My^{(r)} &= Mf(x,t) + (T(x,t) - I)u + Md + u \\ M\dot{s} &= Mv(t) + Mf(x,t) + (T(x,t) - I)u + Md + u \end{aligned}$$

Using the design procedure in [69], the control and adaptation law are given by:

$$\begin{aligned} u &= -Ks + W\hat{\theta} + W_d^T\hat{d} \\ \dot{\hat{\theta}} &= -\Gamma_o W^T s - L_o(\hat{\theta} - \theta^*) \\ \dot{\hat{d}} &= -\Gamma_d W_d s - L_d\hat{d} \end{aligned} \tag{4.4}$$

where

$$W\theta = -Mf - Mv - \frac{1}{2}\dot{M}s - (T - I)u + Gs$$

where the diagonal matrixes $\Gamma_o, \Gamma_d > 0$ are adaptation gains and diagonal matrix $K > 0$

is the control gain matrix. Adaptation filter gains are diagonal matrices L_o, L_d. The matrix $w_d \in R^{l \times m}$, for $\hat{d} \in R^l$ and $u \in R^m$, contains an assumed internal model of disturbance, e.g., a sinusoidal function. If no assumed disturbance content is available then W_d^T is just a truncated identity matrix such that $W_d^T \hat{d}$ is replaced by $\hat{d}$. If no disturbance adaptation is used then $W_d = 0$ and the update law for $\hat{d}$ is removed.

Denote the vector $\hat{a} = [\hat{\theta}^T, \hat{d}]^T$, which is an estimate of the total parameter vector $a = [\theta^T, 0]^T$, where the disturbance adaptation parameter $\hat{d}$ is augmented in a with an assumed nominal value of 0 with $a = [\theta^T, \rho, 0]^T$. Also denote by $e_c = s$ and $C = K$ for this design method. where $\Gamma^{-1} = diag(\Gamma_o^{-1}, \Gamma_d^{-1})$ and $L = diag(L_o, L_d)$. Then the closed loop error dynamics is given by:

$$
\begin{aligned}
M\dot{e}_c &= -Ke_c + W\tilde{\theta} - \frac{1}{2}\dot{M}e_c + Ge_c + W_d^T\hat{d} + Md \\
\dot{\tilde{a}} &= \begin{bmatrix} -\Gamma_o W^T e_c - L_o(\hat{\theta} - \theta^*) - \dot{\theta} \\ -\Gamma_d W_d e_c - L_d\hat{d} \end{bmatrix}
\end{aligned}
$$

where $\tilde{a} = [\tilde{\theta}^T, \hat{d}]^T$. Next, Theorem 4 establishes the properties of the controlled system, see Appendix for proof.

Theorem 4. *If the system given by Equation (4.1) satisfies the assumptions (4.0.1-4.0.5) and (4.2.1-4.2.2) then the adaptive feedback control given by Equation (4.4) yields:*
(i) Uniformly internally exponentially stable and BIBS stable system with state $x_c = [e_c, \tilde{a}]^T$.
(ii) state $x_c = [e_c, \tilde{a}]^T$ *is bounded with*
$\|y - y_r\| \leq \epsilon[c_1\|x_c(t_o)\|e^{-\alpha(t-t_o)} + c_2\int_{t_o}^{t} e^{\alpha(\tau-t)}\|v(\tau)\|\, d\tau]$. *where* c_1, c_2, ϵ *are constants,* $\alpha = \underline{\lambda}(diag(M^{-1}K, L))$, *and* $v = [M^{3/2}d, \Gamma^{-1/2}(L(a^* - a) - \dot{a})]^T$.

4.3.1 Remarks

This section provides some remarks on the design results.

- In order to transform a system to companion form, one may simply successfully differentiate the output y until the control input u appears, see [69, 30] for further discussions on the procedure and conditions for transforming systems into this form.

- Note that the disturbance "d" is not the only possible disturbance in the system but it is the only term that appears as a true input to the dynamics of Equation (4.1). This means that disturbances may appear in the companion form as multiplied by state dependent terms, in which case they are lumped into the time varying parameter θ.

- The assumptions for the input matrix in design II are analogous to those in [82] with constant parameters. In particular, a non-symmetric positive definite matrix is factored into a symmetric positive definite matrix and a unity upper triangular matrix, which is always possible for such a matrix. Note that matrix $T(x,t) - I$ is strictly upper triangular and thus there are no algebraic loops, which is along the lines of the factorizations used in [82, 26].

- The assumption on the reference y_d can be circumvented by using y_d as an output of an r^{th} order low pass filter driven by any bounded piecewise continuous reference.

4.4 Application to Robotic Manipulation

4.4.1 Design for Time-Varying Robotic Manipulators

Consider the rigid body dynamics of time varying robotic manipulators :

$$H(q,t)\ddot{q} + \frac{\partial H(q,t)}{\partial t}\dot{q} + C(q,\dot{q},t)\dot{q} + D(\dot{q},t)\dot{q} + G(q,t) = \tau + d(t) + J^T(q)F(q,\dot{q},t)$$

Where H is the inertia matrix, C is Coriolis matrix, D is damping, G is is gravitation forces, J is the kinematic Jacobian, and F are end effector forces, and τ are motor torques. The following properties are known about such systems:

- $H(q,t)$ is positive definite and uniformly bounded for bounded parameters.

- The matrix $\dot{H} - 2C - \partial H(q,t)/\partial t$ is skew symmetric.

- The following parametrization can be obtained:

$$H(q,t)\ddot{q} + \frac{\partial H(q,t)}{\partial t}\dot{q} + C(q,\dot{q},t)\dot{q} + D(\dot{q},t)\dot{q} + G(q,t)$$
$$= Y(q,\dot{q},\ddot{q})\theta(t)$$

The following assumption is made:

Assumption 4.4.1. *The following parametrization can be obtained* $Y(q,\dot{q},\ddot{q})\theta(t) + J^T(q)F(q,\dot{q},t) = W(q,\dot{q},\ddot{q})a(t)$, *where* $a(t)$ *is a bounded piecewise differentiable vector.*

This simply states that the additional term of end effector torques $J^T F$ can be also linearly parameterized and that the overall parameter vector a is bounded and piecewise differentiable. Note that boundedness of a enforces that parameters in inertia matrix H are continuous but not necessarily smooth, as their derivatives appear in a and thus would otherwise yield unbounded elements of parameter vector a. However, the derivatives of inertial parameters are allowed to be piecewise continuous.

The joint torques are generated using the full state feedback $\tau(q,\dot{q})$. The design is based on the procedure developed in in [69] for the time-invariant case. Let $\tilde{q} = q - q_d$, where $q_d(t)$ is the desired trajectory and use the composite variable $s = \dot{\tilde{q}} + \Lambda\tilde{q} = \dot{q} - \dot{q}_r$, where Λ is a positive definite matrix. Now use the control law:

$$\begin{aligned}
\tau(q,\dot{q},t) &= -Ks + W(q,\dot{q},\dot{q}_r,\ddot{q}_r)\hat{a} + W_d^T\hat{d} \\
W(q,\dot{q},\dot{q}_r,\ddot{q}_r)\hat{a} &= \hat{H}\ddot{q}_r + \hat{C}\dot{q}_r + \hat{G} + \hat{D}\dot{q} \\
&\quad + \frac{1}{2}\frac{\partial \hat{H}}{\partial t}(\dot{q} + \dot{q}_r) + \hat{J}^T(q)\hat{F}(q,\dot{q},t)
\end{aligned}$$

where K is a positive definite gain matrix and using the update laws:

$$\begin{aligned}
\dot{\hat{a}} &= -\Gamma_o W^T s - L_o(\hat{a} - a^*) \\
\dot{\hat{d}} &= -\Gamma_d W_d s - L_d\hat{d}
\end{aligned}$$

The closed loop dynamics can be reduced to :

$$H\dot{s} + Cs + Ks + \frac{1}{2}\frac{\partial H}{\partial t}s = W\tilde{a} + W_d^T\hat{d} + d$$

The system follows the results of Sections 4.1 and 4.2 with $H = M$ and $G = 1/2(\dot{H} - 2C - \partial H(q,t)/\partial t)$ and either design method with $b(t) = 1$ and $B(x) = I$ or $T(x,t) = I$, where I is the identity matrix.

4.4.2 Control of a 2-link Planar Manipulator with Contact

Consider the rigid body dynamics of robotic manipulators :

$$H(q)\ddot{q} + C(q,\dot{q})\dot{q} + G(q) = \tau + d(t) + J^T(q)F(q,t)$$

The following end effector force is considered for contact with a compliant environment:

$$F(q,t) = K_s(t)x + f(t)$$

where x is the end effector position, $K_s = diag(k_{1s}, k_{2s})$ is a diagonal piecewise continuous stiffness matrix and $f_e = [f_1, f_2]^T$ is a piecewise continuous vector of contact forces due to contact position changes and other factors. For a 2-link planar manipulator we have:

$$x = \begin{bmatrix} l_1 c_1 + l_2 c_{12} \\ l_1 s_1 + l_2 s_{12} \end{bmatrix} \quad J = \begin{bmatrix} -l_1 s_1 - l_2 s_{12} & -l_2 s_{12} \\ l_1 c_1 + l_2 c_{12} & l_2 c_{12} \end{bmatrix}$$

where $x = [x_1, x_2]$ is the task space coordinates, l_1, l_2 are link lengths and $c_1 = \cos(q_1)$, $s_1 = \sin(q_1)$, $c_{12} = \cos(q_1 + q_2)$, and $s_{12} = \sin(q_1 + q_2)$. The design is based on the procedure developed in in [69] for the time-invariant case with no contact, which is a special case of the designs in Sections 4.1 and 4.2. The system follows the results of Sections 4.1 and 4.2 with $H = M$ and $G = 1/2(\dot{H} - 2C)$ and either design method with $b(t) = 1$ and $B(x) = I$ or $T(x,t) = I$, where I is the identity matrix.

Consider the modified adaptive controller for a 2-link planar manipulator. The contact

stiffness matrix and forces for the case study under consideration are given by:

$$k_{1s} = \begin{cases} 200 & \text{if } x_2 > 1.5 \\ 0 & \text{otherwise} \end{cases}$$

$$k_{2s} = \begin{cases} 100 & \text{if } x_2 > 1.5 \\ 0 & \text{otherwise} \end{cases}$$

$$f_1 = \begin{cases} 10 & \text{if } x_2 > 1.5 \\ 0 & \text{otherwise} \end{cases}$$

$$f_2 = \begin{cases} 100 & \text{if } x_2 > 1.5 \\ 0 & \text{otherwise} \end{cases}$$

which is a reasonable model representing contact and loss of contact upon reaching the threshold position $x_2 > 1.5$. We will denote the plant parameter vector by:

$$a = \begin{cases} a_2 & \text{if } x_2 > 1.5 \\ a_1 & \text{otherwise} \end{cases}$$

This means $a = a_1$ denotes the non-contact parameter vector, which corresponds to $k_{1s} = k_{2s} = f_1 = f_2 = 0$.

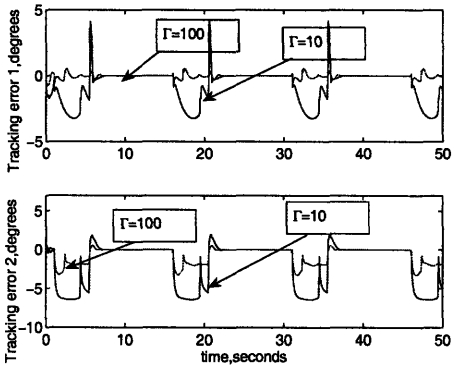

Figure 4-1: Joint tracking errors for different adaptation gain values Γ for modified adaptive controller.

Figure 4-1 simulates the joint tracking tracking error with a reference trajectory of a 2^{nd} order filtered pulse signal of period 15 seconds and width of 5 seconds. The amplitudes of 1 radians and 0.5 radians are used for joints 1 and 2, respectively. The figure displays the expected response to plant switching with jumps at the switching times, due to step changes in parameter vector a and impulse changes in $\dot{a}$. In this case, $a^* = a_1$ and thus zero tracking error is displayed during the intervals where no contact is made, i.e., $a = a_1$, which follows the prediction of the bound in Theorem 3 (or Theorem 4). This is the case since $a^* = a$ during these intervals and thus the exponentially stable closed loop system is unforced. However, relatively large error is seen when contact is established due to change in plant parameters. Increasing the adaptation gain Γ from the nominal value of 10 to 100 displays the same trends but with smaller tracking error during contact as well as during transitions between in-contact and non-contact dynamics.

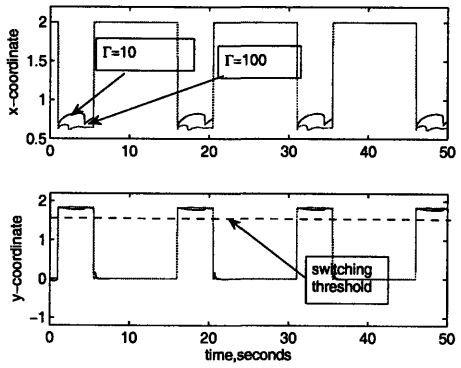

Figure 4-2: Task space coordinates for different adaptation gain values Γ for modified adaptive controller.

Whereas, Figure 4-2 shows the task space coordinates for the scenarios discussed in Figure 4-1. The figure displays the switching threshold of $x_2 = 1.5$, where switching occurs as the system's response crosses this line, which occurs seven times during the displayed time interval. Observe how the jumps in Figure 4-1 coincide with the points where the y-coordinate in the task space crosses this contact switching threshold.

Figure 4-3 shows the joint tracking error in the presence of a sinusoidal disturbance $d_1 = 100\sin(0.3\,t)$ at joint 1 and $d_2 = 50\sin(0.1\,t)$ at joint 2. The tracking error increases

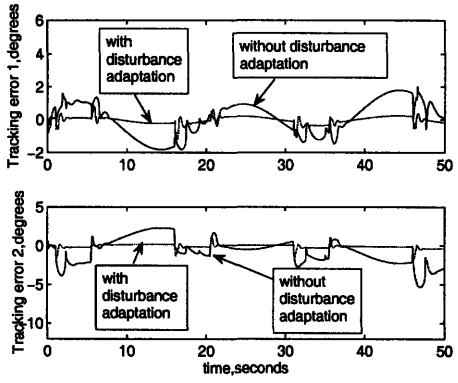

Figure 4-3: Effect of disturbance adaptation on Joint tracking errors for modified adaptive controller.

relative to that of the disturbance free case of Figure 4-1 with a clear sinusoidal content. However, with the addition of a disturbance adaptation vector $\hat{d}$, the tracking error is reduced. This suggests the usefulness of this additional control features, which does not use an prior information about the disturbance content in this case, with $W_d = I$, where I is the identity matrix. Furthermore, if W_d were set to contain a priori information about the sinusoidal content of the disturbance then further performance improvement would be observed as suggested by the well known internal model principle.

4.5 Summary

In this chapter, a detailed robust adaptive control scheme has been presented for linearly-parameterized switched systems in MIMO companion form. The design is based on conventional constructions for such systems with modifications following the developed methodology of Chapter 3. Two different designs have been presented depending on different assumptions on the input matrix. The results have been used to develop controllers for time varying robotic manipulators and are illustrated through a case study for contact-based manipulation via a 2-link planar manipulator.

Chapter 5

Design for Systems in Parametric-Strict Forms

5.1 Introduction

In this chapter, the developed methodology of Chapter 3 is applied to systems in parametric-strict form and parametric-strict output form yielding detailed design procedures. The results are illustrated through a case study for Atomic force microscope (AFM) based imaging and nano-manipulation.

5.2 Backstepping Design for Parametric-Strict Feedback Systems

In this section a robust adaptive controller is presented for systems in parametric strict feedback form based on the backstepping design [33]. The adaptive control literature contains many variants of the design in [33] for systems with constant parameters. Several papers have extended the design procedure to systems with time varying parameters. However, the results are restricted to smoothly varying parameters with known bounds. In these results, projection or other modifications were used to guarantee boundedness, see for example [42, 17]. Such results are not of interest to switching systems where parameter smoothness

is lost and time variation is a persistent intrinsic part of the system's behavior.

Consider systems in parametric strict feedback form given by Equation (5.1):

$$\begin{aligned} \dot{x}_i &= x_{i+1} + \phi_i(x_1, \ldots, x_i)^T\theta, \quad 1 \leq i \leq n-1 \\ \dot{x}_n &= b_n\beta(x)u + \phi_n(x)^T\theta + d \\ y &= x_1 \end{aligned} \tag{5.1}$$

where vector $\theta \in \mathbb{R}^p$ and scalar b_n are plant parameters, ϕ_i and $\beta(x)$ are known functions, and d is a disturbance. The main assumptions for the design are given by:

Assumption 5.2.1. *The states x_i $i = 1 \ldots n$ are measured.*

Assumption 5.2.2. *The sign of b_n is known and constant.*

Assumption 5.2.3. *Parameter vector $\theta \in \mathbb{R}^p$ and scalar $b_n \neq 0 \; \forall \, t$ are piecewise differentiable uniformly bounded functions with finite discontinuities in finite time.*

Assumption 5.2.4. *The vector functions $\phi_i(x_1, \ldots, x_i) \in \mathbb{R}^p \; \forall i = 1 \ldots n$ and scalar function $\beta(x) \in \mathbb{R}$ are known smooth functions and $\beta(x) \neq 0 \; \forall x$.*

Assumption 5.2.5. *The reference trajectory y_r and its first n derivatives $y_r^{(1)}, \ldots, y_r^{(n)}$ are known, bounded and, piecewise continuous.*

Assumption 5.2.6. *$d \in \mathbb{R}$ is uniformly bounded and piecewise continuous.*

5.2.1 Control Design

Using the backstepping tuning functions design procedure [33], with some appropriate modifications we define the following terms to construct our closed loop system:

$$
\begin{aligned}
z_i &= x_i - \alpha_{i-1} - y_r^{(i-1)} \\
w_i &= \phi_i - \sum_{j=1}^{i-1} \frac{\partial \alpha_{i-1}}{\partial x_j} \phi_j \\
\tau_1 &= w_1 z_1 - \Gamma^{-1} L_o (\hat{\theta} - \theta^*) \\
\tau_i &= \tau_{i-1} + w_i z_i \\
\alpha_i &= -c_i z_i - z_{i-1} - w_i^T \hat{\theta} + \frac{\partial \alpha_{i-1}}{\partial \hat{\theta}} \Gamma \tau_i + \sum_{j=2}^{i-1} \frac{\partial \alpha_{j-1}}{\partial \hat{\theta}} \Gamma w_i z_j \\
&\quad + \sum_{j=1}^{i-1} \left[\frac{\partial \alpha_{i-1}}{\partial x_j} x_{j+1} + \frac{\partial \alpha_{i-1}}{\partial y_r^{(j-1)}} y_r^{(j)} + \frac{\partial \alpha_{i-1}}{\partial \theta^{*(j-1)}} \theta^{*(j)} \right]
\end{aligned}
$$

Where $c_i > 0$ are chosen control gains, diagonal adaptation matrices $\Gamma_o, L_o > 0$ and $\hat{\theta}$ are parameter estimates, which will be updated by an adaptation law to be specified. Vector θ^* is an estimate of plant parameters θ to be used in the update law for $\hat{\theta}$. The notation $\alpha_o = z_o = x_o = 0$ and $x_{n+1} = b_n \beta(x) u$ is used for convenience. Also note that by definition, $w_1 = \phi_1$. The following set of control and update laws will be used, which are modifications of those used in the standard backstepping tuning functions design procedure [33] with $\rho = 1/b_n$:

$$
\begin{aligned}
u &= \frac{\hat{\rho}}{\beta(x)} [\alpha_n + y_r^{(n)} + w_d^T \hat{d}] \\
\dot{\hat{\theta}} &= \Gamma_o \tau_n \\
\dot{\hat{\rho}} &= -\gamma_\rho \, sign(b_n) (\alpha_n + y_r^{(n)} + w_d^T \hat{d}) z_n - L_\rho (\hat{\rho} - \rho^*) \\
\dot{\hat{d}} &= -\Gamma_d w_d \, z_n - L_d \hat{d}
\end{aligned}
\tag{5.2}
$$

Where the diagonal matrixes $\Gamma_o, \Gamma_d > 0$ and scalar $\gamma_\rho > 0$ are adaptation gains and adaptation filter gains are diagonal matrices $L_o > 0$ and $L_d > 0$ and scalar $L_\rho > 0$. The vector $w_d \in R^l$ for $\hat{d} \in R^l$ is assumed internal model of disturbance, e.g., a sinusoidal

function, which is set to $w_d = 1$ as a default. If no disturbance adaptation is used then $w_d = 0$ and the update law for $\hat{d}$ is removed.

Denote the vector $\hat{a} = [\hat{\theta}^T, \hat{\rho}, \hat{d}]$, which is an estimate of the total parameter vector $a = [\theta^T, \rho, 0]^T$, where the disturbance adaptation parameter $\hat{d}$ is augmented in $\hat{a}$ with an assumed nominal value of 0 with $a = [\theta^T, \rho, 0]^T$. The chosen parameter estimate vector $a^* = [\theta*^T, \rho^*, 0]^T \in C^{n-1}$, i.e., $n-1$ times continuously differentiable. Also denote by $e_c = z$ for this design method and overall adaptation and filters gains $\Gamma^{-1} = diag(\Gamma_o^{-1}, \gamma_\rho^{-1}|b_n|, \Gamma_d^{-1})$ and $L = diag(L_o, L_\rho, L_d)$. The matrix $W_d = [0_{l\times(n-1)}, w_d]$, $W = [w_1, \ldots, w_n]$, and $W_\rho = [0_{1\times(n-1)}, \alpha_n + y_r^{(n)} + w_d^T\hat{d}]$. If we differentiate z_i and use the definition of α_i and the plant dynamics, we get the closed loop error dynamics, see [33] for analogous details:

$$
\begin{aligned}
\dot{e}_c &= A_z e_c - W^T\tilde{\theta} + b_n W_\rho^T\tilde{\rho} + W_d^T\hat{d} + d \\
\dot{\hat{a}} &= \begin{bmatrix} \Gamma_o W\, e_c - L_o(\hat{\theta} - \theta^*) - \dot{\theta} \\ -\gamma_\rho\, sign(b_n) W_\rho\, e_c - L_\rho(\hat{\rho} - \rho^*) - \dot{\rho} \\ -\Gamma_d W_d\, e_c - L_d\hat{d} \end{bmatrix}
\end{aligned}
$$

Where e_n is the n^{th} unit vector and A_z is given by:

$$
A_z(e_c, \hat{\theta}, t) = \begin{bmatrix} -c_1 & 1 & 0 & \ldots & 0 \\ -1 & -c_2 & 1+\sigma_{2,3} & \ldots & \sigma_{2,n} \\ 0 & -1-\sigma_{2,3} & \ddots & \ddots & \vdots \\ \vdots & \vdots & \ddots & \ddots & 1+\sigma_{n-1,n} \\ 0 & -\sigma_{2,n} & \ldots & -1-\sigma_{n-1,n} & -c_n \end{bmatrix}
$$

Where $\sigma_{i,k} = -\frac{\partial\alpha_{i-1}}{\partial\hat{\theta}}\Gamma_o w_k$. Note that $A_z^T + A_z = -C$, where $C = diag(c_i) > 0$ is a matrix of control gains. Theorem 5 below states the main result of this section.

Theorem 5. *If the system given by Equation (5.1) satisfies the assumptions (5.1.1-5.1.6) then the adaptive feedback control given by Equation (5.2) yields:*

(i) Uniformly internally exponentially stable and BIBS stable system with state $x_c = [e_c, \tilde{a}]^T$.
(ii) state $x_c = [e_c, \tilde{a}]^T$ *is bounded with*
$\|y - y_r\| \leq \epsilon[c_1\|x_c(t_o)\|e^{-\alpha(t-t_o)} + c_2 \int_{t_o}^{t} e^{\alpha(\tau-t)}\|v(\tau)\|\, d\tau]$. *where* c_1, c_2, ϵ *are constants,* $\alpha = \underline{\lambda}(diag(C, L))$, *and* $v = [d, \Gamma^{-1/2}(L(a^* - a) - \dot{a})]^T$.

5.2.2 Remarks

This section provides some remarks on the results of Section 5.1.

- The result applies to systems globally diffeomorphically transformable to the parametric-strict form independent of parameters via a known transformation, see [33] and references therein for conditions for a system to be transformable to this form.

- Note that when $\theta_i = 0\ \forall i \neq n$ the parametric-strict form reduces to the nonlinear controllable canonical form, to which all uniformly strongly controllable linear-time-varying systems are transformable to.

- d is enforced only in the last equation $\dot{x}_n$ yet disturbances at other equations are allowed but they have to be lumped into the vector of time varying parameters θ and adapted for in order to guarantee the same performance. This is the case since they will appear to the closed loop system as terms multiplied by state dependent functions due to the nature of the backstepping procedure. It is assumed that if such disturbances exist they are lumped into the vector of "parameters" θ with the corresponding element of multiplying vector function ϕ_i being unity.

- The assumption on the reference y_r can be circumvented by using y_r as an output of an n^{th} order low pass filter driven by any bounded piecewise continuous reference.

- Other variants of the parametric-strict form are the one with unknown virtual control coefficients and blocks-strict form, follow along the same lines but are significantly lengthier, see [33]. The extension of the modified algorithm to these systems follows by direct analogy.

- Note that it is enforced that the chosen parameter estimate vector $a^* = [\theta*^T, \rho^*, 0]^T \in C^{n-1}$, i.e., $n-1$ times continuously differentiable. This requirement is specific to the backstepping design procedure due the definition of the error dynamics for z. Again this can be circumvented by using a^* as an output of an n^{th} order low pass filter driven by any bounded piecewise continuous choice for a^*.

5.3 Backstepping Design for Parametric-Strict Output Feedback Systems

In this section we discuss the backstepping tuning functions design procedure for parametric output feedback systems [33]. The literature contains a few results extending the design procedure to systems with time varying parameters. However, the results are restricted to smoothly varying parameters as with most adaptive control results. Again only boundedness is concluded without any clear tracking performance claims except when parameters become constant, at least asymptotically. In [43] the input vector parameters, vector $b(t)$ in Equation (5.3) below, is constant and known whereas other parameters are smooth time varying parameters of known bounds. A more recent result by the same authors in [44] applies to linear systems in parametric-strict output form and allows all parameters to be time varying without known bounds but are required to be smooth. Another recent result for linear-time-varying systems with smooth parameters [83] requires a priori information about rapidly varying parameters whereas completely unknown parameters are required to be slowly time varying. Again such results are yet to address switching systems where parameter smoothness is lost and time variation is a persistent intrinsic part of the system's behavior.

Consider systems in the parametric-strict output feedback form:

$$
\begin{aligned}
\dot{x} &= Ax + \phi(y) + \Phi(y)a_p + b\beta(y)u + \bar{d} \\
y &= c^T x \qquad (5.3) \\
A &= \begin{bmatrix} 0 & \\ \vdots & I_{(n-1)\times(n-1)} \\ 0 \ \ldots & 0 \end{bmatrix}, \ b = \begin{bmatrix} 0_{(r-1)\times 1} \\ b_m \\ \vdots \\ b_o \end{bmatrix} \\
c &= \begin{bmatrix} 1 \\ 0_{(n-1)\times 1} \end{bmatrix}, \ \phi(y)^T = \begin{bmatrix} \varphi_{0,1}(y) \\ \vdots \\ \varphi_{0,n}(y) \end{bmatrix} \\
\Phi(y) &= \begin{bmatrix} \varphi_{1,1}(y) \ldots & \varphi_{q,1}(y) \\ \vdots & \vdots \\ \varphi_{1,n}(y) \ldots & \varphi_{q,n}(y) \end{bmatrix}
\end{aligned}
$$

Where vectors a_p and b are unknown system parameters. The vector $\bar{d} = [0, d_2, \ldots, d_n]^T$ is the disturbance. Note the disturbance in the first state equation $d_1 = 0$ since it is enforced that if one exists that it will be augmented in the time varying vector of parameters a_p. This is needed since the effect of such a disturbance will appear in the closed loop dynamics as state dependent terms rather than just a disturbance due to the nature of the backstepping design procedure.

Assumption 5.3.1. *The output y is measured.*

Assumption 5.3.2. *The sign of $b_m \neq 0 \ \forall t$ is known and constant.*

Assumption 5.3.3. *The relative degree $r = n - m \geq 1$ of the system given by Equation (5.3) is a well defined and known constant.*

Assumption 5.3.4. *The zero dynamics of the system given by Equation (5.3) is uniformly exponentially stable.*

Assumption 5.3.5. *Parameter vectors a_p and b are piecewise differentiable bounded functions with finite discontinuities in finite time.*

Assumption 5.3.6. *$\varphi_{i,j}(y)\ \forall i = 0 \ldots q$ and $\forall j = 1 \ldots n$ and $\beta(y)$ are known smooth functions and $\beta(y) \neq 0\ \forall y$.*

Assumption 5.3.7. *The reference trajectory y_r and its first r derivatives $y_r^{(1)}, \ldots, y_r^{(r)}$, are known, bounded and, piecewise continuous.*

Assumption 5.3.8. *$\bar{d} \in \mathbb{R}^n$ is uniformly bounded and piecewise continuous.*

5.3.1 Filter Design

In this section, filters for estimation of unmeasured states are developed. We choose a filter gain vector k such that the matrix $A_o = A - kc^T$ is Hurwitz, which is possible due to observability of the pair (A, c^T) by construction. Therefore, we have the following filter equations [33]:

$$\begin{aligned} \dot{\xi} &= A_o\xi + ky + \phi(y) \\ \dot{\Xi} &= A_o\Xi + \Phi(y) \\ \dot{\lambda} &= A_o\lambda + e_n\beta(y)u \\ v_j &= A_o^j\lambda, \quad j = 0, \ldots, m \\ \Omega^T &= [v_m, \ldots, v_1, v_0, \Xi] \end{aligned} \tag{5.4}$$

where e_i is the i^{th} unit vector.

Now we need to define the error variable of the state estimator ε, which is given by:

$$\varepsilon = x - \left(\xi + \int_0^t \dot{\Omega}^T(\tau)\theta(\tau)d\tau\right)$$

where $\theta = [b, a_p]^T$. From this we have the following estimation error equation:

$$\dot{\varepsilon} = A_0\varepsilon + \bar{d} \tag{5.5}$$

which is an exponentially stable linear system with eigenvalues dictated by choice of filter gain vector k.

5.3.2 Control Design

Based on the backstepping tuning functions design procedure [33], we define the following terms to construct our closed loop system :

$$
\begin{aligned}
z_1 &= y - y_r \\
z_i &= v_{m,i} - \alpha_{i-1} - \hat{\rho}\, y_r^{(i-1)} \quad , i = 2, \ldots, r \\
\omega &= [v_{m,2}, v_{m-1,2}, \ldots, v_{0,2}, \Phi_{(1)} + \Xi_{(2)}]^T \\
\bar{\omega} &= [0, v_{m-1,2}, \ldots, v_{0,2}, \Phi_{(1)} + \Xi_{(2)}]^T \\
\omega_o &= \varphi_{0,1} + \xi_2 \\
\tau_1 &= (w - \hat{\rho}(\bar{\alpha}_1 + \dot{y}_r)e_1)\, z_1 - \Gamma_o^{-1} L_o(\hat{\theta} - \theta^*) \\
\tau_i &= \tau_{i-1} - \frac{\partial \alpha_{i-1}}{\partial y} \omega\, z_i \quad , i = 2, \ldots, r \\
\alpha_1 &= \hat{\rho}\bar{\alpha}_1 \\
\bar{\alpha}_1 &= -(c_1 + d_1)z_1 - \omega_o - \bar{\omega}^T\hat{\theta} \\
\alpha_2 &= -\hat{b}_m\, z_1 - \left[c_2 + d_2 \left(\frac{\partial \alpha_1}{\partial y}\right)^2\right] z_2 + \frac{\partial \alpha_1}{\partial \hat{\theta}} \Gamma \tau_2 \\
&\quad + \left(\dot{y}_r + \frac{\partial \alpha_1}{\partial \hat{\rho}}\right) \dot{\hat{\rho}} + \beta_2 \\
\alpha_i &= -z_{i-1} - \left[c_i + d_i \left(\frac{\partial \alpha_{i-1}}{\partial y}\right)^2\right] z_i + \frac{\partial \alpha_{i-1}}{\partial \hat{\theta}} \Gamma \tau_i \\
&\quad + \left(y_r^{(i-1)} + \frac{\partial \alpha_{i-1}}{\partial \hat{\rho}}\right) \dot{\hat{\rho}} + \beta_i \\
&\quad - \sum_{j=2}^{i-1} \frac{\partial \alpha_{j-1}}{\partial \hat{\theta}} \Gamma \frac{\partial \alpha_{i-1}}{\partial y} \omega\, z_j \quad , i = 3, \ldots, r \\
\beta_i &= \frac{\partial \alpha_{i-1}}{\partial y} \left(\omega_o + \omega^T \hat{\theta}\right) + \sum_{j=1}^{m+i-1} \frac{\partial \alpha_{i-1}}{\partial \lambda_j} (-k_j \lambda_1 + \lambda_{j+1}) \\
&\quad + \sum_{j=1}^{i-1} \left[\frac{\partial \alpha_{i-1}}{\partial a^{*(j-1)}} a^{*(j)} + \frac{\partial \alpha_{i-1}}{\partial y_r^{(j-1)}} y_r^{(j)}\right] + k_i\, v_{m,1} \\
&\quad + \frac{\partial \alpha_{i-1}}{\partial \Xi} (A_o \Xi + \Phi(y)) + \frac{\partial \alpha_{i-1}}{\partial \xi} (A_o \xi + k y + \phi(y))
\end{aligned}
$$

Where constants $c_i, d_i > 0$ and diagonal matrices $\Gamma_o, L_o > 0$ and $a^* = [\theta^*, \rho^*, 0]$ is an estimate of plant parameters θ and ρ to be used in the update laws, to be presented next. The following set of control and update laws are used, which are modifications of those used in the standard backstepping tuning functions design procedure [33]:

$$
\begin{aligned}
u &= \begin{cases} \frac{1}{\beta(y)}[\alpha_r + \hat{\rho} y_r^{(r)} - v_{m,r+1} + w_d^T \hat{d}] & \text{if } r \neq 1 \\ \frac{1}{\beta(y)}[\alpha_1 + \hat{\rho} \dot{y}_r - v_{m,2} + \hat{\rho} w_d^T \hat{d}] & \text{if } r = 1 \end{cases} \\
\dot{\hat{\theta}} &= \begin{cases} \Gamma_o \tau_r & \text{if } r \neq 1 \\ \Gamma_o \bar{\omega} z_1 - L_o(\hat{\theta} - \theta^*) & \text{if } r = 1 \end{cases} \\
\dot{\hat{\rho}} &= \begin{cases} -\gamma_\rho \, sign(b_m)[\bar{\alpha}_1 + \dot{y}_r] z_1 - L_\rho(\hat{\rho} - \rho^*) \\ \qquad\qquad \text{if } r \neq 1 \\ -\gamma_\rho \, sign(b_m)[\bar{\alpha}_1 + \dot{y}_r + w_d^T \hat{d}] z_1 - L_\rho(\hat{\rho} - \rho^*) \\ \qquad\qquad \text{if } r = 1 \end{cases} \\
\dot{\hat{d}} &= -\Gamma_d w_d \, z_r - L_d \hat{d}
\end{aligned}
$$

where the diagonal matrixes $\Gamma_o, \Gamma_d > 0$ and scalar $\gamma_\rho > 0$ are adaptation gains and adaptation filter gains are diagonal matrices $L_o > 0$, $L_d > 0$ and scalar $L_\rho > 0$. The vector $w_d \in R^l$ for $\hat{d} \in R^l$ is assumed internal model of disturbance, e.g., a sinusoidal function, which is set to $w_d = 1$ as a default. If no disturbance adaptation is used then $w_d = 0$ and the update law for $\hat{d}$ is removed. It can be seen that the relative degree $r = 1$ case is similar, with the exception that some terms are omitted in the update law for $\hat{\theta}$, whereas the term $w_d^T \hat{d}$ is included in the update law for $\hat{\rho}$.

Denote the vector $\hat{a} = [\hat{\theta}^T, \hat{\rho}, \hat{d}]$, which is an estimate of the total parameter vector $a = [\theta^T, \rho, 0]^T$, where the disturbance adaptation parameter $\hat{d}$ is augmented in $\hat{a}$ with an assumed nominal value of 0 with $a = [\theta^T, \rho, 0]^T$ with the chosen parameter estimate vector $a^* = [\theta*^T, \rho^*, 0]^T \in C^{r-1}$, i.e., $r - 1$ times continuously differentiable. Also denote by $e_c = [z^T, \varepsilon^T]^T$ for this design method and overall adaptation and filters gains $\Gamma^{-1} = diag(\Gamma_o^{-1}, \gamma_\rho^{-1}|b_m|, \Gamma_d^{-1})$ and $L = diag(L_o, L_\rho, L_d)$. The matrix $W_d = [0_{l \times (r-1)}, w_d]$, W_θ and W_ρ are given below:

$$
\begin{aligned}
W_\varepsilon &= \begin{bmatrix} 1 \\ -\frac{\partial \alpha_1}{\partial y} \\ \vdots \\ -\frac{\partial \alpha_{r-1}}{\partial y} \end{bmatrix} \in \mathbb{R}^r \\
W_\theta^T &= \begin{cases} W_\varepsilon \omega^T - \hat{\rho}(\bar{\alpha}_1 + \dot{y}_r) e_1 e_1^T & \text{if } r \neq 1 \\ \bar{\omega}^T & \text{if } r = 1 \end{cases} \in \mathbb{R}^{r \times p} \\
W_\rho &= \begin{cases} (\bar{\alpha}_1 + \dot{y}_r) e_1 & \text{if } r \neq 1 \\ \bar{\alpha}_1 + \dot{y}_r + w_d^T \hat{d} & \text{if } r = 1 \end{cases} \in \mathbb{R}^r
\end{aligned}
$$

If we differentiate z_i and use the definition of α_i and the plant dynamics, we get the closed loop error dynamics:

$$
\begin{aligned}
\dot{e}_c &= \begin{bmatrix} A_z z - W_\theta^T \tilde{\theta} + W_\varepsilon \varepsilon_2 + b_m W_\rho \tilde{\rho} + W_d^T \hat{d} \\ A_0 \varepsilon \end{bmatrix} + d \\
\dot{\hat{a}} &= \begin{bmatrix} \Gamma_o W_\theta z - L_o(\hat{\theta} - \theta^*) - \dot{\theta} \\ -\gamma_\rho \, sign(b_m) W_\rho z - L_\rho(\hat{\rho} - \rho^*) - \dot{\rho} \\ -\Gamma_d W_d z - L_d \hat{d} \end{bmatrix}
\end{aligned}
$$

Where $e_c = [z^T, \varepsilon^T]^T$ and the overall disturbance $d = [0_{1\times r}, \bar{d}]^T$ with A_z given by :

$$
A_z = \begin{bmatrix}
-c_1 - d_1 & \hat{b}_m & 0 & \dots & \dots & 0 \\
-\hat{b}_m & -c_2 - d_2(\frac{\partial \alpha_1}{\partial y})^2 & 1 + \sigma_{2,3} & \sigma_{2,4} & \dots & \sigma_{2,r} \\
0 & -1 - \sigma_{2,3} & \ddots & \ddots & \ddots & \vdots \\
\vdots & -\sigma_{2,4} & \ddots & \ddots & \ddots & \sigma_{r-2,r} \\
\vdots & \vdots & \ddots & \ddots & \ddots & 1 + \sigma_{r-1,r} \\
0 & -\sigma_{2,r} & \dots & -\sigma_{r-2,r} & -1 - \sigma_{r-1,r} & -c_r - d_r(\frac{\partial \alpha_{r-1}}{\partial y})^2
\end{bmatrix}
$$

Where $\sigma_{i,k} = \frac{\partial \alpha_{i-1}}{\partial \hat{\theta}} \Gamma_o \frac{\partial \alpha_{k-1}}{\partial y} \omega$.

Theorem 6 below states the main result of this section for the backsepping based design procedure for systems in parametric-strict output feedback form.

Theorem 6. *If the system given by Equation (5.3) satisfies the assumptions (5.2.1-5.2.8) then the adaptive feedback control given by Equations (5.6) and filter Equations (5.4) yields:*
(i) Uniformly internally exponentially stable and BIBS stable system with state $x_c = [e_c, \tilde{a}]^T$.
(ii) states $x_c = [e_c, \tilde{a}]^T$, x, *and filter states* Λ, ξ *are bounded with tracking error satisfying:* $\|y - y_r\| \leq \epsilon[c_1\|x_c(t_o)\|e^{-\alpha(t-t_o)} + c_2 \int_{t_o}^{t} e^{\alpha(\tau-t)}\|v(\tau)\|\, d\tau]$. *where* c_1, c_2, ϵ *are constants,* $\alpha = \underline{\lambda}(diag(P^{-1}C, L))$, *and* $v = [P^{1/2}d, \Gamma^{-1/2}(L(a^* - a) - \dot{a})]^T$.

5.3.3 Remarks

This section provides some remarks on the results of Section 5.2.

- The result applies to systems globally diffeomorphically transformable to the parametric-strict output form, see [33] and references therein for conditions for a system to be transformable to this form. Note that unlike the full state feedback design this transformation is neither required to be known nor parameter independent.

- Note that when $\Phi(y) = Iy$ and $\beta(y) = 1$ the parametric-strict-output form reduces to the observable canonical form, to which all uniformly strongly observable linear-time-varying systems are transformable.

- Note that the definition of ε given by Equation (5.5) differs from that in standard backstepping designs [33] due to allowing time varying parameters. Note, however, that it reduces to the same quantity when parameters are constant and filters are initialized at zero.

- The assumption 5.2.3 for $r \geq 1$ simply suggests that the plant is strictly proper. Note that the relative degree zero case can also be dealt with by augmenting the plant with a stable pole. Then the control design is carried out for this effective relative degree 1 system. Then the controller is implemented via passing the obtained control signal through the augmented low pass filter (stable pole) mentioned above.

- Note that the disturbance in the first state equation $d_1 = 0$ since it is enforced that if one exists that it will be augmented in the time varying vector of "parameters" a_p in order to guarantee the same performance. This is the case since they will appear to the closed loop system as terms multiplied by state dependent functions due to the nature of the backstepping procedure. It is assumed that if such disturbances exist they are lumped into the vector of "parameters" a_p with the corresponding element of multiplying vector function ϕ_i being unity.

- The assumption on the reference y_r can be circumvented by using y_r as an output of an r^{th} order low pass filter driven by any bounded piecewise continuous reference.

- Note that it is enforced that the chosen parameter estimate vector $a^* = [\theta*^T, \rho^*, 0]^T \in C^{r-1}$, i.e., $r-1$ times continuously differentiable. This requirement is specific to the backstepping design procedure due the definition of the error dynamics for z. This can be circumvented by using a^* as an output of an r^{th} order low pass filter driven by any bounded piecewise continuous choice of a^*.

5.4 Application to Atomic Force Microscope Based Nano-manipulation

The use of atomic force microscopy (AFM) as a nano-manipulation system has been generating considerable interest in recent years. This is attributed to its success as an imaging system to detect topographic and material properties at sub-nanometer resolution as well as its compatibility with many samples and ambient conditions. Nano-manipulation is important in nano-manufacturing such as printing, lithography, and assembly. Another important application is in biological object manipulation enabling disease characterization, drug discovery, and bio-system synthesis.

In the last few years, nano-manipulation of certain objects via AFM's has been demonstrated by biologists, chemists, and material scientists. More recently, the robotics community has taken interest in developing AFM-based nano-manipulation systems that allow scientists and engineers to systematically perform certain tasks. This has been primarily

focused on developing and/or integrating haptic devices for tele-operation, appropriate visualization interfaces, and calibration, e.g. [19, 24, 35]. However, the work in this area has highlighted, e.g. [80], the difficulty in achieving repeatable and stable operation due to sensitivity to parametric variations and disturbances at the nano-scale among other factors. This suggests the need for developing appropriate controls guaranteeing stable, repeatable, and fast nano-manipulation. The basic principle of the AFM operation is based on using a

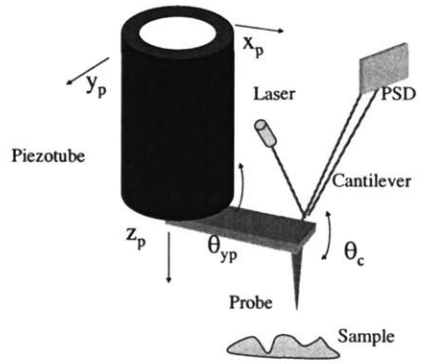

Figure 5-1: Principle of AFM operation.

micro-cantilever with a sharp object at its tip to probe a surface. The cantilever is mounted on a piezoelectric tube, which can translate both laterally and vertically, see Figure 5-1. As the probe approaches the surface, an interaction force causes the cantilever to deflect. Therefore, light from a laser source reflects off the cantilever's tip and the corresponding change in cantilever deflection is recorded via a position sensitive split photodetector (PSD). This sensor measurement is then compared to a chosen detector output reflecting a desired manipulation such as cutting, indentation, and pushing. Additional sensor measurements of the piezotube's extensions are typically available for nano-manipulation.

5.4.1 AFM Dynamical Model

The model presented here includes the first mode for each of the three degrees-of-freedom of interest, where extensions to include higher modes can be made by direct analogy between this work and that in [11, 12]. The model considers the vertical extension z_p and bending θ_{yp}, about the y-axis in Figure 5-1, for the piezotube scanner. In addition, the bending of the cantilever, θ_c relative to the tube's base is included. The governing equations are given by:

$$\ddot{\theta}_{yp} + 2\zeta_{\theta p}\omega_{\theta p}\dot{\theta}_{yp} + \omega_{\theta p}^2\theta_{yp} = a_{\theta p}u \tag{5.6}$$

$$\ddot{z}_p + 2\zeta_{zp}\omega_{zp}\dot{z}_p + \omega_{zp}^2 z_p = a_{zp}u \tag{5.7}$$

$$\ddot{\theta}_c + 2\zeta_c\omega_c\dot{\theta}_c + \omega_c^2\theta_c = a_1\ddot{\theta}_{yp} + a_2\ddot{z}_p + a_e M_e \tag{5.8}$$

$$y_m = \theta_c + \theta_{yp} \tag{5.9}$$

Where ζ is damping ratio and ω is natural frequency. The 1^{st} two differential Equations (5.6-5.7) describe the dynamics of the two piezotube flexible modes of interest. The voltage given to the piezotube vertical axes z_p generates tube strain in the extension and bending modes. Though it is desired that the tube only extends or retracts to a given voltage in the same axis, this ideal behavior is not achieved in practice. The reason is that an inevitable tube eccentricity leads to axes coupling as observed in [10]. The effect of the piezotube coupling on an image of a 70° included angle silicon grating, identified in a commercial AFM, is shown in Figure 5-2. In Figure 5-2, this coupling leads to an included angle of about 76° for the image. The coupling in other axes is not discussed here as it is not relevant to the control of probe-surface interaction but rather in positioning of the scanner, which is usually done in open loop, see [13] for details.

The dynamics of the cantilever's bending angle, θ_c relative to the tube's base, is shown in Equation (5.8). Note that since θ_c is relative to the tube's base acceleration terms due to tube bending θ_{yp} and vertical extension z_p need to be included. Whereas, M_e is the moment about the y-axis due to the interaction with the probed surface, for which a more

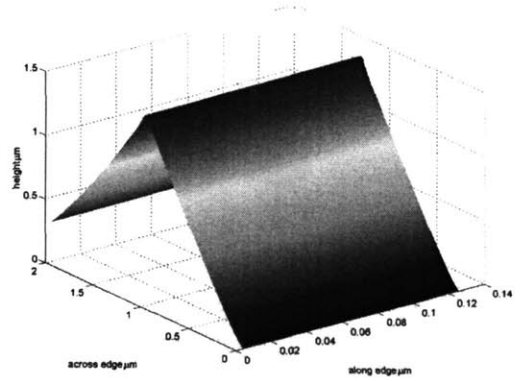

Figure 5-2: Experimental demonstration of effect of Piezotube coupling on an AFM image.

detailed analysis and discussion is presented in the next section. Finally, the measurement y in Equation (5.9) is that of the vertical optical detector's deflection, i.e., the absolute angular deviation of a laser beam reflected off the cantilever. This represents the sum of the piezotube bending and cantilever bending relative to the tube base.

Experimental frequency response results of key AFM dynamics have been reported in earlier efforts [11, 12]. Typical values of piezotube lateral extension, vertical extension, and cantilever bending 1^{st} resonances are of the order of few hundred Hz, few kHz, and tens to hundreds of kHz, respectively.

Probe-Surface Interaction

The interaction, with the environment (surface) is discussed in this section, see Figure 5-3 for a schematic.The forces acting on the probe are of the elastic and dissipative type. The normal forces, such as Van der Waals force, are a nonlinear function of the relative separation between the probe and the contacted surface, see Figure 5-4 where separation is defined to be nonnegative during contact. Other forces include dissipative forces are a function of the velocity between the probe and the manipulated object. The aforementioned forces yield a total force with components f_x, f_y, f_z shown in Figure 5-3, which yield the

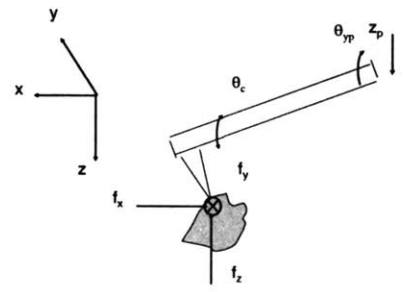

Figure 5-3: Schematic of Probe-surface Interaction.

moment M_e acting on the cantilever's bending dynamics. Therefore, retaining *linear terms* in the modeled states (probe position and velocity) we can approximate M_e at an operating point, as done in modeling of AFM imaging systems [11], as follows:

$$M_e \approx \alpha_1 \theta_{yp} + \alpha_2 z_p + \alpha_3 \theta_c + \alpha_4 \dot{\theta}_{yp} + \alpha_5 \dot{z}_p + \alpha_6 \dot{\theta}_c + d_f \tag{5.10}$$

where α_i for $i = 1 \ldots 6$ are appropriate constants from linearizing at an operating point. The terms above from θ_p and z_p appear due to the fact that the total velocity and position of the probe are not only a function of θ_c since θ_c is measured relative to the tube's base. Whereas, the first order terms due to the manipulated surface's height changes as well as higher order nonlinearities, will be represented as an external forcing disturbance d_f. This disturbance accounts for changing the cantilever's deflection during manipulation. The primary effect of the Moment M_e is changing the effective stiffness and damping of the cantilever through $\alpha_3 \theta_c$ and $\alpha_6 \dot{\theta}_c$, respectively.

Note that the coefficients α_i will generally be *time varying* due to the time variation of the relative position and velocity between the probe and surface since α_i are the outcome of linearization of forces, such as Van der Waals. Linearization is then made about a trajectory rather than a setpoint value if the relative position and velocity between the probe and surface are time varying, which yields time varying coefficients α_i, see [11, 12] for experimental demonstrations at different operating points. Furthermore, parameter jumps due to transition between out-of-contact and in-contact dynamics at different points in the sur-

face will cause *switching* in the parameters α_i, which suggests a switched system's model. Therefore, the overall system is being represented by a *linear time varying switching system* with the same local structure.

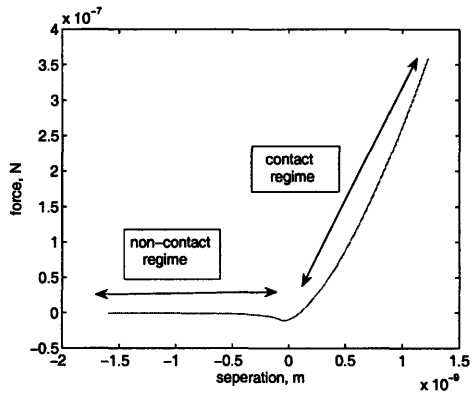

Figure 5-4: Force separation curve based on Van der Waals-Maugis Model

5.4.2 Control Simulations

In this section the backstepping-based adaptive control procedure of Section 5.2 is applied to the AFM system. Since the surface forces acting on the cantilever depend nonlinearly on the probe-surface separation, which is unknown, these nonlinearities cannot be used usefully in a model-based control design since they depend on the separation between the probe and the unknown surface. Therefore, the linearized time varying model using Equation (5.10) will be used for control design yet the plant will be implemented in the simulations using the original nonlinear force of Figure 5-4. The linearized time varying model falls under the class of parametric strict output feedback systems of Section 5.2. The work by [12] has utilized backstepping based adaptive control to demonstrate robust AFM imaging, which is an important step towards AFM automation. The modified algorithm used here will be used not only for AFM imaging but also for nano-manipulation.

The case study under consideration uses plant parameters from an experimental frequency response data of Figure 5-5 as the nominal unforced model, i.e., when no contact is made. The adaptation gains $\Gamma_o = I$ and $\gamma_\rho = 1$, filter gains $L = 100I$, and feedback gain

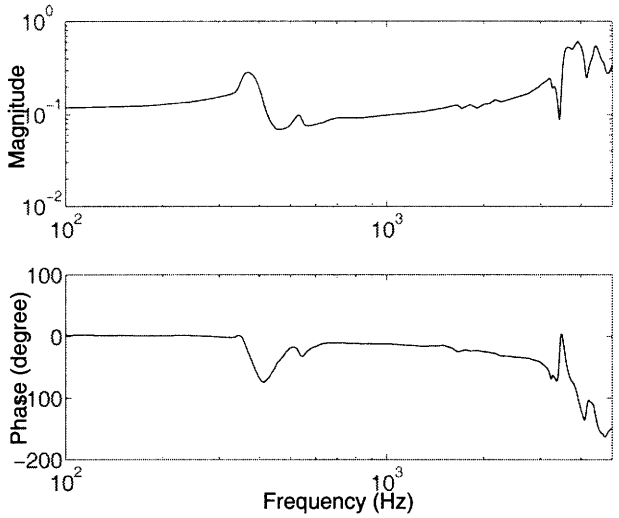

Figure 5-5: Experimental frequency response from Piezotube input voltage to PSD detector output.

$c = 100$ are chosen, where I is the identity matrix. The choice for c and L correspond to a closed loop bandwidth of 100 rad/sec, which is typical for AFM systems. The simulations shown are for the probe scanning a $2\mu m$ steps at a frequency of $2Hz$.

First we consider the control system's response when imaging the sample of interest. Figure 5-6 shows height profile image of the step-like sample along a scanned cross section in addition to the the profile of the sample itself, which are almost identical. This corresponds to a tracking error in Figure 5-7, which is almost zero everywhere except at a few points where the step change occurs. In Figure, 5-7 the transient error due to the step changes is about $18nm$, which is reduced to about $9nm$ with increasing adaptation gain γ_ρ, as predicted by the theory of Section 5.2. Observe that this performance has been achieved with a choice of parameter estimate a^* matching the out-of-contact dynamics of the system from the experimental frequency response data of Figure 5-5. Note that the used force curve of Figure 5-4 causes the effective cantilever's stiffness to change from $1N/m$ to about $250N/m$ for the in-contact dynamics, which corresponds to large uncertainty in system poles and zeros, see [12, 11].

Next, we consider AFM-based nano-manipulation with the same $2\mu m$ steps sample being scanned at a frequency of $2Hz$. The reference trajectory for the detector output

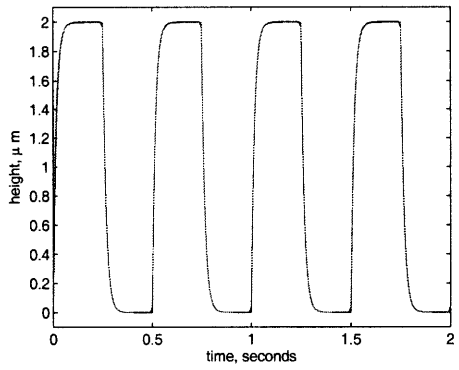

Figure 5-6: AFM height profile images and imaged step-like sample.

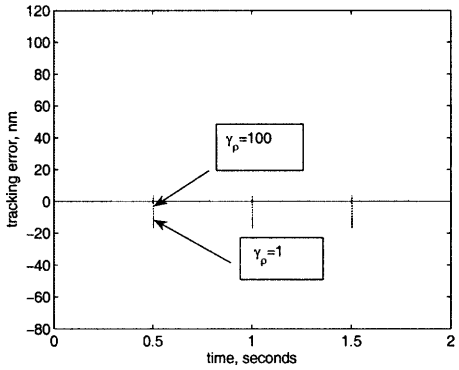

Figure 5-7: Tracking error for AFM imaging of a step-like sample.

is a $2Hz$ pulse that corresponds to an amplitude of $200nm$ for the cantilever's vertical deflection. This requires the probe to maintain contact with the top of the steps at a $200nm$ cantilever's deflection and stay out-of-contact with the steps when traversing the bottom of the steps with a zero deflection of the cantilever, see Figure 5-8. This task is achieved at minimal tracking error less than $2nm$, expect at initial contact establishment, as shown in Figure 5-9.

The enforced manipulation task of Figure 5-8 corresponds to switching in plant dynamics due to switching between contact and non-contact portions of the force curve of Figure 5-4. This corresponds to changes in plant dynamics between the non-contact dynamics and the contact-dynamics modes of Figure 5-4. In this example, the rapid transition between non-contact and in-contact modes causes the effective cantilever's stiffness to switch from

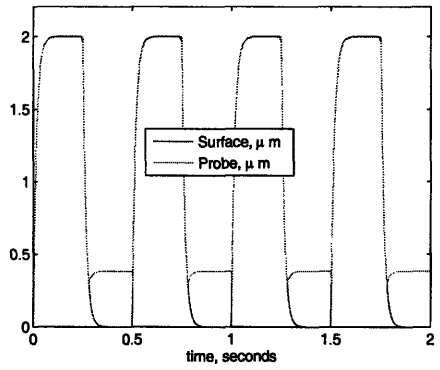

Figure 5-8: Probe position and surface for AFM nano-manipulation task.

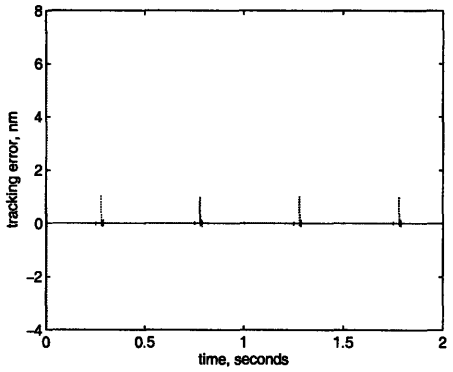

Figure 5-9: Tracking error for AFM nano-manipulation task.

$1\ N/m$ to about $250N/m$, which affects both poles and zeros of the plant at a given operating point. This can be seen from the system's response in Figure 5-10 as the separation is nonnegative during contact, which corresponds to a nonzero contact force of about $17\mu N$. Whereas, when the probe moves away from the surface the separation is negative and the contact force goes to zero. Clearly the force undergoes larger jumps and transients during these mode transitions yet the tracking error remains very small as seen in Figure 5-9 with a closed loop bandwidth of only 100 rads/sec. The adaptive controller performs very well under such large changes in system dynamics.

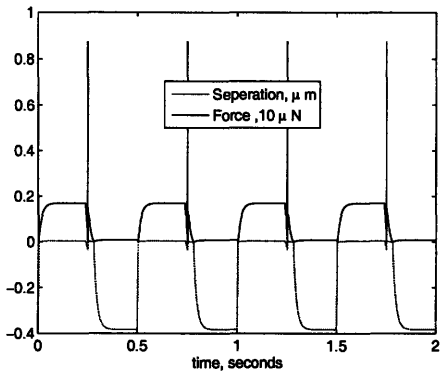

Figure 5-10: Contact force and probe-surface separation for AFM nano-manipulation task

5.5 Summary

In this chapter, detailed robust adaptive control schemes have been presented for linearly-parameterized switched systems in parametric-strict form and parametric-strict output feedback form. The design is based on conventional constructions for such systems with modifications following the the developed methodology of Chapter 3. The results are illustrated through a case study for AFM based nano-manipulation.

Chapter 6

Switching and Parameter Varying Control

6.1 Introduction

In this chapter, controller switching and variation are introduced within the proposed architecture of Chapter 3. Although stability and dynamic response of the system are guaranteed by the proposed method without any need to switch between different controllers, controller switching and adjustment are introduced within the proposed architecture: 1) if mode-specific information (identified data, candidate models) are to be utilized, and 2) for allowing more design degree of freedom for performance optimization.

The focus of this chapter is on adjusting and updating the chosen parameter estimate a^*, which can be any piecewise continuous bounded function. This allows for reducing the effect of parametric uncertainty through reducing size of input $a^* - a$ independent of system bandwidth and control gains. In fact, one of the main strengths of the controller design used here is the ability to adjust a^* with no effect on system stability due its variation or its mismatch with the ideal value a. This simply the case since its only a bounded input to the closed loop system. This gives rise to two types of problems relating to well known methods of gain scheduling and multiple model control.

6.2 Properties of The Modified Adaptation Law

Recall the modified adaptation law introduced in Chapter 3:

$$\dot{\hat{a}} = f_a - L(\hat{a} - a^*) \tag{6.1}$$

Where $\hat{a}$ is the parameter estimate, a^* is an additional chosen estimate of the plant parameter vector, L is a filter gain, and Γ is the adaptation (learning) gain. One possible interpretation of the estimator in Equation (6.1) is that it minimizes the following cost using a gradient algorithm with learning rate matrix Γ:

$$\begin{aligned} \hat{a} &= \arg\min V_E \\ V_E &= V_o + \frac{1}{2}(\hat{a} - a^*)^T \Gamma^{-1} L(\hat{a} - a^*) \\ \dot{\hat{a}} &= -\Gamma \nabla_{\hat{a}} V_E \end{aligned}$$

Where $f_a = -\Gamma \nabla_{\hat{a}} V_o$, i.e., the update law minimizing the original cost V_o associated with standard adaptive control according to a gradient update with learning rate Γ. The following remarks summarize some key points about the estimator:

- The quadratic term in the cost V_E is a penalty term that pulls the estimate $\hat{a}$ towards the guess a^* rather than allowing a completely unconstrained estimation, as with standard adaptive control using cost V_o, with the size of the matrix $\Gamma^{-1}L$ representing the strength of this penalty. Therefore, the smaller $\Gamma^{-1}L$ the less effect the choice of a^* has on the performance, which is consistent with tracking error bounds obtained in Chapter 3.

- From a statistical estimation point of view, the quadratic term in the cost V_E is a type of regularization [39] with a^* as the mean value of a and $\Gamma^{-1}L$ as the inverse of the covariance matrix for the estimator's search. Therefore, the larger $\Gamma^{-1}L$ is the higher confidence the estimator has in in the initial guess a^* and thus $\hat{a}$ remains close to a^*.

- When the size of the matrix $\Gamma^{-1}L$ approaches zero, then the estimator would approach the ideal estimator in the sense that it minimizes the prediction error even if

a^* is very far from the actual a.

- Practical control considerations limit the choice of the matrix $\Gamma^{-1}L$ since very large Γ would amplify measurement noise an introduce excessive oscillations in the control. Whereas, a small L would yield low control bandwidth.

- The use of a^* is this estimator allows for a good method to utilize data and available information in influencing or biasing the estimation while allowing for the estimator to fine tune the estimate $\hat{a}$ relative to the chosen value of a^* with a specified confidence level.

Given this interpretation of a^* we would like to develop methods to adjust and improve the choice of a^* as an indirect method to improve the estimate $\hat{a}$ while maintaining the strong stability and robustness capabilities of the control systems developed in Chapters 3-5.

6.3 Parameter Scheduling Control

In a scheduled switching scheme a pre-determined but variable control action is used, which can allow for utilizing any a priori available knowledge about changes in the process's dynamics as a function of time. In particular, a^* will be used as a scheduled parameter analogous to gain scheduling and Linear parameter varying (LPV) control methods. Yet *the key feature* here is that unlike existing techniques for gain scheduling and parameter scheduling control [40, 62, 70], stability of the system is guaranteed and the dynamic response of the system is specified by a fixed exponential stability rate α. The scheduled control variable a^* could be updated in a discrete or a continuous way. Given a discrete set of candidate models we can update a^* as follows:

1. Given a set of K candidate models associated with different operating modes obtain the corresponding set of candidate parameter vectors $\{a_k | k = 1, 2, \ldots K\}$.

2. Implement a controller with $a^* = a_1$, which is the "best guess" for the initial operating condition.

3. Every specified sampling period T set a^* according to :

$$a^* = a_k \quad \text{if mode k is detected}$$

This simply sets the "best guess controller" corresponding to the operating condition, e.g., from a look-up table. Whereas, the sampling period T is introduced in the supervisor to avoid chattering. Alternatively, a smooth interpolation between a_k values could be used. The detection of a mode is usually done through a pre-determined event, which is either a time instant, a measured variable, e.g., the output, reaching a certain threshold, or even an external trigger. For example a time-based schedule can be represented by:

$$a^* = a_k \quad t_{k-1} \leq t < t_k$$

Alternatively, we can continuously update a^* according to scheduled function $g(t)$ which depends on a continuously monitored variable. This is common in some applications such as flight control where the Mach number are monitored and used to generate an estimate of system parameters according to empirical models. In this case the update given by Equation (3.6) can be replaced with:

$$\begin{aligned} \dot{\hat{a}} &= f_a(e_c, \hat{a}, t) - L(\hat{a} - a^*) + \dot{a^*} \\ a^* &= g(t) \end{aligned}$$

Where we have used $a^* = g(t)$ with the scheduled function $g(t)$. Note the added term $\dot{a^*}$, which transforms the input perturbation v of Theorem 1 in Chapter 3 to $v = [P^{1/2}d, \Gamma^{-1/2}(L(a^* - a) + (\dot{a^*} - \dot{a})]^T$. This means we have direct means to reduce not only parametric uncertainty $a^* - a$ but also parameter variation $\dot{a^*} - \dot{a}$ independent of the size of gains Γ and L, which can be used to attenuate these uncertainties. In particular, when $d = 0$ and the estimate $g(t) = a(t)$, the tracking error goes to zero. The extra term $\dot{a^*}$ is usually not used since such information is not assumed to be available in general. However, this is consistent with LPV control design assumptions [70, 40], yet with guaranteed stability and no concern if $g \neq a$. However, it is assumed that this estimate, $g(t)$, is a better guess of the

actual value of $a(t)$ than a single constant guess else controller scheduling is unnecessary.

6.3.1 Parameter Scheduling Control Simulations

Consider the following 2^{nd} order plant of relative degree 1 of Chapter 3:

$$\begin{aligned} \dot{x}_1 &= a_1 x_1^3 + x_2 + (1 + x_1^2) b_1 u + d \\ \dot{x}_2 &= a_2 x_1 + (1 + x_1^2) b_2 u \\ y &= x_1 + n \end{aligned} \tag{6.2}$$

Where u, d, and n are the control signal, disturbance, and measurement noise, respectively. Let $a_1 = -3, a_2 = -2, b_1 = 5, b_2 = 4$ be the nominal plant parameter values parameterized by a parameter vector a and let $a^* = a$ be the choice corresponding to the non-switching adaptive control procedure for this system. The control design is based on the backstepping design procedure [33], which is modified along the lines of the developed methodology, see Chapter 5 for detailed design procedures. Let us choose the nominal gains $C = 10$ (feedback gain), adaptation filter gain $L = 10I$, where I is the identity matrix, then we have from Theorem 1 that the decay rate $\alpha = 10$ rad/sec. This should yield a settling time of at most 0.4 seconds for the closed loop system. Also the nominal value of the adaptation gain $\Gamma = I$ will be used. The nominal disturbance is set to $d = 0$.

First consider switching the plant parameter a_2 according to:

$$a_2 = \begin{cases} 98 & \text{if } 10 \leq t < 20 \\ -2 & \text{otherwise} \end{cases}$$

This yields three operating modes for the system, which starts at the nominal parameter values, switches parameter a_2, and then switches back to the nominal operating conditions. Figure 6-1 shows the response of the system tracking a setpoint of 2. Clearly, the tracking error is zero in mode 1 (before $t = 10$ seconds) and mode 3 (after $t = 20$ seconds) since $a^* = a$ during these modes yet the large switch in a_2 from its nominal value causes large

error during the time interval $t \in (10, 20)$. However, introducing a time-driven scheduled controller switching at times 10 and 20 seconds to match changes in a_2, yields perfect tracking except for small transient error during mode transitions from which the system settles within the pre-specified 0.4 seconds (for a closed loop bandwidth of 10 rads/seconds). The figure also shows that choosing a better guess of a, even if not an exact match, improves tracking error since it reduces the size of the input $a^* - a$. This is seen in the inexact switching case where a^* uses 70% of a_2 instead of a_2 for the 2^{nd} mode's parameter estimate. Whereas, Figure 6-2 shows the response of the parameter estimates $\hat{a}$ with the exact scheduled controller. As expected, the estimate corresponding to a_2 responds to step changes in input a^* at the controller switching times.

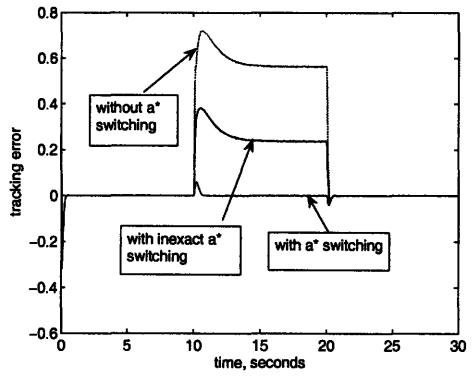

Figure 6-1: Tracking error for standard and scheduled adaptive controller for plant switching of a_2.

Next, Figure 6-3 reproduces the situation of Figure 6-1 but with the addition of a disturbance $d = 5\ \sin(2\pi t)$, see Equation (6.2). Again the same trend is seen with controller switching improving tracking error. This Figure highlights that reducing the size of input $a^* - a$ improves tracking error independent of the presence of disturbances as predicted by the analysis of Chapter 3.

Now consider an output-based switching of a_2 depending on operating regime:

$$a_2 = \begin{cases} 98 & \text{if } y > 3 \\ -2 & \text{otherwise} \end{cases}$$

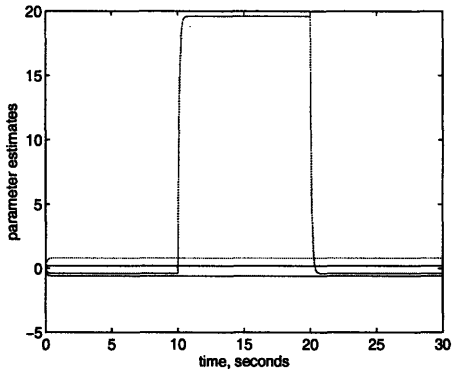

Figure 6-2: Parameter estimates for scheduled adaptive controller for plant switching of a_2.

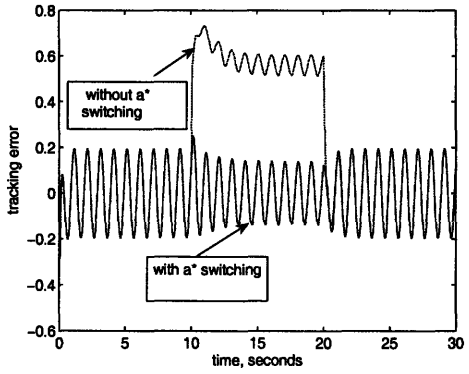

Figure 6-3: Tracking error for standard and scheduled adaptive controller for plant switching of a_2 with sinusoidal disturbance.

Figure 6-4 shows the response of the systems with the standard and switched controller for tracking a reference of 2 except at the time period $t \in (10, 20)$ where a step change in reference occurs from 2 to 4 at $t = 10$ seconds and back to a reference of 2 at $t = 20$ seconds. This choice of reference forces the system with output-based switching to behave similarly to the time-driven switching system of Figure 6-1. In Figure 6-4, output based switching of a^* was used instead of time-driven switching and the performance is similar to that of Figure 6-1 with the exception of brief oscillations during the transition for the case without controller switching. It is interesting to note that despite the oscillations in the non-switching controller case, the case with scheduled switching controller displays very

little difference from the time-based scheduling case.

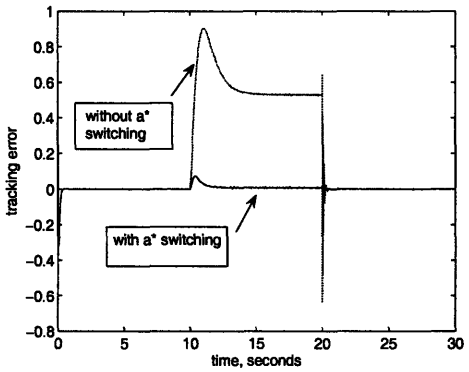

Figure 6-4: Tracking error for standard and scheduled adaptive controller for plant switching of a_2 for output driven switching.

Next, consider switching the plant parameter a_1 according to:

$$a_1 = \begin{cases} 2 & \text{if } 10 \leq t < 20 \\ -3 & \text{otherwise} \end{cases}$$

Note that changing the sign of a_1 from a negative to a positive value causes the plant to become unstable. Figure 6-5 reproduces the situation in Figure 6-1 but using a_1 switching. Observe that for non-switching controller, the tracking error oscillates during mode 2 unlike in Figure 6-1 where the $a^* - a$ mismatch yields a constant error. This is the case since during mode 2 the plant becomes unstable, a_1 positive, yet the nominal a^* estimate used assumes a stable plant, negative a_1. However, the scheduled switching controller eliminates these oscillations and yields performance similar to that seen in earlier situations. An interesting observation when the plant is unstable is that overshoot during mode transitions is larger than with stable plants, which is expected since an unstable plant is harder to control at least during transients. Figure 6-6 shows how switching the scheduled controller slightly earlier, at $t = 9$ seconds instead of $t = 10$ seconds, can significantly reduce the overshoot due to plant switching from a value of 1.8 to 0.8, which are contrasted with a value of 2.2 for the standard non-switching controller.

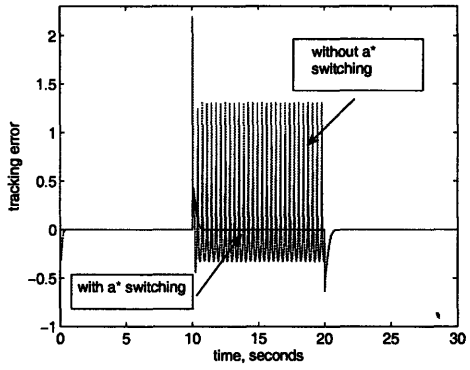

Figure 6-5: Tracking error for standard and scheduled adaptive controller for plant switching of a_1.

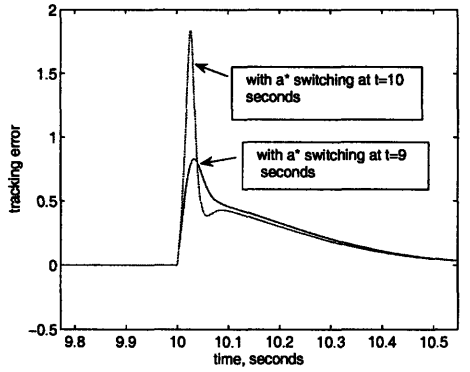

Figure 6-6: Effect of controller switching time on tracking error for scheduled adaptive controller for plant switching of a_1.

6.4 Multiple Model Control

In this section, another approach to utilize available modeling data about the controlled system is presented. In particular, the multiple model algorithm, which has received considerable interest in the last several years in the control community, will be used in two different implementations.

This line of work is known as multiple model adaptive or supervisory control were a plant is assumed to belong to a set of known plants from available data and candidate controllers are switched between based on estimation to control the plant. The supervisory

control work of [1, 86] and related references therein, uses LTI controllers and estimation-based switching between controllers is made in order to implement the best possible controller. As noted by the authors the problem of freezing an unstable plant/controller configuration is a concern to safety. Furthermore, the stability of the overall system, even when each frozen configuration is stable, needs to be verified via conservative and usually difficult to satisfy conditions. Other methods based on a conventional adaptive control architecture have been developed via re-initializing the adaptation by switching between fixed estimates or resetting the adaptive estimate during transients. However, as suggested by the authors in [49, 29, 52], these efforts are solely for improving transients, which is possible only if such fixed estimates are good. All of these efforts were for a an LTI plant yet a few of the multiple model control schemes considered infrequent jumps and slowly varying parameters of a linear system [86]. Similar ideas were introduced for classes of nonlinear systems, see for instance [31, 75].

On the other hand, the developed approach to multiple model control relies on adjusting the chosen estimate a^* by switching between different candidate plant parameter vectors. In this regard, the known candidate data models will be represented by the aforementioned candidate plant parameter vectors and a multiple model estimation scheme will be used to update a^*. Therefore, adjusting the estimate a^* by switching between different candidates, which can be any piecewise continuous bounded function, such that $\|a^* - a\|$ is reduced will improve tracking error. Note that unlike most of the existing approaches such as that in [1] there is no concern here in having an unstable plant/controller configuration by picking a "wrong controller" since any a^* will not destabilize the system and controller switching of a^* does not introduce any concern with overall system stability unlike in [1] where an average dwell time condition needs to be satisfied.

6.4.1 The Multiple Model Estimator

This section describes the multiple model estimator, which will be used with the multiple model algorithms of the next two sections. The focus is on systems in parametric-strict output feedback form. Whereas, the full state feedback case of Chapter 5 and the compan-

ion form systems of Chapter 4 are ignored since they are similarly treated with more states measured. Recall from Chapter 5 that that parametric output feedback systems are given by:

$$\begin{aligned}
\dot{x} &= Ax + \phi_0(y) + \sum_{j=1}^{p} \phi_j(y)^T \theta_i + b\beta(y)u + \bar{d} \\
y &= c^T x \\
A &= \begin{bmatrix} 0 & \\ \vdots & I_{(n-1)\times(n-1)} \\ 0\ldots & 0 \end{bmatrix}, \; b = \begin{bmatrix} 0_{(\rho-1)\times 1} \\ b_m \\ \vdots \\ b_o \end{bmatrix}, \; c = \begin{bmatrix} 1 \\ 0_{(n-1)\times 1} \end{bmatrix}
\end{aligned} \tag{6.3}$$

where known vector functions $\phi_j(y) = [\phi_{j,1}(y), \ldots, \phi_{j,n}(y)]^T$, with $0 \leq j \leq p$. Also $\theta = [\theta_1, \theta_2, \ldots, \theta_m]^T$ with θ_i and b_i the unknown system parameters. The vector $\bar{d}$ is the disturbance. The objective of the multiple model estimator is to adjust the estimate a^*

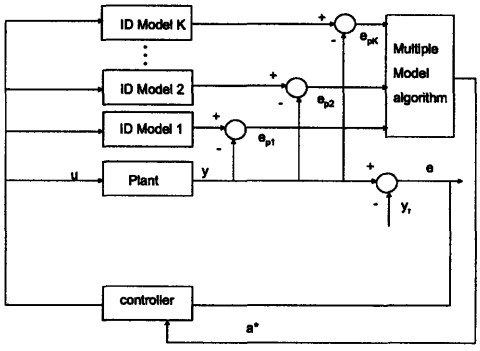

Figure 6-7: Schematic of Multiple Model Architecture.

so that the closer a^* is to the actual plant parameter a, the better the tracking error is as suggested by chapter 3. The idea is to construct K observers (identification models) for the system given by Equation (6.3) each parameterized by values corresponding to a candidate parameter vector from the set of parameter vectors $\{a_k | k = 1, 2, \ldots K\}$, see Figure 6-7 for

a schematic. These vectors correspond to available data. The k^{th} observer is given by:

$$\begin{aligned} \dot{x}_k &= Ax_k + k(y - c^T x_k) + \Phi(y)\theta_k + b_k\beta(y)u \\ y_k &= c^T x_k \end{aligned} \tag{6.4}$$

Where A and c given by Equation (6.3) and filter gain vector k is chosen such that the matrix $A - kc^T$ is Hurwitz, which is possible due to observability of the pair (A, c^T) by construction. Using Equations (6.3) and (6.4) we get:

$$\begin{aligned} \dot{\tilde{x}}_k &= (A - kc^T)\tilde{x}_k + v_k \\ e_{pk} &= C\tilde{x}_k \end{aligned}$$

where

$$v_k = \Phi(y)\Delta\theta_k + \Delta b_k u + \bar{d}$$

where $\tilde{x}_k = x - x_k$ is the state estimation error and $\Delta\theta_k = \theta - \theta_k$, and $\Delta b_k = b - b_k$. The system above is a linear system with $\tilde{x}_k$ driven by an input v_k composed of model mismatch terms and process noise . Therefore, if we pick $A - kc^T$ as a Hurwitz matrix , which is possible since the candidate models are detectable, we have an internally exponentially stable system with $\tilde{x}_k$ as a state. We can see that the size of the state estimation error $\tilde{x}_k = x - x_k$ is proportional to the size of the model mismatch $a - a_k$ represented by the terms $\Delta\theta_k = \theta - \theta_k$, and $\Delta b_k = b - b_k$. Note that the disturbance and measurement noise also contribute to the size of the prediction error. Thanks to the ability of the basic algorithm developed in Chapter 3, perturbations depending on $\Phi(y)$ and u are bounded for any bounded choice of a^* and thus the multiple model estimation is possible. Note that if y was unbounded due to an implemented destabilizing controller, the prediction error would go unbounded even for the best model unless its a perfect match $\Delta\theta_k = \Delta b_k = 0$. Next, two different algorithms to adjust and update a^* using the estimators of Equation (6.4) are discussed.

6.5 Maximum likelihood Based Multiple Model Algorithm

This algorithm is based on a maximum likelihood concept in the sense that it picks the most likely model (parameter vector), among a finite set, given data observations. This entails a conditional probability, that if the prediction error of one model is small then this model is likely close to the actual plant. Therefore, one seemingly reasonable choice is to set:

$$a^* = \arg\min_{a_k} |e_{pk}|^2$$

This sets the current value of a^* to the one from the set $\{a_k | k = 1, 2, \ldots K\}$ with smallest prediction error $e_{pk} = y - y_k$. However, it is typically a better choice to replace this instantaneous cost with an integral cost such that past measurements are also included. In addition, a forgetting factor is included to adjust how much of this past data is relevant, this is important for time varying systems, which yields:

$$a^* = \arg\min_{a_k} \mu_k \tag{6.5}$$

where the k^{th} monitoring signal μ_k is given by:

$$\mu_k = \int_{t_o}^{t} e^{-\lambda(t-\tau)} |e_{pk}(\tau)|^2 d\tau\,, \quad \mu_k(t_o) = 0 \; \forall \, k \tag{6.6}$$

where $\lambda > 0$ is a forgetting factor.

In summary, the maximum likelihood based multiple model scheme is given by the following procedure:

1. Given a set of K candidate models obtain the corresponding set of candidate parameter vectors $\{a_k | k = 1, 2, \ldots K\}$.

2. Implement an initial controller with $a^*[0] = a_1$, which is the choice with highest prior probability (an arbitrary choice would be used if all have the same probability).

3. Simultaneously simulate K parallel observers (identification models) with the k^{th} observer for the k^{th} candidate model parameterized by a parameter vector a_k accord-

ing to Equation (6.4).

4. Obtain the prediction errors $\{e_{pk} = y - y_k | k = 1, 2, \ldots K\}$, where y is the output of the actual plant and y_k is the output of the k^{th} identification system.

5. Construct the monitoring signals μ_k with a chosen forgetting factor λ according to Equation (6.6).

6. Every specified sampling period T set

$$a^*[T(i+1)] = \arg\min_{a_k} \mu_k$$

and set $i = i + 1$.

6.5.1 Relation to Maximum Likelihood Estimation

The algorithm discussed is closely related to the maximum likelihood estimation algorithm [39], where one wants to maximize the likelihood of obtaining the data, which has been actually observed. The optimal parameter estimate is thus the one which maximizes this likelihood:

$$a^* = \arg\max_{a_k} L(y(t)|a_k, Y(t))$$

Where $L(y|a_k, Y)$ is the likelihood function associated with each model, a conditional probability function, which will be assumed gaussian with mean y_k and variance σ^2 :

$$L(y|a_k, Y) = \frac{1}{\sqrt{2\pi}\sigma} \exp[-\frac{1}{2\sigma^2}(y - y_k)^2]$$

Where Y is a vector representing past observations of measurement y. The problem is equivalent to:

$$a^* = \arg\max_{a_k} \ln L(y|a_k, Y) \tag{6.7}$$

Substituting the assumed form for the likelihood function $L(y|a_k, Y)$ in Equation (6.7) we get:

$$\begin{aligned} a^* &= \arg\max_{a_k} -\ln\sqrt{2\pi}\sigma - \frac{1}{2\sigma^2}(y - y_k)^2 \\ &= \arg\min_{a_k} |e_{pk}|^2 \end{aligned} \tag{6.8}$$

Which is the same criteria used earlier. The above result is obtained by ignoring constants in the maximization and due to the fact that $\max f = \min(-f)$. Then introducing a forgetting factor gives the final criteria used in Equation (6.5). However, the main problem with this approach arises here due to the hypothesis that $|y - y_k|$ small implies $\|a - a_k\|$ small, which is weakened as the contribution of process and measurement noise increases. The next case study will analyze the response of the algorithm under various situations.

6.5.2 Maximum likelihood Based Multiple Model Control Simulations

Consider the following linear 2^{nd} order plant of relative degree 1:

$$\begin{aligned} \dot{x}_1 &= \theta_1 x_1 + x_2 + b_1 u + d \\ \dot{x}_2 &= \theta_2 x_1 + b_2 u \\ y &= x_1 + n \end{aligned} \tag{6.9}$$

Where u, d, and n are the control signal, disturbance, and measurement noise, respectively.

The control design is based on the backstepping design procedure [33], which is modified along the lines of the developed methodology, see Chapter 5 for detailed design procedures. Let us choose the nominal gains $C = 10$ (feedback gain), adaptation filter gain $L = 10I$, where I is the identity matrix, then we have from Theorem 1 that the decay rate $\alpha = 10$ rad/sec. This should yield a settling time of at most 0.4 seconds for the closed loop system. Also the nominal value of the adaptation gain $\Gamma = I$ will be used. The nominal disturbance is set to $d = 0$ and the system is forced to track a setpoint reference of 2. The

plant parameter values are given by $\theta_1 = -3, b_1 = 5$ and:

$$\theta_2 = \begin{cases} 98 & \text{if } 10 \leq t < 20 \\ -2 & \text{otherwise} \end{cases}$$

$$b_2 = \begin{cases} 4 & \text{if } t \leq 20 \\ 24 & \text{otherwise} \end{cases}$$

This yields three operating modes for the system, for which the overall parameter vector a switches. We are given five candidate models M_i for the multiple model estimation, which correspond to parameter vectors a_i:

$$\begin{aligned} M_1(s) &= \frac{5s+4}{s^2+3s+2} \Rightarrow a_1 \\ M_2(s) &= \frac{5s+4}{s^2+3s-98} \Rightarrow a_2 \\ M_3(s) &= \frac{5s+24}{s^2+3s+2} \Rightarrow a_3 \\ M_4(s) &= \frac{10s+500}{s^2+30s+20} \Rightarrow a_4 \\ M_5(s) &= \frac{2s+20}{s^2+03s+100} \Rightarrow a_5 \end{aligned}$$

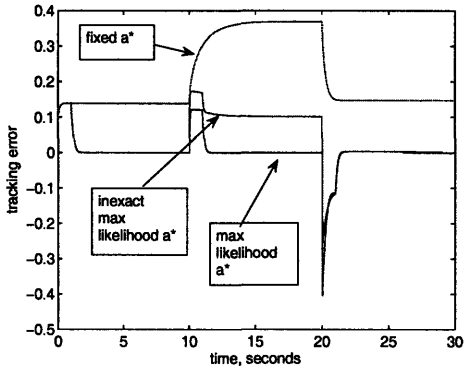

Figure 6-8: Tracking error for exact and inexact maximum likelihood based multiple model adaptive controller.

Note that since each model is an LTI system, we have used transfer functions to rep-

resent them for simplicity. The actual system switches between models $1, 2$ and 3 in that order, whereas models 4 and 5 are incorrect models for the situation under consideration. When switching from mode 1 (model 1) to mode 2 (model 2) the poles of the system change and the system becomes unstable. Whereas, switching from mode 2 to 3 (model 3) the poles are switched back to mode 1 values but the zero location is changed. In addition, these switches all cause changes in the DC gain of the plant. In the simulations, the system is initialized with an incorrect model $a^* = a_5$, the supervisor uses a sampling time of $T = 1$ second, and a forgetting factor of $\lambda = 2$ rads/seconds unless otherwise specified.

Figure 6-8 shows the response of the switching system with a maximum likelihood based multiple model controller and a fixed a^* controller with $a^* = a_5$, which is the model used for initializing the multiple model algorithm. The multiple model controller quickly switches the choice of a^* from the initial incorrect vector a_5 to the actual value a_1 using the multiple model estimator, which yields zero tracking error. The same trend continues when the plant switches to mode 2 and mode 3 at times $t = 10$ and $t = 20$ seconds, respectively. Whereas, the fixed a^* controller, although remains stable, maintains a larger tracking error which changes with the mismatch between the choice $a^* = a_5$ and the actual active model a_i. The Figure also shows the response of the maximum likelihood controller when the plant is perturbed by changing parameters θ_2 and b_2 to:

$$\theta_2 = \begin{cases} 198 & \text{if } 10 \leq t < 20 \\ -2 & \text{otherwise} \end{cases}$$

$$b_2 = \begin{cases} 4 & \text{if } t \leq 20 \\ 44 & \text{otherwise} \end{cases}$$

As a result the actual models used by the multiple model controller do not match any of the actual system modes. Nevertheless, the multiple model estimator still improves the tracking error significantly compared to the fixed model controller and chooses the closest available models. Figure 6-9 shows the response of the implemented a^* vector generated by the multiple model estimator, which undergoes switching in its elements consistent with the observed tracking response of Figure 6-8.

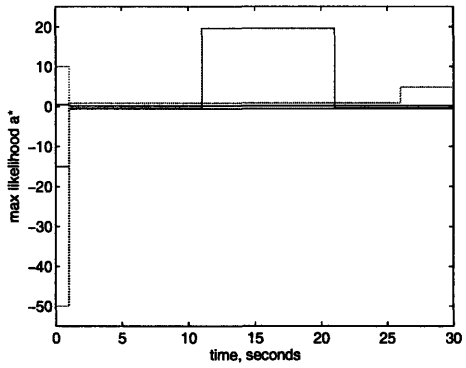

Figure 6-9: Implemented maximum likelihood based multiple model a^* for adaptive controller.

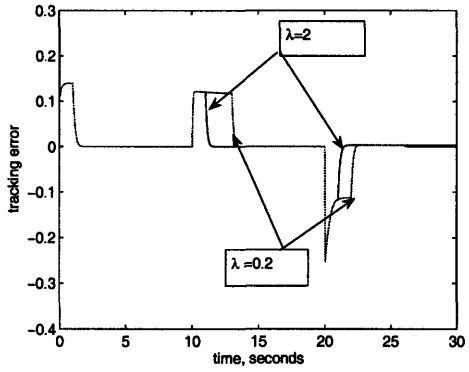

Figure 6-10: Effect of forgetting factor λ on tracking error for maximum likelihood based multiple model adaptive controller.

Next, Figure 6-10 shows the effect of the choice of forgetting factor λ in the estimator on the multiple model controller's response to plant switching. The multiple model control situation of Figure 6-8 with $\lambda = 2$ is repeated and contrasted with the same controller using a forgetting factor of $\lambda = 0.2$ for the maximum likelihood estimation. Clearly, the controller with smaller forgetting factor responds slower to plant switching and thus the tracking error remains large for a longer period of time before zero tracking error is achieved by both controllers. This highlights the importance of the choice of an adequate forgetting factor relative to the time scale of the plant of interest. However, a very large forgetting factor may yield excessive adjustment and switching of the controller depending

on the models used and the system's monitored response.

In addition, Figure 6-11 tests the effect of different initializations of the multiple model maximum likelihood based estimator. The standard choice of $a^* = a_5$ is contrasted with $a^* = a_1$, which is the correct choice for mode 1 of the system. The response is identical with the exception that the first controller switch made from $a^* = a_5$ to $a^* = a_1$ is eliminated since the correct choice $a^* = a_1$ is already used.

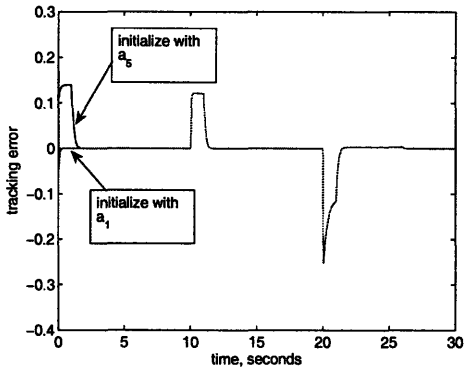

Figure 6-11: Effect of initial a^* on tracking error for maximum likelihood based multiple model adaptive controller.

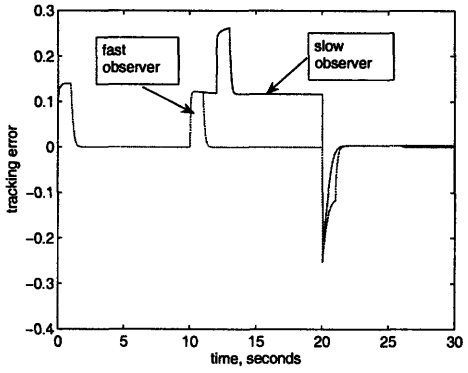

Figure 6-12: Effect of observer (identification model) gain on tracking error for maximum likelihood based multiple model adaptive controller.

Next, Figure 6-12 demonstrates the effect of observer (identification model) dynamics' speed through reducing the observer gain k in Equation (6.4). The eigenvalues of the

observer's system matrix $A-kc^T$ have been reduced from $-88, -11$ to about $-0.08, -0.01$, which is very slow compared to the plant switching speed. Therefore, the algorithm fails to adequately identify the correct model within an acceptable time. Another important parameter to be tuned in the algorithm is the sampling period T. The effect of increasing the sampling period from the nominal $T = 1$ seconds to $T = 10$ seconds is shown in Figure 6-13. The result is a slower algorithm response, which fails to react soon enough to the plant transitions.

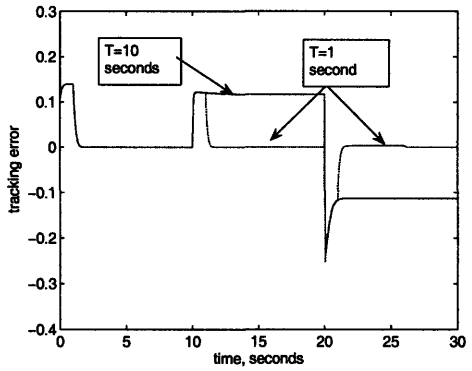

Figure 6-13: Effect of sampling period T on tracking error for maximum likelihood based multiple model adaptive controller.

Figure 6-14 tests the effectiveness of the multiple model controller in the presence of disturbances (process noise). The disturbance $d = 100\sin(2\pi t)$ is used in Equation (6.9). The same trend continues with the multiple model controller outperforming the fixed $a^* = a_5$ controller, as in Figure 6-8. The only observed difference is the sinusoidal contribution to the tracking error due to the disturbance yet reducing the effect of parametric uncertainty and variation on tracking error is similarly achieved. It is interesting to note that the actual chosen a^* values by the estimator do not match those of the plant, see Figure 6-15, unlike in the disturbance free case of Figure 6-9. This is observed for the third mode only but is generally expected since the estimator does not account for disturbances.

Nevertheless, the maximum likelihood based controller performs almost as well as an exact switching controller, Figure 6-14, which is chosen to switch to the right model at the mode switching times, i.e., assumes exact plant information. This is seen as the responses

of the multiple model and exact switching controllers' match except at the first $1-2$ seconds for each mode within which the multiple model controller identifies and switches to the "best" controller. However, it is expected that a multiple model estimator of this type may select inappropriate models if process noise is excessively large, relative to the difference between models, and not accounted for in the estimator as in a Kalman filter, for example.

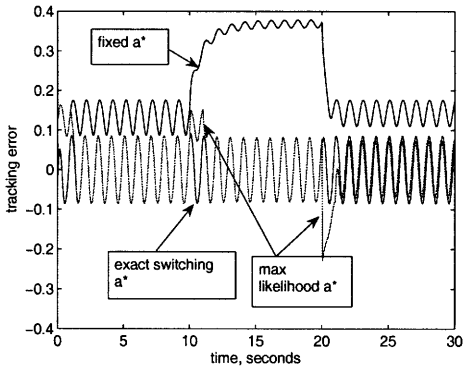

Figure 6-14: Tracking error for maximum likelihood based multiple model and fixed $a*$ adaptive controller with sinusoidal disturbance.

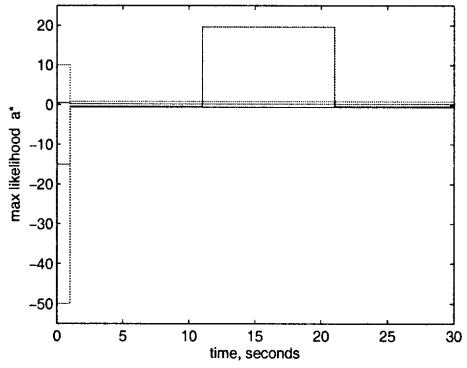

Figure 6-15: Implemented maximum likelihood based multiple model $a*$ for adaptive controller with sinusoidal disturbance.

6.6 Bayesian Based Multiple Model Algorithm

This section presents an alternative algorithm to update a^*, which is based on the Bayesian approach to learning. In particular, a prior probability $P_k = prob(a = a_k)$ is assigned to each candidate model (can use $P_k(0) = 1/K \; \forall \, k$ for K candidate models unless more specific information is available) and then these probabilities are updated to form weights for their corresponding candidate parameters a_k, in order to compute a^* as a weighted average:

$$a^* = \sum_{k=1}^{K} w_k a_k \tag{6.10}$$

This is simply the expected value for a discrete probability problem as this one where the k^{th} weight w_k is given by:

$$w_k(i) = \frac{P_k(i)}{\sum_{k=1}^{K} P_k(i)} \; \forall \, k \tag{6.11}$$

The posterior probability of the k^{th} model P_k is updated as follows:

$$P_k(i+1) = \frac{e^{-c|e_{pk}(i)|^2} P_k(i)}{\sum_{k=1}^{K} e^{-c|e_{pk}(i)|^2} P_k(i)} \; \forall \, k \tag{6.12}$$

Where, $c > 0$ is a tuning factor, reflecting the inverse of the variance and effecting the speed of convergence of the estimation.

In summary, the Bayesian based multiple model scheme is given by the following procedure:

1. Given a set of K candidate models obtain the corresponding set of candidate parameter vectors $\{a_k | k = 1, 2, \ldots K\}$ with prior probabilities $P_k(0)$(use $P_k(0) = 1/K$ $\forall \, k$ unless more specific information is available).

2. Implement an initial controller with $a^*[0] = \sum_{k=1}^{K} w_k(0) a_k$, where $w_k(0)$ are computed according to Equations (6.11), respectively.

3. Simultaneously simulate K parallel observers (identification models) with the k^{th}

observer for the k^{th} candidate model parameterized by a parameter vector a_k according to Equation (6.4).

4. Obtain the prediction errors $\{e_{pk} = y - y_k | k = 1, 2, \ldots K\}$, where y is the output of the actual plant and y_k is the output of the k^{th} identification system.

5. Every specified sampling period T construct the posterior probabilities $P_k(i)$ and weights $w_k(i)$ according to Equations (6.12) and Equations (6.11), respectively.

6. Every specified sampling period T set a^* according to :

$$a^*[T(i+1)] = \sum_{k=1}^{K} w_k(i) a_k$$

and set $i = i + 1$.

6.6.1 Relation to Bayesian Learning

The Bayes rule in probability states that:

$$P(A_k|B) = \frac{P(B|A_k)P(A_k)}{P(B)}$$

Which means that probability that event A_k occurs given event B is given by the conditional probability $P(B|A_k)$ times the probability of A_k occurring itself divided by the probability of B occurring. Given a discrete probability problem, this can be re-written as:

$$P(A_k|B) = \frac{P(B|A_k)P(A_k)}{\sum_{i=1}^{n} P(B|A_i)P(A_i)}$$

In terms of the multiple model problem, the posterior probability of model k being correct given the observed data is given by:

$$P_k(i+1) = \frac{p(y(i)|a_k, Y(i-1))\, P_k(i)}{\sum_{k=1}^{K} p(y(i)|a_k, Y(i-1))\, P_k(i)} \quad \forall\, k \tag{6.13}$$

where $P_k(i)$ the prior probability of model k, $Y(i-1) = [y(i-1), y(i-2), \ldots, y(0)]$ is the past observed data up to step i, and $p(y(i)|a_k, Y(i-1))$ is the conditional probability density of the observed data given a_k and past observations.

The developed algorithm assumes independent samples y_k for models a_k and that the conditional probability density $p(y(i)|a_k, Y(i-1))$ is gaussian with mean y_k and variance $1/(2c)$:

$$p(y(i)|a_k, Y(i-1)) = e^{-c|e_{pk}(i)|^2} \; \forall \, k$$

Substituting this in Equation (6.13) yields the used update expression in Equation (6.12).

6.6.2 Bayesian Based Multiple Model Control Simulations

Consider the following linear 2^{nd} order plant of relative degree 1 :

$$\begin{aligned} \dot{x}_1 &= \theta_1 x_1 + x_2 + b_1 u + d \\ \dot{x}_2 &= \theta_2 x_1 + b_2 u \\ y &= x_1 + n \end{aligned} \tag{6.14}$$

where u, d, and n are the control signal, disturbance, and measurement noise, respectively.

The control design is based on the backstepping design procedure [33], which is modified along the lines of the developed methodology, see Chapter 5 for detailed design procedures. Let us choose the nominal gains $C = 10$ (feedback gain), adaptation filter gain $L = 10I$, where I is the identity matrix, then we have from Theorem 1 that the decay rate $\alpha = 10$ rad/sec. This should yield a settling time of at most 0.4 seconds for the closed loop system. Also the nominal value of the adaptation gain $\Gamma = I$ will be used. The nominal disturbance is set to $d = 0$ and the system is forced to track a setpoint reference of 2. The

plant parameter values are given by $\theta_1 = -3, b_1 = 5$ and:

$$\theta_2 = \begin{cases} 98 & \text{if } 10 \leq t < 20 \\ -2 & \text{otherwise} \end{cases}$$

$$b_2 = \begin{cases} 4 & \text{if } t \leq 20 \\ 24 & \text{otherwise} \end{cases}$$

This yields three operating modes for the system, for which the overall parameter vector a switches. We are given five candidate models M_i for the multiple model estimation, which correspond to parameter vectors a_i:

$$\begin{aligned} M_1(s) &= \frac{5s+4}{s^2+3s+2} \Rightarrow a_1 \\ M_2(s) &= \frac{5s+4}{s^2+3s-98} \Rightarrow a_2 \\ M_3(s) &= \frac{5s+24}{s^2+3s+2} \Rightarrow a_3 \\ M_4(s) &= \frac{10s+500}{s^2+30s+20} \Rightarrow a_4 \\ M_5(s) &= \frac{2s+20}{s^2+03s+100} \Rightarrow a_5 \end{aligned}$$

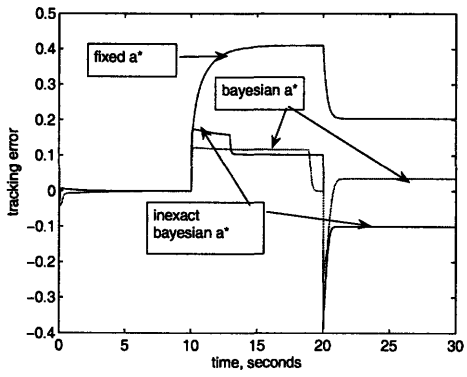

Figure 6-16: Tracking error for exact and inexact Bayesian based multiple model adaptive controller.

Note that since each model is an LTI system, we have used transfer functions to represent them for simplicity. The actual system switches between models $1, 2$ and 3 in that

order, whereas models 4 and 5 are incorrect models for the situation under consideration. When switching from mode 1 (model 1) to mode 2 (model 2) the poles of the system change and the system becomes unstable. Whereas, switching from mode 2 to 3 (model 3) the poles are switched back to mode 1 values but the zero location is changed. In addition, these switches all cause changes in the DC gain of the plant. In the simulations, the system is initialized with prior probabilities $P_k(0) = 1/5$ for all k, meaning each model is assumed to have the same probability. The supervisor uses a sampling time of $T = 0.01$ seconds, and a tuning factor of $c = 10$ unless otherwise specified.

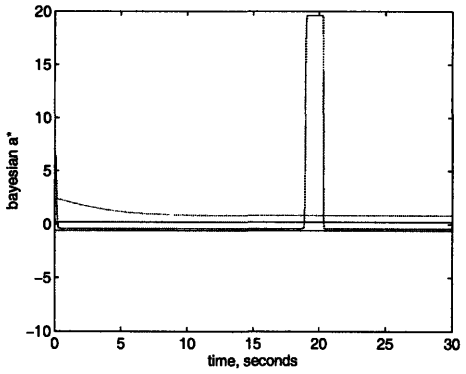

Figure 6-17: Implemented Bayesian based multiple model a^* for adaptive controller.

Figure 6-16 shows the response of the switching system with a multiple model Bayesian controller for the same situation of Figure 6-8. The tracking error is shown with a Bayesian controller and a fixed a^* controller with a^* as the average of vectors a_i from the five models, which is the initial choice for the Bayesian learning algorithm with $P_k(0) = 1/5$. The Bayesian multiple model estimator quickly adjusts a^*, which significantly improves tracking error compared to the fixed a^* controller. Nevertheless, the Bayesian multiple model controller is unable to yield zero tracking for any of the modes unlike the maximum likelihood multiple model controller of Figure 6-8. This can be seen from the corresponding a^*, see Figure 6-17, which does not select the best current model and switch after each mode change as the maximum likelihood based a^* of Figure 6-9 does. The Figure also shows the response of the controller when the plant is perturbed by changing parameters θ_2 and b_2 to:

$$\theta_2 = \begin{cases} 198 & \text{if } 10 \leq t < 20 \\ -2 & \text{otherwise} \end{cases}$$

$$b_2 = \begin{cases} 4 & \text{if } t \leq 20 \\ 44 & \text{otherwise} \end{cases}$$

As a result the actual models used by the controller do not match any of the actual system modes. Nevertheless, the Bayesian estimator still improves the tracking error significantly compared to the fixed model controller.

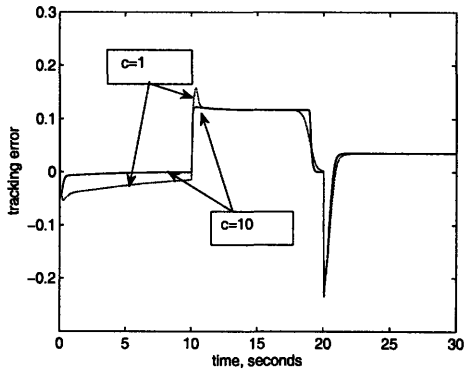

Figure 6-18: Effect of tuning factor c on tracking error for Bayesian based multiple model adaptive controller.

Next, Figure 6-18 shows the effect of the choice of tuning factor c in the Bayesian estimator on the multiple model controller's response to plant switching. The control situation of Figure 6-16 with $c = 10$ is repeated and contrasted with the same controller using a tuning factor of $c = 1$. Clearly, the controller with smaller tuning factor responds slower to plant switching and thus the tracking error remains large for a longer period of time. This highlights the importance of the choice of an adequate tuning factor. However, a large tuning factor yields premature learning and quick convergence to a fixed controller that may be inadequate. This is the case since c reflects the inverse of the variance for a normal distribution and thus a large c suggests high confidence in prior data and thus little learning is needed.

In addition, Figure 6-19 tests the effect of different initializations of the Bayesian estimator. The standard choice of $P_k(0) = 1/5$ is contrasted with $P_1(0) = P_2(0) = P_3(0) = 1/3$ and $P_4(0) = P_5(0) = 0$. The latter choice corresponds to zero prior probability for models 4 and 5, which are incorrect models. This is clearly a better initialization choice for the algorithm since it ignores the incorrect models. Therefore, the tracking error is reduced and the learning is quicker with the modified initial conditions for a tuning factor of $c = 1$. Note that the use of these different initial conditions for the nominal tuning factor $c = 10$ yielded very little improvement in tracking.

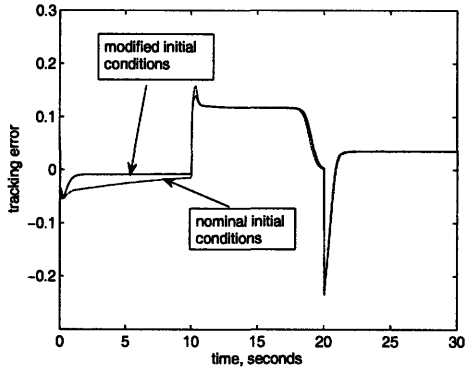

Figure 6-19: Effect of initial a^* on tracking error for Bayesian based multiple model adaptive controller.

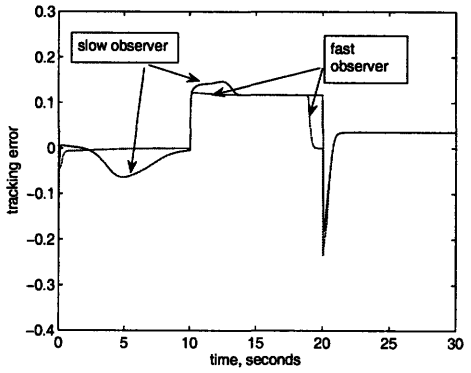

Figure 6-20: Effect of observer (identification model) gain on tracking error for Bayesian based multiple model adaptive controller.

Next, Figure 6-20 demonstrates the effect of observer (identification model) dynamics'

speed through reducing the observer gain k in Equation (6.4). The eigenvalues of the observer's system matrix $A-kc^T$ have been reduced from $-88, -11$ to about $-0.08, -0.01$, which is very slow compared to the plant switching speed. Therefore, the algorithm fails to adequately identify the correct model within an acceptable time. Another important parameter to be tuned in the algorithm is the sampling period T. The effect of increasing the sampling period from the nominal $T = 0.01$ seconds to $T = 1$ seconds is shown in Figure 6-21. The result is a slower and rougher response due to the coarse discrete-time updates.

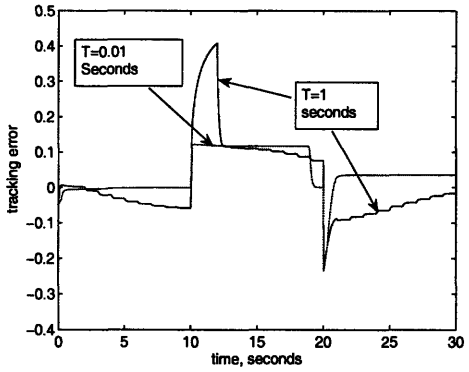

Figure 6-21: Effect of sampling period T on tracking error for Bayesian based multiple model adaptive controller.

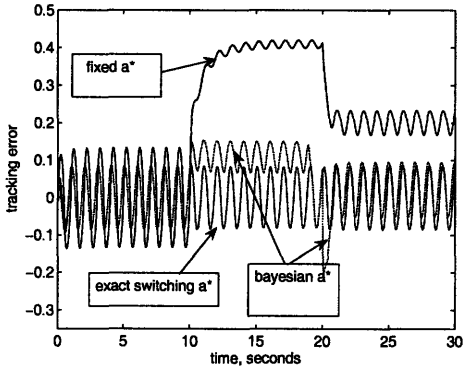

Figure 6-22: Tracking error for Bayesian based multiple model $a*$ adaptive controller with sinusoidal disturbance.

Figure 6-22 shows the response of the Bayesian controller in the presence of distur-

bances (process noise). The disturbance $d = 100\sin(2\pi t)$ is used in Equation (6.14). The same trend continues with the Bayesian controller outperforming the fixed a^* controller, as in the disturbance free case of Figure 6-16. It is interesting to note that the actual chosen a^* values by the estimator do not change much compared to the disturbance free case, see Figure 6-23 and Figure 6-17. Recall that Figure 6-15 shows an incorrect choice of models for the maximum likelihood multiple model algorithm with disturbances. This is an advantage for the Bayesian estimation algorithm over the multiple model algorithm since it does not attempt to choose the single best model, which could be poorly estimated in the presence of large process noise.

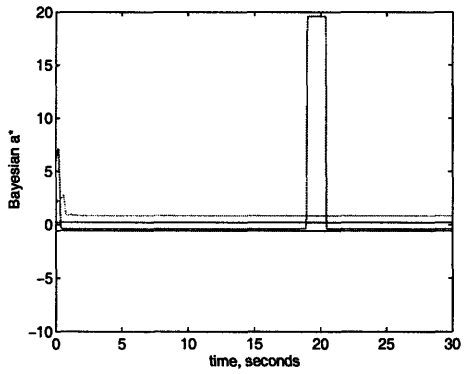

Figure 6-23: Implemented Bayesian based multiple model $a*$ for adaptive controller with sinusoidal disturbance.

6.7 Remarks

- The simple scheduled control results of Section 6.2 eliminates stability concerns with conventional gain scheduling and LPV techniques [70]. Furthermore, there is no controller redesign and tuning needed for each operating mode but simply a candidate vector of plant parameters a_k is used as the "controller" for each mode.

- The two approaches used for multiple model control have a different interpretation. The likelihood method returns the single most likely model (parameter) whereas the Bayesian method gives a weighted average of models.

- The Bayesian method is more dependent on a reliable prior probabilities in the sense that a model given a zero initial weight would never enter in the weighted average. Whereas, the likelihood method is more sensitive to good data as only one of the candidate models is chosen at a certain time period.

- Both approaches guarantee a bounded a^* since the multiple model algorithm can only select one of the given constant a_k values at a given period of time. Whereas, the Bayesian algorithm uses $a^* = \sum_{k=1}^{K} w_k a_k$ where $\sum_{k=1}^{K} w_k = 1$ by construction and thus $a^* \leq \max_k a_k$.

- In terms of implementation, the supervisor for the maximum likelihood based algorithm is just a system that computes the costs for each model and identifies the one of minimum cost every given period of time. Whereas, the supervisor in the Bayesian algorithm is a discrete-time nonlinear system with P_k as states and w_k as outputs.

- The sampling period T is enforced to be large enough to avoid chattering and excessive switching in the maximum likelihood based algorithm. Whereas in the Bayesian based algorithm, since it's a discrete-time system, it's made as small as possible to smooth out the implementation.

- Observe that from Sections 6.4.1 and 6.5.1 that the assumed likelihood function $L(y|a_k, Y)$ in the maximum likelihood based algorithm and the assumed conditional probability density $p(y(i)|a_k, Y(i-1))$ in the Bayesian based algorithm are similarly Gaussian with mean y_k for the k^{th} model. The main differences being the discrete-time nature of the used Bayesian algorithm and its explicit dependence on the choice of variance $1/(2c)$.

- Other versions of the multiple model maximum likelihood based algorithm could be used where the cost is a weighted sum of the prediction error $|e_{pk}|^2$ and an integral as the one used in Equation (6.6), see [48].

- Other Bayesian based variants of the multiple model estimator could be used such as a Kalman filter based algorithm with the tuning factor c updated with time for each

model using the covariance in the Klamn filter, see for instance [18]. Alternatively, if any information is assumed about the transition probabilities from one mode to the other, then such information could be used to improve the Bayesian based algorithm's response to plant switching, see for instance [28] for markovian switching systems.

- In case excessive process noise confuses the learning, a dead-zone could be introduced in the update law to avoid unnecessary adjustments to a^* if tracking error is below an acceptable threshold. This is more likely with the maximum likelihood algorithm, which chooses the single most likely identification model, which does not account for the presence of a disturbance. Alternatively, a Kalman filter could be used instead of an observer if covariance information about process noise is assumed available.

- As mentioned in Chapter 5, if the backstepping procedure is used $a^* \in C^{r-1}$, i.e., $r-1$ times continuously differentiable is required, where r is the relative degree of the plant. This can be circumvented by using a^* as an output of an r^{th} order low pass filter driven by any bounded piecewise continuous a^* produced by any of the switching algorithms discussed in this chapter.

6.8 Performance of Multiple Model Control Algorithms

In this section, the performance of multiple model control algorithms is discussed. It is a nontrivial task to predict how successful these algorithms would perform since following learning theory to see when the estimation of an accurate model will be made is neither trivial nor conclusive. This is the case since the tracking error may still be improved even if the best candidate model is not chosen, see for instance Figures 6-14 and 6-15. The presented algorithms can only theoretically guarantee stability and well defined dynamic response, via specified decay rate α, and that tracking error is reduced with decrease in size of $a^* - a$. The ability of such a learning algorithm to improve the tracking error depends on quality of used models, the tuning of the multiple model algorithm, and nature of the plant. As the figures in Sections 6.4.2 and 6.5.2 have demonstrated, observer gain k, sampling

period T, tuning factor c, and forgetting factor λ can significantly impact the system's behavior if they are poorly chosen. However, clear guidelines to choose these algorithm parameters in order to optimize performance are available:

- Choose observer (identification model) gain vector k such that the eigenvalues of the Hurwitz matrix $A - kc^T$ have large enough real parts for convergence to be fast enough relative to plant switching in order to detect it. Note that an excessively large gain k would amplify measurement noise.

- The sampling period T for a maximum likelihood algorithm has to be fast enough to allow for sufficiently fast controller switching/adjustment but not too fast to induce chattering due to excessive controller switching.

- The sampling period T for a Bayesian algorithm has to be fast enough to allow for sufficiently fast controller switching/adjustment and smoothen the discrete-time implementation, thus is typically much smaller than that of the maximum likelihood algorithm.

- The forgetting factor λ in the maximum likelihood based algorithm has to be large enough to detect switching but not too fast to overreact to unimportant transients.

- Tuning factor c in the Bayesian based algorithm has to be large enough to react to plant switching but not too fast to yield premature convergence, which depends on the size of $|e_{pk}|$. This is usually directly coupled to choice of observer gain since the input-output gain of the observer dynamics changes the size of its output $|e_{pk}|$.

These guidelines require some trial and error tuning to identify the appropriate values for the plant of interest but are usually not very sensitive to small changes. It is noteworthy that although the closed loop bandwidth of the control system will affect the performance of these learning algorithms, it is not included in the parameters to be adjusted. This is the case since it is a given control specification independent of choice of controller. Fortunately, when plan switching is too fast relative to the closed loop bandwidth, then its effect is attenuated due to system roll-off as shown in the analysis and simulations of Chapter 3.

Finally, it is assumed that good and well defined models/modes are available to the algorithm designer. Otherwise it is best to rely solely on optimizing feedback and adaptation gains as discussed in Section 3.3.2.

6.9 Summary

In this chapter, algorithms for time varying adjustment of the developed adaptive controllers using additional available data models are developed. Adjusting and updating the chosen parameter estimate a^* is proposed with no effect on system stability due its variation or its mismatch with the ideal plant parameters a. As a result, stable parameter scheduling and multiple model control algorithms are obtained. Two types of multiple model algorithms are presented, which are based on maximum likelihood and Bayesian learning techniques. Case studies and performance considerations have been discussed.

Chapter 7

Conclusions and Recommendations

The work presented in this thesis provides a leading effort in the synthesis of controllers for classes of time-varying switched systems. Switched systems are those governed by differential equations, which undergo vector field switching due to sudden changes in model characteristics. Such systems arise in many applications such as mechanical systems with contacts, electrical systems with switches, and thermal-fluidic systems with valves and phase changes.

The developed control methodology guarantees system stability, under typical adaptive control assumptions, for systems with piecewise differentiable bounded parameters and piecewise continuous disturbances without requiring a priori knowledge on such parameters or disturbances. A leakage-type adaptive controller is shown to achieve internal exponential and BIBS stability without need for persistence of excitation. The effect of plant variation and switching is reduced to piecewise continuous and impulsive inputs acting on this BIBS stable closed loop system. This, in turn, provides a separation between the robust stability and robust performance control problems. The developed methodology provides clear guidelines for steady-sate and transient performance optimization. In the presented simulations, the proposed controller demonstrated superior robustness of stability and performance as well as practical usability relative to non-adaptive and other adaptive methods such as projection and deadzone adaptive controllers.

The presented adaptive control methodology has been used to develop detailed control schemes for different classes of nonlinear switched systems. A robust adaptive con-

trol scheme has been presented in Chapter 4 for linearly-parameterized switched systems in MIMO companion form. The results are illustrated through a case study for contact-based manipulation via a 2-link planar manipulator. Furthermore, robust adaptive control schemes have been presented in Chapter 5 for linearly-parameterized switched systems in parametric-strict form and parametric-strict output feedback form. The results are illustrated through a case study for AFM based nano-manipulation.

In Chapter 6, algorithms for time varying adjustment of the developed adaptive controllers using additional available data models are developed. Adjusting and updating the chosen parameter estimate a^* is proposed with no effect on system stability due its variation or its mismatch with the ideal plant parameter vector a. As a result, stable parameter scheduling and multiple model control algorithms are obtained. Two types of multiple model algorithms are presented, which are based on maximum likelihood and Bayesian learning techniques.

The classes of systems for which the developed methodology applies are characterized by linearly-parameterized dynamics of known structure, exponentially stable zero dynamics, known and constant relative degrees and signs of the control direction, which are typical adaptive control assumptions. Detailed design procedures have been provided for certain important classes of systems. Future work should consider developing detailed design procedures for more classes of systems that fall under this methodology.

In addition, extensions to the work relaxing some of these typical adaptive control assumptions such as exponentially stable zero dynamics and linearly-parameterized dynamics would be of high value. However, this would require more fundamental work on adaptive control systems since successful adaptive control results for such systems are limited even in the constant parameters case. Such results typically involve significant modifications to typical adaptive control systems and thus would require more stand alone developments in order to extend them to switched systems, see for instance nonlinearly-parameterized systems in [31] and weakly non-minimum phase systems in [38]. It would also be of interest to relax other assumptions such as known and constant relative degree and sign of control direction, though they appear to be rarely violated in practical control applications. This appears to be possible since the adaptive control literature already contains some re-

sults relaxing some of these assumptions for some limited classes of systems with constant parameters though through somewhat different architectures, see for instance [85].

On the other hand, utilizing the ability of the developed control systems to perform stable gain scheduling and data-based control would be an important area of future development. The stability characteristics and nature of the control system's architecture has allowed for stable gain scheduling and data-based control design by adjusting a parameter vector in the adaptation law referred to as a^*. Future work should take further advantage of this capability by investigating other variants of maximum likelihood and Bayesian based learning algorithms, which already exist in the learning and estimation literature. It is expected that some versions of these algorithms may prove to be more effective than the ones presented in this thesis for some problems. Furthermore, any other method to adjust the parameter estimate vector a^* should be considered as long as this vector remains bounded since there would be no concerns with system stability. This is an important problem, which has been actively researched even for simpler time-invariant plants for which the stability of the closed loop system has been a limiting factor due to the choice of control architecture used.

Bibliography

[1] Anderson, B.D.O., Brinsmead, T.S., Liberzon, D., and Morse,A.S. Multiple model adaptive control with safe switching. *Int. J. Adaptive Control Signal Process.*, 15, 445-470, 2001.

[2] Angeli, D., and E. Mosca. Lyapunov-Based Switching Supervisory Control of Nonlinear Uncertain Systems. *IEEE Transactions On Automatic Control*, 47 (3), 500-505, 2002.

[3] Bedrosian, D., and J. Vlach. Time-Domain Analysis of Networks with Internally Controlled switches. *IEEE Transactions on Circuits and Systems-I: Fundamnetal Theory and Applications*, 39(3), 199-212, 1992.

[4] Branicky, M.S. Multiple Lyapunov functions and other stability tools for switched and hybrid systems. *IEEE Transactions on Automatic Control*, 43(4), 475-482, 1998.

[5] Cheng, D. Stabilization of Planar Switched Systems. *Systems and Control Letters*, 51, 79-88, 2004.

[6] Chang, T. Nonlinear Observer Design Using Contraction Theory with Application to Heat Exchangers Having Varying Phase Transition, *Ph.D. Thesis, Dept. of Mech. Eng., Massachusetts Institute of Technology*, 2006.

[7] Chang, Y. An Adaptive H^{∞} Tracking Control for a Class of Nonlinear Multiple-Input Multiple-Output (MIMO) Systems. *IEEE Transactions on Automatic Control*, 46 (9), 1432-1437, 2001.

[8] Decarlo, R. A. , Branicky, M. S., Pettersson,S., and B. Lennartson. Perspectives and Results on the Stability Stabilizability of Hybrid Systems, *Proceedings of The IEEE*, 88 (7), 1069-1082, 2000.

[9] DE JONG, H. Modeling and Simulation of Genetic Regulatory Systems: A Literature Review, *Journal Of Computational Biology*, 9 (1), 67-103, 2002.

[10] O. M. El Rifai, and K. Youcef-Toumi. Coupling in Piezoelectric Tube Scanners Used in Scanning Probe Microscopes, *American Control Conference*, Arlington, VA, June 2001.

[11] El Rifai,O. M. and K. Youcef-Toumi. Trade-offs and Performance Limitations in Mechatronic Systems: A Case Study, *Annual Reviews in Control*, 2, 2004.

[12] El Rifai,O. M. and K. Youcef-Toumi. On Automating Atomic Force Microscopes: An Adaptive Control Approach, *Control Engineering Practice*, 15(3), 349-361, 2007.

[13] El Rifai, K., El Rifai, O., and K. Youcef-Toumi. Modeling and Control of AFM-based Nano-manipulation Systems, *IEEE Conference on Robotics and Automation*, Barcelona, Spain, April 2005..

[14] El Rifai, K., El Rifai, O., and K. Youcef-Toumi. On Robust Adaptive Switched Control, *American Control Conference* , Portland, OR, June 2005.

[15] El Rifai, K.,and K. Youcef-Toumi. Robust Adaptive Scheduled Switched Control, *Conference on Decision and Control*, Seville, Spain, December 2005.

[16] Engel, S., G. Frehse, and E. Schnieder (Eds.) Modeling, Analysis, and Design of Hybrid Systems, LNCIS, *Springer Verlag*, 2002.

[17] Ge, S. and J. Wang. Robust Adaptive Tracking for Time-Varying Uncertain Nonlinear Systems With Unknown Control Coefficients, *IEEE Transactions on Automatic Control*, 48(8), 1463-1369, 2003.

[18] Fekri, S., Athans, M. and A. Pascoal. RMMAC: A Novel Robust Adaptive Control Scheme . Part I: Architecture, *IEEE Conference on Decision and Control*, Atlantis, Paradise Island, Bahamas, December 2004.

[19] Grange, S. , Conti,F., Helmer, P., Rouiller, P. and C. Baur. The Delta Haptic Device as a Nanomanipulator, *SPIE Microrobotics and Microassembly III*, Boston, MA, November 2001.

[20] Hespanha, J.P., Liberzon, D., Morse, A.S., Anderson, B.D.O., Brinsmead, T.S., and F.D. Bruyne. Multiple model adaptive control, Part 2: switching. *Int. J. Robust Nonlinear Control*, 10, 909-929, 2000.

[21] Hespanha, J.P., S. A. Morse. Switching between stabilizing controllers. *Automatica*, 38, 1905-1917, 2002.

[22] Hespanha, J.P.,Liberzon, D., S. A. Morse. Overcomingthe limitations of adaptive control by means of logic-based switching, *Systems and Control Letters*, 49, 49-65, 2003.

[23] Hespanha, J.P. Uniform Stability of Switched Linear Systems: Extensions of LaSalle's Invariance Principle, *IEEE Transactions on Automatic Control*, 49(4), 470-482, 2004.

[24] Horiguchi,S., Sitti,M., and H. Hashimoto. Visualization Interface for AFM-based Nano Manipulation, *IEEE Int. Symp. on Industrial Electronics*, Slovenia, July 1999.

[25] Hu, Z.,Zhang, B., and W. Deng. Output controllability of switched power converters as switched linear systems. *Power Electronics and Motion Control Conference*,Riga, Latvia, August 2004.

[26] Imai, A., Costa, R., Hsu, L., Tao, G., and P. Kokotovic. Multivariable MRAC using high frequency gain matrix factorization. *IEEE transactions on Automatic Control*, 49 (7), 1152-1157, 2004.

[27] Ioannou P. and J. Sun. Robust Adaptive Control, *Prentice-Hall*, 1996.

[28] Johnston, L. and V. Krishnamurthy. An Improvement to the Interacting Multiple Model (IMM) Algorithm,*IEEE Transactions On Signal Processing*, 49 (12), 2909-2923, 2001.

[29] Kalkkuhl, J., Johansen, T.A., and J. Ldemann. Improved Transient Performance of Nonlinear Adaptive Backstepping Using Estimator Resetting Based on Multiple Models, *IEEE transactions on Automatic Control*, 47(1), 136-140, 2002.

[30] Khalil, H. Nonlinear Systems, 2nd Ed., *Prentice-Hall*, 1995.

[31] Kojic, A., A. M. Annaswamy. Adaptive control of nonlinearlyparameterized systems with a triangular structure, *Automatica*, 38, 115123, 2002.

[32] Koutsoukos, X. D., and P. J. Antsaklis. Design of Stabilizing Switching Control Laws for Discrete and Continuous-Time Linear Systems Using Piecewise-Linear Lyapunov Functions, *International Journal of Control*, 75(12), 2002.

[33] Krstic, M., Kanellakopoulos, I., and P. V. Kokotovic. Nonlinear and Adaptive Control Design, *Wiley*, 1995.

[34] Kypuros, J. and R. Longoria. Model Synthesis for Design of Switched Systems Using a Variable Structure System Formulation, *ASME Journal Of Dynamic Systems, Measurement, And Control*, 125, 618-629 ,2003.

[35] Li,G., Xi, N. and M. Yu. Calibration of AFM Based Nanomanipulation System, *IEEE Int. Conference on Robotics and Automation*, New Orleans, LA, April 2004.

[36] Liberzon, D., and A.S. Morse. Basic Problems in Stability and Design of Switched Systems, *IEEE Control Systems Magazine*, 19, 59-70, 1999.

[37] Liberzon, D. Switching in Systems and Control, *Birkhauser*, 2003.

[38] Lin, Z. and . Tao Adaptive Control of a Weakly Nonminimum Phase Linear System. *IEEE Transactions On Automatic Control*, 45 (4), 824-829, 2000.

[39] Ljung, L. System Identification: Theory for the User, *Prentice-Hall*, 2nd Ed. 1999.

[40] Lu, B., and F. Wu. Control Design of Switched LPV systems Using Multiple Paramter-Dependent Lyapunov Functions, *American Control Conference*, Boston, MA, 2004

[41] Lucente, G., Montanari, M., and C. Rossi. Modelling of a car driveline for servo-actuated gear-shift control, *Symposium on Industrial Electronics* , Dubrovnik, Croatia, June, 2005.

[42] Marino, R. and P. Tomei. Robust Adaptive State-Feedback Tracking for Nonlinear Systems. *IEEE Transactions on Automatic Control*, 43(1), 84-89, 1998.

[43] Marino, R. and P. Tomei. An Adaptive Output Feedback Control for a Class of Nonlinear Systems with Time-Varying Parameters. *IEEE Transactions on Automatic Control*, 44 (11), 2190-2194, 1999.

[44] Marino, R. and P. Tomei. Control of linear time-varying systems. *Automatica*, 39, 651659, 2003.

[45] Mhaskar, P., El-Farra, N., and P. Christofides. Predictive Control of Switched Nonlinear Systems With Scheduled Mode Transitions. *IEEE Transactions on Automatic Control*, 50 (11), 1670-1680, 2005.

[46] Morselli, R., Zanasi, R., and P. Ferracin. Modelling and simulation of static and Coulomb friction in a class of automotive systems.*International Journal of Control*,79 (5), 508520, 2006.

[47] P.Mosterman. Mode transition behavior in hybrid dynamic systems.*Winter Simulation Conference*,New Orleans, Louisiana, December, 2003.

[48] Narendra, K.S., and J. Balakrishnan. Adaptive Control Using Multiple Models. *IEEE Transactions on Automatic Control*, 42(2), 171-187, 1997.

[49] Narendra, K.S., Driollet, O.A., Feiler, M. , and K. George. Adaptive control using multiple models, switching and tuning.*Int. J. Adaptive Control Signal Process*, 17, 2003.

[50] Owen, W. , Croft, E. The Reduction of Stick-Slip Friction in Hydraulic Actuators. *IEEE/ASME Transactions On Mechatronics*, 8 (3), 362-371, 2003.

[51] Pan, Y., Dagci, O. and U. Ozguner. Variable Structure Control of Electronic Throttle Valve. *Vehicle Electronics Conference*, Tottori, Japan, September, 2001.

[52] Paul, A., M., Safonov. Model Reference Adaptive Control Using Multiple Controllers and Switching. *Conference on Decision and Control*, Maui, Hawaii, USA, December, 2003.

[53] de Wit, C., Kolmanovsky, I., and J. Sun. Adaptive Pulse Control of Electronic Throttle. *American Control Conference*. Arlington, Virginia, June, 2001.

[54] Pan, Z. and T. Basar. Adaptive controller design and disturbance attenuation for SISO linear systems with noisy measurements.*European Control Conference*, Brussels, Belgium, July, 1997.

[55] Pagilla, P., and Y.Zhu. Adaptive Control of Mechanical Systems With Time-Varying Parameters and Disturbances. *ASME Journal Of Dynamic Systems, Measurement, And Control*, 126, 520-530, 2004.

[56] J. Qiu. An Electrothermally-Actuated Bistable MEMS Relay for Power Applications, *Ph.D. Thesis, Dept. of Mech. Eng., Massachusetts Institute of Technology*, 2003.

[57] Rao, R.,Aufderheide, B., and B. Bequette. Experimental Studies on Multiple-Model Predictive Control for Automated Regulation of Hemodynamic Variables, *IEEE Transactions On Biomedical Engineering*, 50 (3), 277-288, 2003.

[58] Raupach, C. and J. Melbert. Advanced Injection System by Means of Sensor Actuator Function.*SAE World Congress* Detroit, Michigan, April 2005.

[59] Rodrigues,L. and B. El-Kebir. Piecewise-linear H-infinity controller synthesis with applications to inventory control of switched production systems. *Automatica*, 42, 1245-1254, 2006.

[60] Rossi,C.,Tilli,A., and A. Tonielli. Robust Control of a Throttle Body for Drive by Wire Operation of Automotive Engines,*IEEE Transactions On Control Systems Technology*, 8 (6), 993-1002, 2000.

[61] Rugh, W.J. Linear System Theory. Upper Saddle River, NJ: *Prentice-Hall*, 1996.

[62] Rugh, W.J. and J.S. Shamma. Research on Gain Scheduling. *Automatica*, 36 (10), 1401-1425, 2000.

[63] Shapiro, B. Ed. NSF Workshop on Control and System Integration Micro- and Nano-Scale Systems, 2004.

[64] Shorten, R.N., K.S. Narendra, and O. Mason . A Result on Common Quadratic Lyapunov Functions. *IEEE Transactions on Automatic Control*, 48(1), 110-113, 2003.

[65] Shorten, R.N., and K.S. Narendra . On Common Quadratic Lyapunov Functions for Pairs of Stable LTI Systems Whose System Matrices Are in Companion Form . *IEEE Transactions on Automatic Control*, 48(4), 618-621, 2003. .

[66] Sitti, M. Teleoperated and Automatic Nanomanipulation Systems using Atomic Force Microscope Probes, *IEEE Conference on Decison and Control*, Maui, Hawaii, December 2003.

[67] Sitti, M. Ed. NSF Workshop on Future Directions in Nano-Scale Systems, Dynamics and Control, 2003.

[68] Slotine, J.J.E., and Coetsee, J.A. Adaptive Sliding Controller Synthesis for Nonlinear Systems,*Int. Journal of Control*, 43(4), 1986.

[69] Slotine, J.J.E., and Li, W. Applied Nonlinear Control, Upper Saddle River, NJ: *Prentice-Hall*, 1991.

[70] Stilwell, D.J, and W. J. Rugh. Stability and L2 gain properties of LPV systems. *Automatica*, 38, 1601-1606, 2002.

[71] Sulchek,T., Yaralioglu, G., Quate, C., and S.C. Minne. Characterization and optimization of scan speed for tapping-mode atomic force microscopy, *Review of Scientific Instruments*, 73(8), August 2002.

[72] Tao, G. Adaptive Control Design and Analysis,*Wiley and Sons*, 2003.

[73] Tomei, P. Robust Adaptive Control of Robots with Arbitrary Transient Performance and Disturbance Attenuation. *IEEE Transactions on Automatic Control*, 44 (3), 654-658 ,1999.

[74] Van der Schaft, A. and J. M. Schumacher. An Introduction to Hybrid Dynamical Systems. New York: *Springer Verlag*, 2000.

[75] Vu, L., Chatterjee, D. and D. Liberzon. Input-to-state stability of switched systems and switching adaptive control Control. *Automatica*, 43, 639-646, 2007.

[76] Xu, H., and P. Ioannou. Robust Adaptive Control for a Class of MIMO Nonlinear Systems With Guaranteed Error Bounds. *IEEE Transactions on Automatic Control*, 48 (5), 728-742, 2003.

[77] Yang, T. Impulsive Systems and Control: Theory and Applications, *Nova Science*, 2001.

[78] Zhai, G., Hu, B., Yasuda, K. and A. N. Michel . Stability Analysis of Switched Systems with Stable and Unstable Subsystems: An Average Dwell Time Approach. *American Control Confrence*, Chicago, IL, 200-204, 2000.

[79] Zhai, G. Hu, B. Yasuda, K. and A. N. Michel. Disturbance Attenuation Properties of Time- Controlled Switched Systems, *Journal of the Franklin Institute*, 338 (7), 765-779, 2001.

[80] Zhai,G., H. Lin and P. J. Antsaklis. Quadratic Stabilizability of Switched Linear Systems with Polytopic Uncertainties. *International Journal of Control*, 76,(7), 747-753, 2003.

[81] Zhang, D. Adaptive Control of Switched Systems. *IEEE Conference on Decision and Control*, Maui, Hawaii USA, December 2003.

[82] Zhang, X., Dawson, D.,de Queiroz, M., and B. Xian. Adaptive Control for a Class of MIMO Nonlinear Systems with Non-Symmetric Input Matrix . *IEEE Conference on Control Applications*, Taipei, Taiwan, September 2004.

[83] Zhang, Y., Fidan, B., and P.Ioannou. Backstepping Control of Linear Time-Varying Systems With Known and Unknown Parameters. *IEEE Transactions on Automatic Control*, 48 (11), 1908-1925, 2003.

[84] Zhendong S., S.S. Geb. Analysis and synthesis of switched linear control systems. *Automatica*, 41, 181-195, 2005.

[85] Zhengtao, D. Adaptive Output Feedback Stabilization of Nonlinear Systems of Any Relative Degree with Unknown High-Frequency Gains.*IEEE Transactions On Automatic Control*, 3 (10), 1442-1446, 1998.

[86] Zhivoglyadov, P. V. , Middleton, R. H., and M. Fu, Localization Based Switching Adaptive Control for Time-Varying Discrete-Time Systems.*IEEE Transactions on Automatic Control*, 45 (4), 752-755, 2000.

Appendix A

Proofs

In this appendix, the proofs of the theorems presented in this thesis are provided. First, a few basic mathematical notations are introduced for convenience.

A.1 Mathematical Background and Notations

Vector $x \in \mathbb{R}^n$, if x is an n-dimensional vector. Whereas, matrix $A \in \mathbb{R}^{n \times m}$, if A is an $n \times m$ matrix.

In this thesis, $\overline{\lambda}(.)$ and $\underline{\lambda}(.)$ denote the maximal and minimal eigenvalues of a matrix. Whereas, $\overline{\sigma}(.)$ and $\underline{\sigma}(.)$ denote the maximal and minimal singular values of a matrix. $\|.\|$ the euclidian norm of a vector and the spectral norm (maximum singular value) of matrix. Also $diag(.,.,\ldots)$ denotes a block diagonal matrix.

Let I denote the identity matrix and superscript T denote transpose. A matrix A is called symmetric if $A = A^T$ and positive definite if $x^T A x > 0 \; \forall x \neq 0$, which is denoted by $A > 0$. A matrix A is Hurwitz if and only if the real part of each eigenvalue is negative. A matrix A is called diagonal if and only if its off diagonal elements are all zero.

A.2 Proof of Theorem 1

The major part of the proof follows standard exponential stability and BIBS stability arguments [30], but is slightly modified to yield less conservative bounds by taking advantage

of the quadratic nature of the Lyapunov function.

Proof.

Without loss of generality we assume that $P^{-1}C > 0$, which is true since we have $C > 0$ and we can upper (or lower) bound it in Equation (3.5) by a positively scaled identity matrix, in which case the product of this matrix with $P^{-1} > 0$ is positive definite. Let $x_c = [e_c, \tilde{a}]^T$ and $z_c = Sx_c$, where $S = diag(P^{1/2}, \Gamma^{-1/2})$ a symmetric positive definite matrix. Using the Lyapunov function $V(e_c, \tilde{a}) = e_c^T P e_c + \tilde{a}^T \Gamma^{-1} \tilde{a}$ and the result from Equation (3.5), we have for the system given by Equation (3.7):

$$\begin{aligned} \dot{V}(x_c) &= -2x_c^T SQSx_c + 2x_c^T S^2 \bar{v} \\ &= -2z_c^T Q z_c + 2z_c^T v \end{aligned}$$

where $Q = diag(P^{-1/2}CP^{-1/2}, \Gamma^{-1/2}L\Gamma^{1/2})$, $\bar{v} = [d, L(a^* - a) - \dot{a}]^T$ and $v = S\bar{v}$. But we have $V = \|z_c\|^2$, which means:

$$\frac{1}{2}\frac{d}{d\tau}\|z_c\|^2 = -z_c^T Q z_c + z_c^T v \leq -\alpha\|z_c\|^2 + \|z_c\|\|v\|$$

where $\alpha = \underline{\lambda}(Q) = \underline{\lambda}(diag(P^{-1}C, L))$ by similarity. Hence

$$\|z_c\| \left(\frac{d}{d\tau}\|z_c\| + \alpha\|z_c\| - \|v\| \right) \leq 0$$

When $\|z_c\| \neq 0$ we have:

$$\frac{d}{d\tau}\|z_c\| \leq -\alpha\|z_c\| + \|v\|$$

Integrating and re-arranging we then have:

$$\|z_c(t)\| \leq \|z_c(t_o)\| e^{-\alpha(t-t_o)} + \int_{t_o}^{t} e^{\alpha(\tau - t)} \|v(\tau)\| \, d\tau$$

Note that if $\|z_c\| = 0$ then the above bound would still be valid. By definition of $\|z_c\| =$

$\|S\,x_c\|$ we can get that:

$$\|x_c(t)\| \;\leq\; b_1\|x_c(t_o)\|e^{-\alpha(t-t_o)} + b_2\int_{t_o}^{t} e^{\alpha(\tau-t)}\|v(\tau)\|\,d\tau$$

with $b_1 = \|S\|\|S^{-1}\|$ and $b_2 = \|S^{-1}\|$. Internal exponential stability is shown by letting $v = 0$ above. BIBS stability is shown by denoting $v_o = \sup_{t\geq t_o}\|v(t)\| < \infty$, then from the last expression we have:

$$\|x_c(t)\| \;\leq\; b_1\|x_c(t_o)\|e^{-\alpha(t-t_o)} + \frac{b_2}{\alpha}v_o$$

Now to get the tighter bound in part (ii) square both sides in the expression for $\|z\|$ and using the expansion $\|z_c\|^2 = \|P^{1/2}e_c\|^2 + \|\Gamma^{-1/2}\tilde{a}\|^2$ we have:

$$\|P^{1/2}e_c\|^2 \;\leq\; \left(\|z_c(t_o)\|e^{-\alpha(t-t_o)} + \int_{t_o}^{t} e^{\alpha(\tau-t)}\|v(\tau)\|\,d\tau\right)^2$$

Using the fact that $\|P^{1/2}e_c\| \geq \|e_c\|/\|P^{-1/2}\|$ we have:

$$\|e_c\| \;\leq\; c_1\|x_c(t_o)\|e^{-\alpha(t-t_o)} + c_2\int_{t_o}^{t} e^{\alpha(\tau-t)}\|v(\tau)\|\,d\tau$$

which is the required expression in part (ii) with $c_1 = \|S\|\|P^{-1/2}\|$ and $c_2 = \|P^{-1/2}\|$. The states are bounded by BIBS stability for piecewise continuous bounded inputs, which leaves us with verifying boundedness when $\dot{a}$ contains infinitely many dirac-delta functions due to discontinuities in a. The closed loop system is given by:

$$\dot{x}_c \;=\; f(x_c, t)$$

where the vector field $f(x_c, t) = [f_e(e_c, \tilde{a}, t) + d, f_a(e_c, \hat{a}, t) - L(\hat{a} - a^*) - \dot{a}]^T$. The solution of the system satisfies:

$$\begin{aligned} x_c &= x_c(t_o) + \int_{t_o}^{t} f(x_c(\tau), \tau)\,d\tau \\ &= x_{cc} + \int_{t_o}^{t} [0, -\dot{a}(\tau)]^T\,d\tau \end{aligned}$$

where x_{cc} is the solution of the same dynamic system with bounded input $[d, L(a^* - a)]^T$ (i.e. without input $\dot{a}$), which is bounded by part (i). Therefore, by boundedness of parameter vector a, then state x_c is bounded. □

A.3 Proof of Theorem 2

Proof.

The problem is equivalent to that of Theorem 1 with the exception that the adaptation gain matrix $\Gamma^{-1} = diag(\Gamma_o^{-1}, \gamma_\rho^{-1}|b|, \Gamma_d^{-1})$ depends on the time varying scalar $b(t)$. The proof of Theorem 1 is extended to deal with this technicality next. Without loss of generality we assume that $P^{-1}C > 0$, which is true since we have $C > 0$ and we can upper (or lower) bound it in Equation (3.5) by a positively scaled identity matrix, in which case the product of this matrix with $P^{-1} > 0$ is positive definite. Let $x_c = [e_c, \tilde{a}]^T$ and $z_c = S\,x_c$, where $S = diag(P^{1/2}, \Gamma^{-1/2})$ a symmetric positive definite matrix with $\Gamma^{-1} = diag(\Gamma_o^{-1}, \gamma_\rho^{-1}|b|, \Gamma_d^{-1})$. Using the Lyapunov function $V(e_c, \tilde{a}, \tau) = e_c^T P e_c + \tilde{a}^T \Gamma^{-1} \tilde{a}$ and the result from Equation (3.5), we have for the system given by Equation (3.7):

$$\begin{aligned} \dot{V}(x) &\leq -2x_c^T S Q(t) S x_c + 2x_c^T S^2 \bar{v} \\ &\leq -2z_c^T Q(t) z_c + 2z_c^T v \end{aligned}$$

where matrix $Q(t) = diag(P^{-1/2} C P^{-1/2}, \Gamma_o^{-1/2} L_o \Gamma_o^{1/2}, l_\rho - 1/2 \frac{d \ln |b(\tau)|}{d\tau}, \Gamma_d^{-1/2} L_d \Gamma_d^{1/2})$, $\bar{v} = [d, L(a^* - a) - \dot{a}]^T$ and $v = S\bar{v}$. But we have $V = \|z\|^2$:

$$\begin{aligned} \frac{1}{2}\frac{d}{d\tau}\|z_c\|^2 &\leq -z_c^T Q(t) z_c + z_c^T v \\ &\leq -\bar{\alpha}\|z_c\|^2 + \|z_c\|\|v\| \end{aligned}$$

where $\bar{\alpha} = \underline{\lambda}(Q) = \underline{\lambda}(diag(P^{-1}C, L_o, l_\rho - 1/2 \frac{d \ln |b(\tau)|}{d\tau}, L_d))$ by similarity. Since $\underline{\lambda}(P^{-1}C) > 0$ and $\underline{\lambda}(L_o)$, $\underline{\lambda}(L_d) > 0$ we assume without loss of generality that $\bar{\alpha} = l_\rho - 1/2 \frac{d \ln |b(\tau)|}{d\tau}$ since this is the worst case scenario as all other eigenvalues of Q are positive and constant. Else the proof would follow that of Theorem 1. Hence, $\bar{\alpha}(\tau) = \alpha - \frac{1}{2}\frac{d}{d\tau} \ln |b(\tau)|$, where

$\alpha = l_\rho > 0$.

$$\|z_c\| \left(\frac{d}{d\tau} \|z_c\| + \bar{\alpha} \|z_c\| - \|v\| \right) \leq 0$$

Therefore if $\|z_c\| \neq 0$ we have:

$$\frac{d}{d\tau} \|z_c\| \leq -\bar{\alpha} \|z_c\| + \|v\|$$

Note that if $\|z_c\| = 0$ the above bound would still be valid. Using the integration factor $e^{\int_0^\tau \bar{\alpha}(\tau) d\tau}$ we then have:

$$\int_{t_o}^{t} \frac{d}{d\tau} \left(\|z_c(\tau)\| e^{\int_0^\tau \bar{\alpha}(\tau) d\tau} \right) d\tau \leq \int_{t_o}^{t} e^{\int_0^\tau \bar{\alpha}(\tau) d\tau} \|v(\tau)\| \, d\tau$$

Consider the integration factor used above the integral

$$\int_0^\tau \bar{\alpha}(\tau) d\tau = \alpha\tau - \frac{1}{2} \int_0^\tau \frac{d}{d\tau} \ln |b(\tau)| d\tau$$

Note that the integral in the right hand side of the expression above exists since b has a constant sign and its piecewise differentiable. Note that due to the boundedness of $|b(t)| \; \forall t$ the integral in the right hand side of the expression above is necessarily bounded since it equals $\ln(|b(\tau)|/|b(0)|)$. Integrating the expression:

$$\int_{t_o}^{t} \frac{d}{d\tau} \left(\|z_c(\tau)\| e^{\int_0^\tau \bar{\alpha}(\tau) d\tau} \right) d\tau \leq \int_{t_o}^{t} e^{\int_0^\tau \bar{\alpha}(\tau) d\tau} \|v(\tau)\| \, d\tau$$

we get

$$\begin{aligned} \|z_c(t)\| \leq & \sqrt{\frac{|b(t)|}{|b(t_o)|}} \|z_c(t_o)\| e^{-\alpha(t-t_o)} \\ & + \sqrt{|b(t)|} \int_{t_o}^{t} \frac{e^{\alpha(\tau-t)} \|v(\tau)\|}{\sqrt{|b(\tau)|}} \, d\tau \end{aligned}$$

Therefore, the boundedness of $b(t)$ implies that $\exists$ constants b_{max} and b_{min}, which are maximum and minimum values of the bounded parameter b, respectively. This yields:

$$\begin{aligned}\|z_c(t)\| &\leq \sqrt{\frac{|b_{max}|}{|b(t_o)|}}\|z_c(t_o)\|e^{-\alpha(t-t_o)} \\ &\quad + \sqrt{\frac{|b_{max}|}{|b_{min}|}}\int_{t_o}^{t} e^{\alpha(\tau-t)}\|v(\tau)\|\,d\tau\end{aligned}$$

Therefore, we are left with an expression analogous to that of Theorem 1 and the stability result follows with the only difference is the bounds' dependence on constants b_{max} and b_{min}. In particular, we have $c_1 = \sqrt{|b_{max}|/|b(t_o)|}\|S\|\|P^{-1/2}\|$ and $c_2 = \sqrt{|b_{max}|/|b_{min}|}\|P^{-1/2}\|$. □

A.4 Proof of Theorem 3

Proof.

The result follows by direct application of Theorem 2 using the Lyapunov function:

$$\begin{aligned}V(e_c,\tilde{a}) &= s^T M s + \tilde{\theta}^T\Gamma^{-1}\tilde{\theta} + |b(t)|\frac{\tilde{\rho}^2}{\gamma} + \hat{d}^T\Gamma_d^{-1}\hat{d} \\ &= e_c^T P e_c + \tilde{a}^T\Gamma^{-1}\tilde{a}\end{aligned}$$

with $P = M$, $C = K$ and $\epsilon = \max_i 1/\lambda^{r_i-1}$. Note that the additional term $s^T\dot{M}s$ in $\dot{V}$ cancels with that in $\dot{s}$ and the term $s^TGs = 0$ by skew symmetry of G. Note that $P = M(x,t)$ yet the boundedness of M, from design assumptions, eliminates any concern with the state dependence of M. □

A.5 Proof of Theorem 4

Proof.

The result follows by direct application of Theorem 1 using the Lyapunov function:

$$\begin{aligned} V(e_c, \tilde{a}) &= s^T M s + \tilde{\theta}^T \Gamma^{-1} \tilde{\theta} + \hat{d}^T \Gamma_d^{-1} \hat{d} \\ &= e_c^T M e_c + \tilde{a}^T \Gamma^{-1} \tilde{a} \end{aligned}$$

with $P = M$, $C = K$ and $\epsilon = \max_i 1/\lambda^{r_i - 1}$. Note that the additional term $s^T \dot{M} s$ in $\dot{V}$ cancels with that in $\dot{s}$ and the term $s^T G s = 0$ by skew symmetry of G and that boundedness of M, from design assumptions, eliminates any other concern from that fact that $M(x, t)$. This differs from the result of Theorem 2 by the fact that Γ does not depend on a parameter b, as $\Gamma^{-1} = diag(\Gamma_o^{-1}, \Gamma_d^{-1})$ and $L = diag(L_o, L_d)$, thus Theorem 1 is used directly. □

A.6 Proof of Theorem 5

Proof.

The result follows by direct application of Theorem 2 using the Lyapunov function:

$$\begin{aligned} V(e_c, \tilde{a}) &= z^T z + \tilde{\theta}^T \Gamma_o^{-1} \tilde{\theta} + |b_n(t)| \frac{\tilde{\rho}^2}{\gamma} + \hat{d}^T \Gamma_d^{-1} \hat{d} \\ &= e_c^T e_c + \tilde{a}^T \Gamma^{-1} \tilde{a} \end{aligned}$$

with $P = I$, $C = diag(c_i)$ and $\epsilon = 1$ by definition of $z_1 = y - y_r$.

□

A.7 Proof of Theorem 6

Proof.

The result of part (i) follows by direct application of Theorem 2 using the Lyapunov func-

tion:

$$\begin{aligned} V(e_c, \tilde{a}) &= z^T z + 2\sum_{i=1}^{r} \varepsilon^T \frac{P_o}{d_i}\varepsilon + \tilde{\theta}^T \Gamma_o^{-1}\tilde{\theta} + |b_m(t)|\frac{\tilde{\rho}^2}{\gamma} \\ &\quad + \tilde{d}^T \Gamma_d^{-1}\hat{d} \\ &= e_c^T P\, e_c + \tilde{a}^T \Gamma^{-1}\tilde{a} \end{aligned}$$

where, $P = diag(I, 2\sum_{i=1}^{r} \frac{P_o}{d_i})$, $C = diag(C_o, D)$, $C_o = diag(c_1, \ldots, c_r)$, and the matrix $D = diag(d_o, 3/4d_o, d_o, \ldots, d_o)$, where $d_o = \sum_{i=1}^{r} \frac{1}{d_i}$. The constant $\epsilon = 1$ by definition of $z_1 = y - y_r$.

For part (ii) the boundedness of x_c follows from part (i). The boundedness of other signals x, Λ and ξ is proven next, which differs slightly from that usually done in [33] due to the modified definition of ε. From boundedness of $e_c = [z, \varepsilon]^T$ and reference y_r, this proves boundedness of y since $z_1 = y - y_r$, which shows boundedness of ξ and Ξ by stability of the filter dynamics and smoothness of ϕ and Φ. By the boundedness of y and uniform exponential stability of the zero dynamics, then u is bounded, see [33] for more analogous details. Therefore, v_i are also bounded by filter construction and thus Λ and $\dot{\Lambda}$ are bounded. By boundedness of y, u then from Equation (5.3), we have that $\dot{x} - Ax$ is bounded. Therefore, expanding Equation (5.5) we get:

$$\dot{x} - Ax + kc^T\varepsilon - \dot{\varepsilon} - \dot{\Omega}^T\theta = -A\left(\xi + \int_0^t \dot{\Omega}^T(\tau)\theta(\tau)d\tau\right)$$

From above the right hand side of this equation is bounded since $\dot{x} - Ax$, ε, $\dot{\varepsilon}$, $\dot{\Omega}$, and θ are all bounded. Therefore, by boundedness of ε and the right hand side of the equation above as well as the definition of ε, then x is also bounded.

□